The North Sea: Satellite Colour Atlas

P. M. Holligan,*† T. Aarup† and S. B. Groom‡

Abstract—Satellite imagery of the North Sea from the Coastal Zone Color Scanner (CZCS) shows complex seasonal changes in the optical and biological properties of surface waters, features which have not been resolved, hitherto, through direct observations from ships. Selected scenes for the period 1979–1986, presented as single band (channel 3), colour composite (channels 1 + 2 + 3) and chlorophyll (channels 1/3 or 2/3) images, are used to demonstrate the relative surface distributions between February and October of suspended sediments, coccolithophores and plant pigments. Comparisons are made also with sea surface temperature images from the Advanced Very High Resolution Radiometer (AVHRR). Quantitative evaluation of the CZCS data is restricted by a lack of contemporary *in situ* optical and biological measurements. However, chlorophyll and Secchi disc distributions, determined by measurements from research ships have been compared qualitatively with images from the Southern Bight (13 May 1986) and for the east central North Sea (24 August 1984 and 24 October 1985). Mini series of CZCS images are presented to show the annual coccolithophore blooms, the development of the spring bloom in 1980 in the eastern and north western parts of the North Sea, advection and mixing processes in the Skagerrak, June 1983 and summer chlorophyll distributions in the German Bight.

1. INTRODUCTION

FOR continental shelf seas, such as the North Sea, the distributions of biological properties, including plankton type and abundance, are related to hydrographic properties such as temperature, salinity, turbidity, etc. (FRASER, 1965). With the introduction in the mid-1960s of methods for continuous measurements of water properties, the nature and cause of such relationships have attracted much attention (e.g. STEELE and HENDERSON, 1979), particularly in the context of studies on tidal mixing (PINGREE *et al.*, 1978) and advection (REID *et al.*, 1983).

Since the mid-1970s the introduction of satellite remote sensing (for a general account see ROBINSON, 1985) has made it possible to observe directly large-scale distributions of physical and biological parameters. The Coastal Zone Color Scanner (CZCS) on the Nimbus-7 satellite was launched in 1978 and was operational for about 8 years (to June 1986). The instrument had sensors for visible light designed to measure variations in surface water constituents that absorb and scatter sunlight. The Advanced Very High Resolution Radiometer (AVHRR) instruments on the TIROS-N and NOAA series of satellites (launched in 1979) have sensors for thermal infra-red radiation which provide images of sea surface temperature. These two sensors provided a powerful new approach to studies of the biology of shelf seas, and one that gives an essential spatial and temporal framework for the interpretation of experimental observations from ships.

* Plymouth Marine Laboratory, Plymouth PL1 3DH, U.K.
† Bigelow Laboratory for Ocean Sciences, West Boothbay Harbor, ME 04575, U.S.A.
‡ NERC Computer Services, Image Analysis Unit, Polytechnic South West, Plymouth PL4 8AA, U.K.

Ocean colour can be defined as the spectral or wavelength composition of radiance exiting the ocean surface in the visible waveband (approximately 400–700 nm). It is frequently expressed as reflectance which is the ratio of upwelling to downwelling irradiance. At any wavelength the reflectance is dependent upon the absorption and scattering properties of the water as well as dissolved and particulate constituents (dissolved organic matter, phytoplankton cells, suspended mineral particles, etc).

Although the precise interpretation of CZCS imagery for coastal waters presents several fundamental problems related to complex optical processes (HØJERSLEV, 1982), the images show structures that can be related to the distributions of surface water properties and to well-known hydrographic features such as fronts, banks and river plumes. They present a form of information that is quite distinct from any provided by ships or moored instruments, the most obvious differences being the spatial synopticity of a single pass and temporal changes observed from passes on successive days (BOXALL and ROBINSON, 1987).

Little use has been made of the CZCS archive of the North Sea even though successful pre-launch experiments were carried out off the French and Dutch coasts in 1977 (SØRENSEN, 1979) and in the German Bight in 1978 (GIENAPP, 1982). This is partly because marine scientists in Europe have not had easy access to appropriate image processing systems, whereas in laboratories equipped for remote sensing work there is often no expertise in oceanography. A further problem is that frequent cloud cover over the North Sea, even in summer, makes it difficult to plan validation experiments on ships. Nevertheless, the archive contains many clear scenes, and represents by far the largest body of information on the optical properties of the North Sea. For a region where commercial exploitation has caused so much concern about a wide range of environmental issues (MILNE, 1987), it seems remarkable that only a few scenes have been analysed (GIENAPP and STURM, 1983; SINGH *et al.*, 1983; FISCHER and DOERFFER, 1987; AARUP *et al.*, 1989). The objective of this Atlas is to demonstrate the various types of information provided by the CZCS, to indicate further uses for the archive, and to prepare the way for more effective use of future satellite colour sensors. The final product is largely descriptive because there are so few relevant sea-truth measurements for the North Sea at times of clear imagery, and because many of the problems of quantitative interpretation of reflectance signatures for coastal waters have yet to be resolved (HØJERSLEV, 1982).

2. HYDROGRAPHY OF THE NORTH SEA

General accounts of the hydrography of the North Sea are given by LEE (1980) and REID *et al.* (1988). Only those aspects that are of direct relevance to the interpretation of the satellite imagery are considered here.

Topographically the North Sea can be divided into three parts (Figs 1 and 2): the Southern Bight (51–54°N) with water depths generally <40 m; the central North Sea (54–57°N) with water depths of 40–100 m except for shallower areas on the Dogger Bank and along the western coastline of Denmark; and the northern North Sea (north of 57°N) which includes an area of shelf water 100–200 m deep and the Norwegian Channel with water depths from 200 to >700 m in the Skagerrak between Denmark and Norway.

The strongest tidal currents (Fig. 3) occur in the Southern Bight, the German Bight, off the eastern coastline of Scotland and between Orkney and Shetland. The combination of variations in water depth and in tidal currents leads to the development of distinct

hydrographic regimes during the summer months when a seasonal thermocline extends over most of the central and northern North Sea in response to solar heating. This effect is shown clearly by numerical models of the $H/\bar{u}^3$ stratification parameter (H = water depth, $\bar{u}$ = average horizontal tidal stream velocity) which predict the distributions of stratified and well-mixed waters in summer (Fig. 4) (PINGREE and GRIFFITHS, 1978). The transitional, or frontal zones are characterized by strong horizontal gradients in surface or bottom water temperatures (see Fig. 9). In contrast to the shelf waters which are well mixed in the winter by tidal action and winds, the deeper waters of the Norwegian Channel exhibit thermohaline stratification throughout the year (SVANSSON, 1975).

Seasonal changes in surface temperature (Figs 5 and 6) are most pronounced in the southern and eastern parts of the North Sea, where the water is relatively shallow and influenced by the more extreme continental climate. Seasonal variations in surface salinity (Figs 7 and 8) are relatively slight, the most significant being the decrease in salinity of the Norwegian coastal waters during summer as a result of fresh water flowing out from the Baltic Sea (SVANSSON, 1975; LARSSON and RHODE, 1979). It is important to note that there is considerable annual variability in these mean temperature and salinity distributions in response to climatic forcing (solar radiation, wind, rainfall etc.).

Vertical density gradients in winter are very slight except in the Norwegian Channel. The development of a strong thermocline, reinforced in the northeastern North Sea by lower surface salinities in summer, is illustrated in Fig. 9. Horizontal changes in the degree of stratification are aligned closely with the predicted positions of tidal fronts (Fig. 4), which give rise to strong gradients in surface and/or bottom water temperatures. In general, surface temperature boundaries or fronts are most marked in the spring and early summer as the thermocline is developing and are most persistent in deeper regions, where the temperature contrast is maintained by relatively slow warming of the mixed waters.

Inspection of the surface temperature and salinity charts shows clearly the influence of warm (in winter), high salinity (>35) Atlantic water entering the North Sea through the English Channel and around the north of Scotland. These inflows, together with the effects of the Earth's rotation (Coriolis force), drive the cyclonic pattern of circulation in the North Sea (Fig. 10). Variations in the strength of the advective currents are determined largely by the wind stress, with additional effects due to seasonal changes in density structure (e.g. Fig. 9). The Norwegian coastal current is a quite distinct dynamic feature (MORK, 1981) influenced by deep inflow from the Atlantic, surface outflow from the Baltic and the spring snow-melt, as well as by the general circulation of the North Sea. In contrast, the currents in the central North Sea tend to be weak and variable in direction.

Tidal mixing and seasonal stratification also have a profound influence on surface turbidity (Figs 11 and 12). The highest turbidity values occur during winter in the shallow water areas subjected to strong tidal action (EISMA and KALF, 1987, Fig. 3). Weaker mixing in summer, as a result of stratification of the water column and of lower mean wind speeds, causes a general reduction in the turbidity levels. This effect is most pronounced off the west coast of Denmark, where the water is shallow and weak stratification in the summer inhibits the re-suspension of particulate matter in the surface waters. In the Southern Bight, the effects of the inflow of relatively clear water from the English Channel throughout the year and of the easterly advective flow in summer are apparent.

The distribution of dissolved organic matter, or Gelbstoff, in the surface waters (Fig. 13) is related to salinity. High values, which significantly modify water colour and
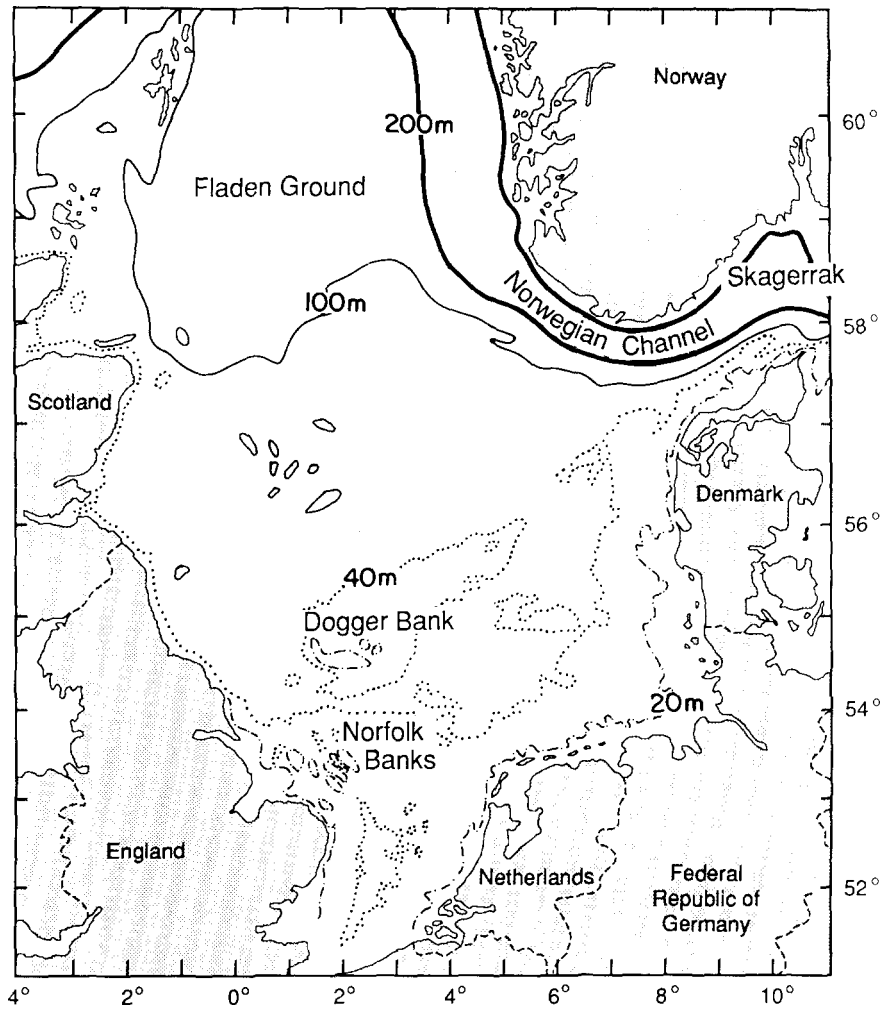
Fig. 1.   Bathymetry of the North Sea (adapted from LEE and RAMSTER, 1981).
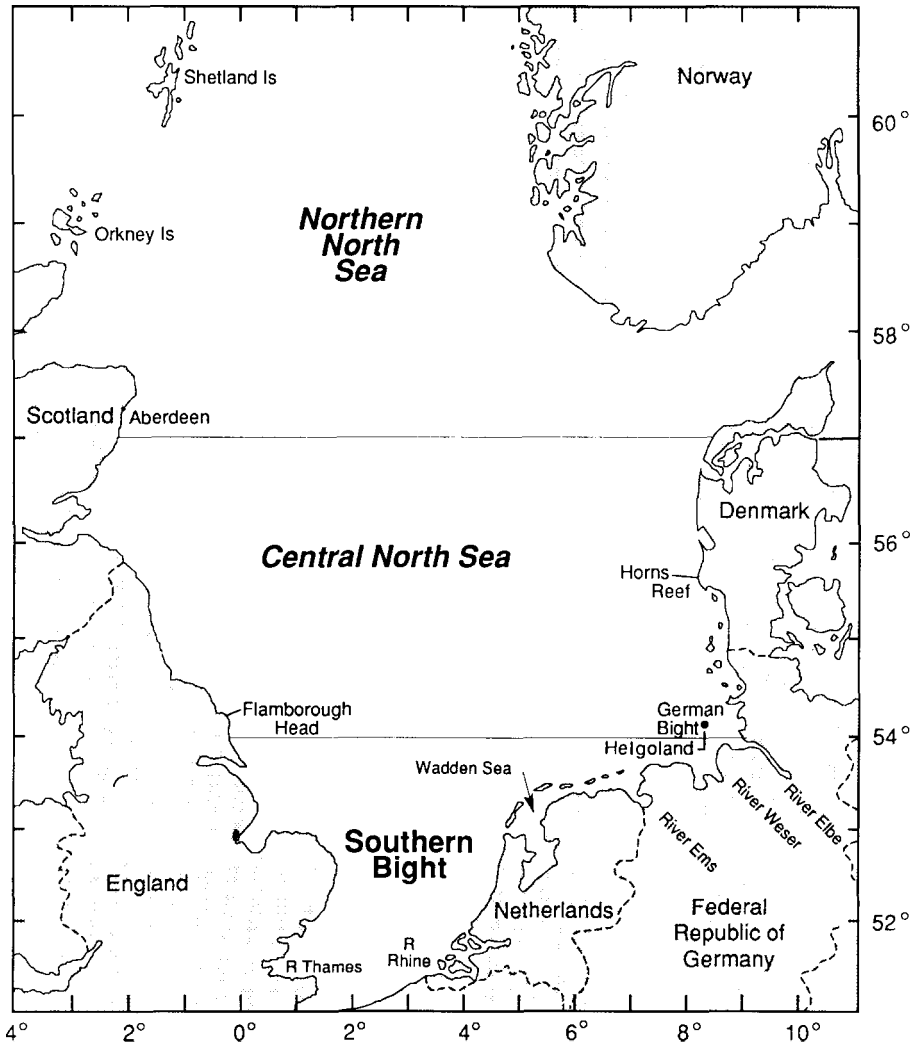
Fig. 2. Geographic subdivisions of the North Sea, and locations referred to in the text.
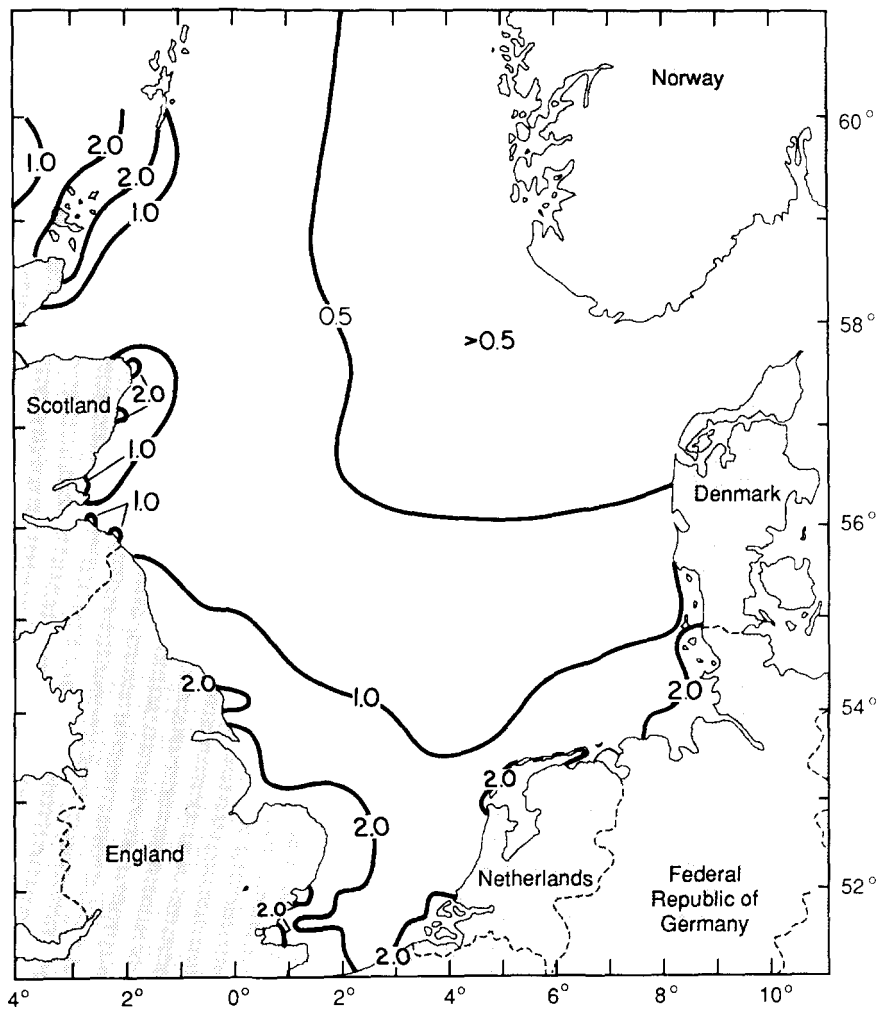
Fig. 3. Maximum tidal current speed (knots) during mean spring tides (Lee and Ramster, 1981).
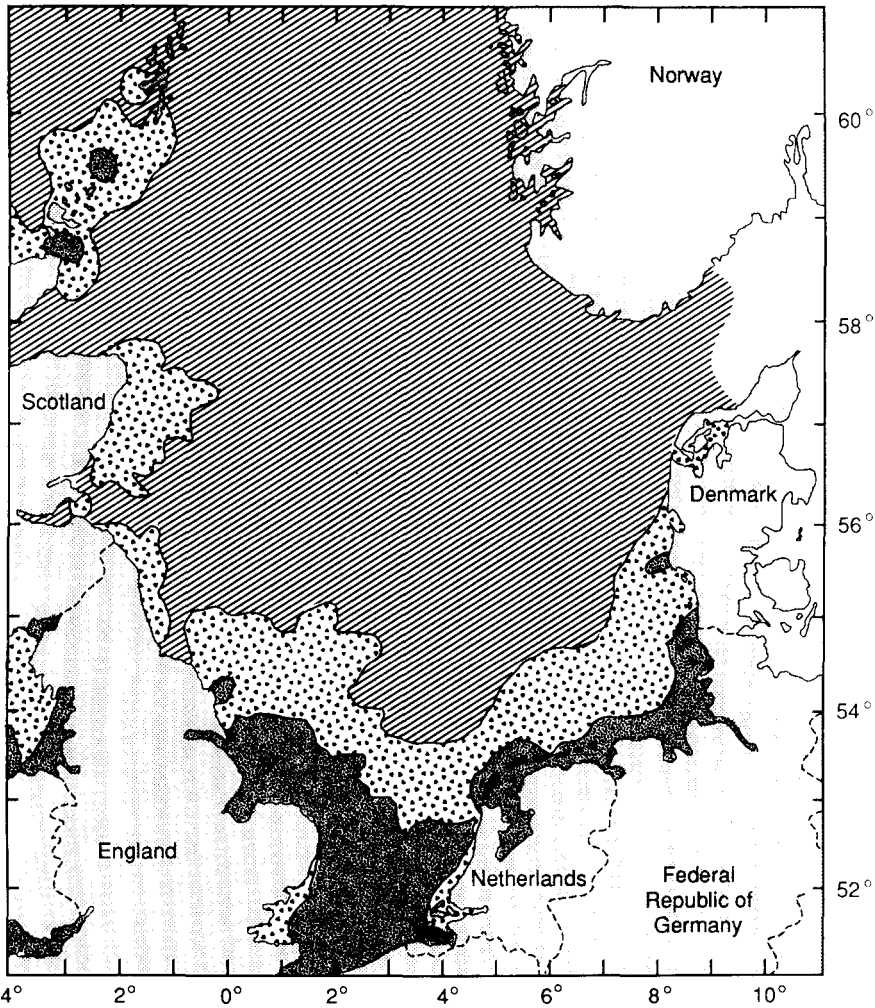
Fig. 4. Predicted distributions of stratified ▨, transitional (frontal) ▨ and well-mixed waters ▨ during the summer months from a numerical model of the stratification parameter, S (PINGREE and GRIFFITHS, 1978).
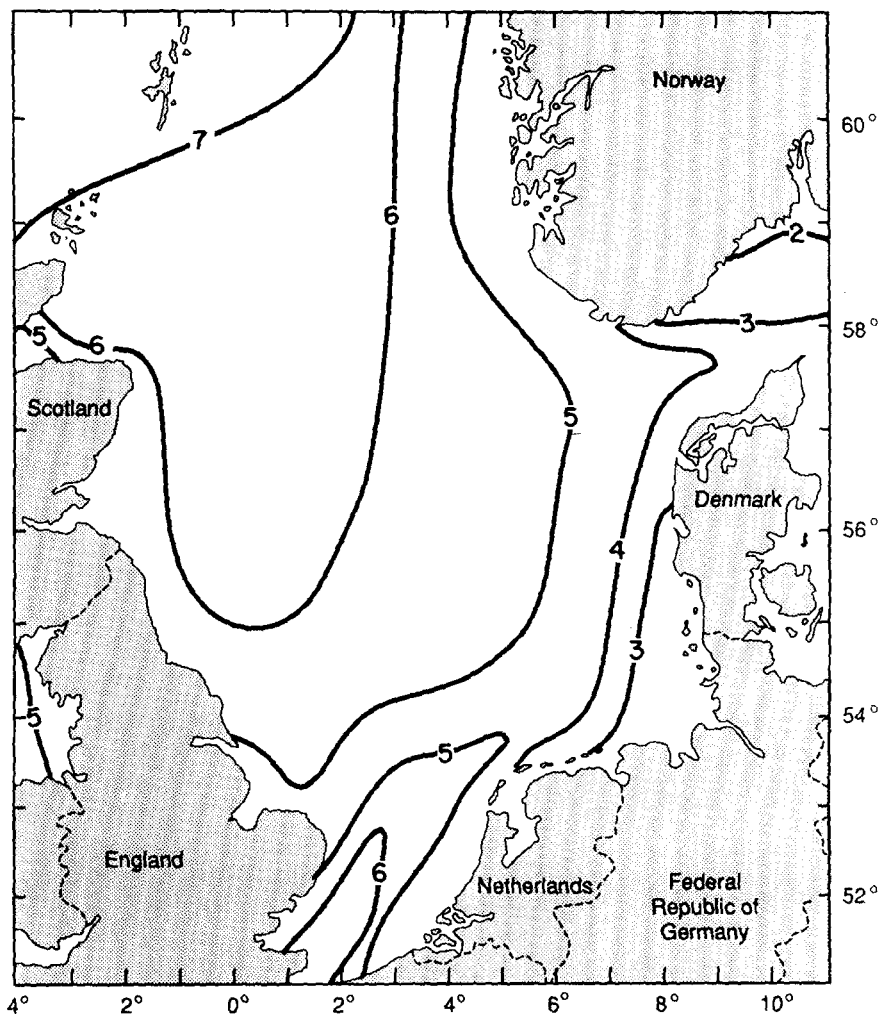
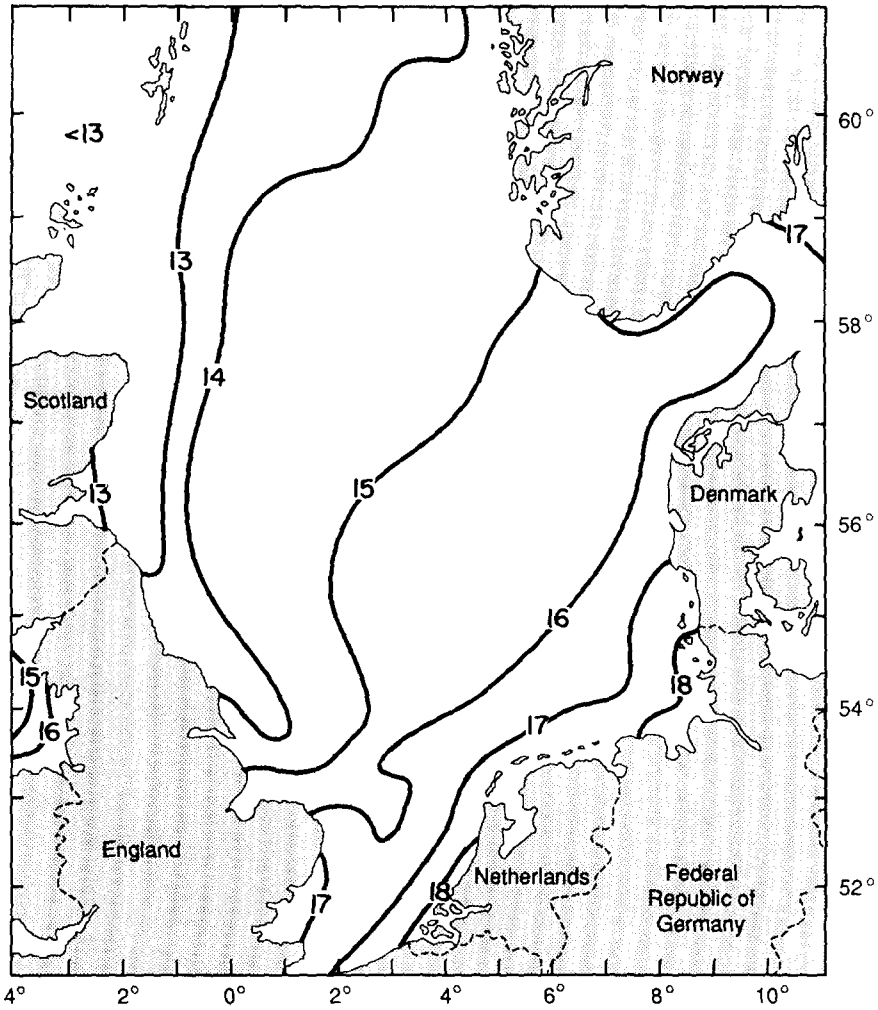Fig. 5.   Mean winter (February) sea surface temperature, °C (LEE and RAMSTER, 1981).

Fig. 6. Mean summer (August) sea surface temperature, °C (LEE and RAMSTER, 1981).
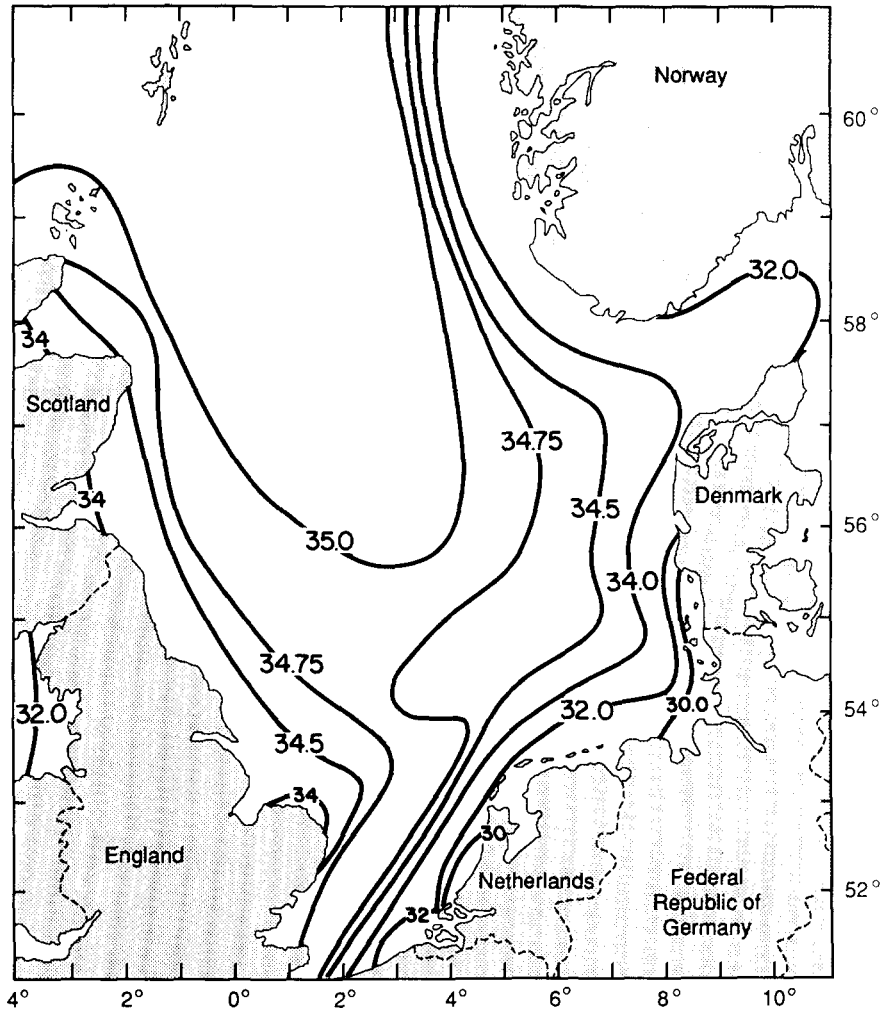
Fig. 7.   Mean winter (February) sea surface salinity (LEE and RAMSTER, 1981).
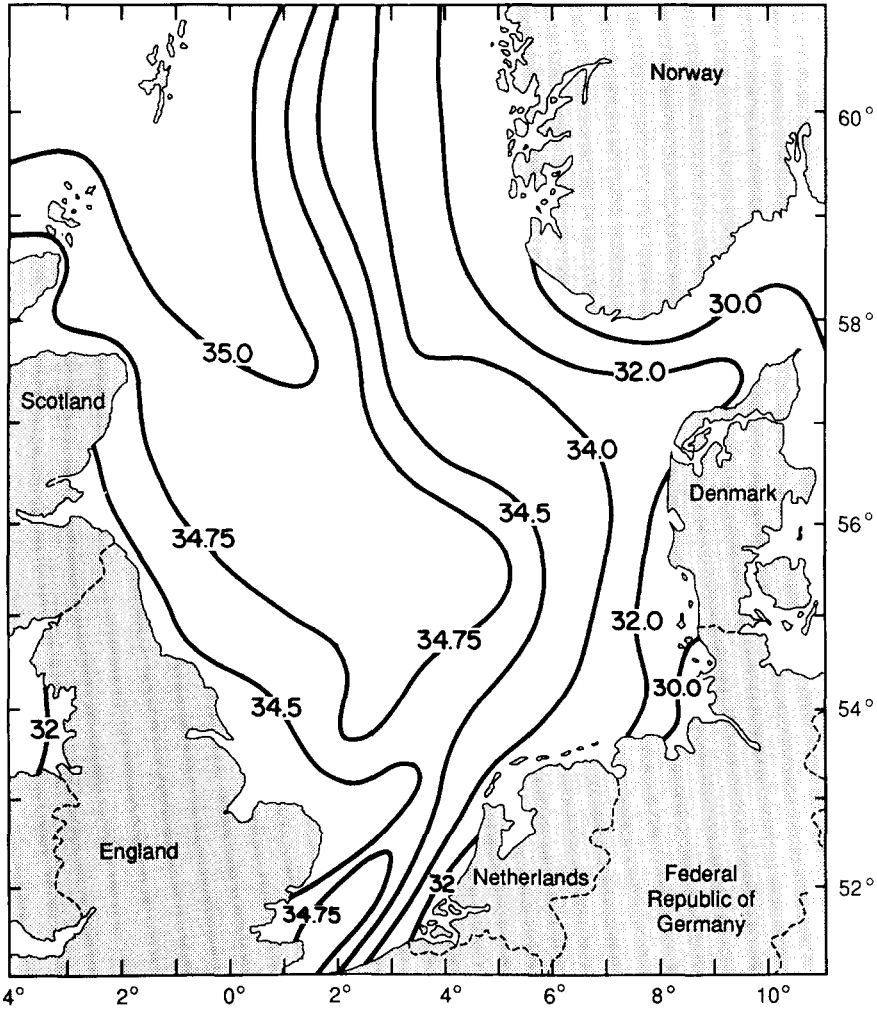
Fig. 8.   Mean summer (August) sea surface salinity (LEE and RAMSTER, 1981).
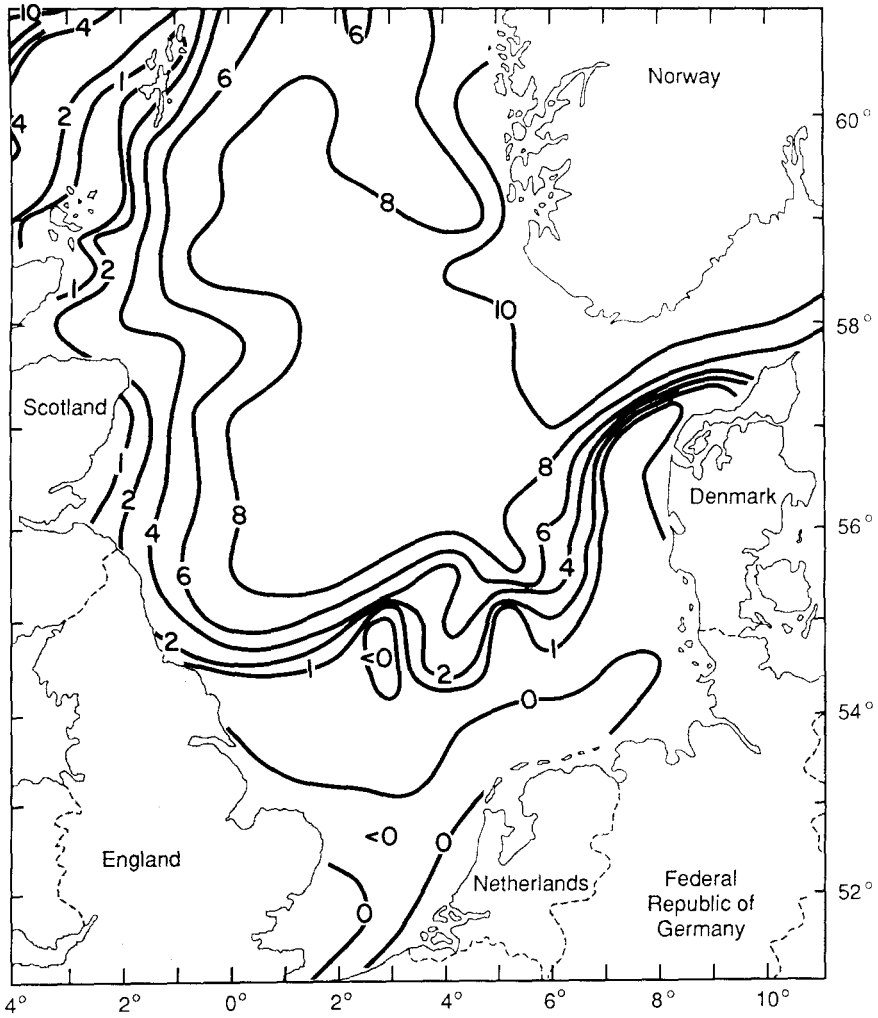
Fig. 9. Surface-to-bottom temperature difference (°C) for August 1980 (from PRAHM-
RODENWALD, 1982).
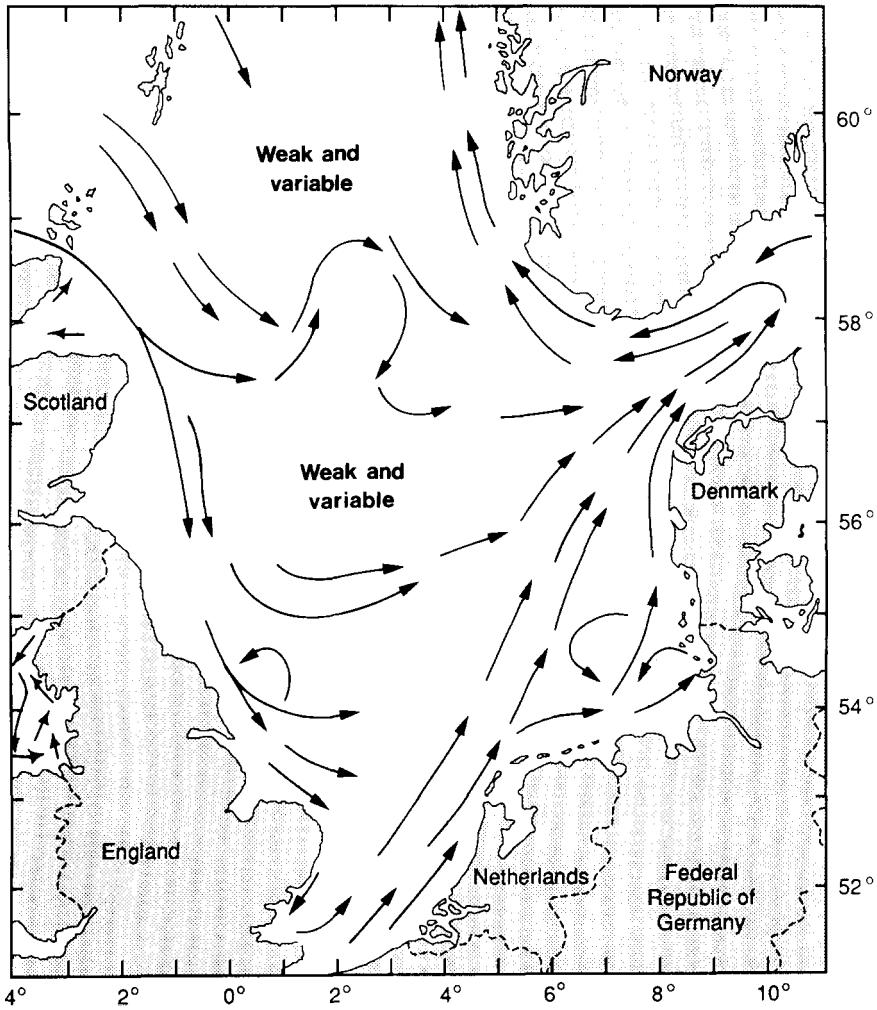
Fig. 10. Generalized near-surface pattern of water movement in the North Sea based on charts presented by LEE and RAMSTER (1981), BACKHAUS and MAIER-REIMER (1983) and PINGREE and GRIFFITHS (1980).
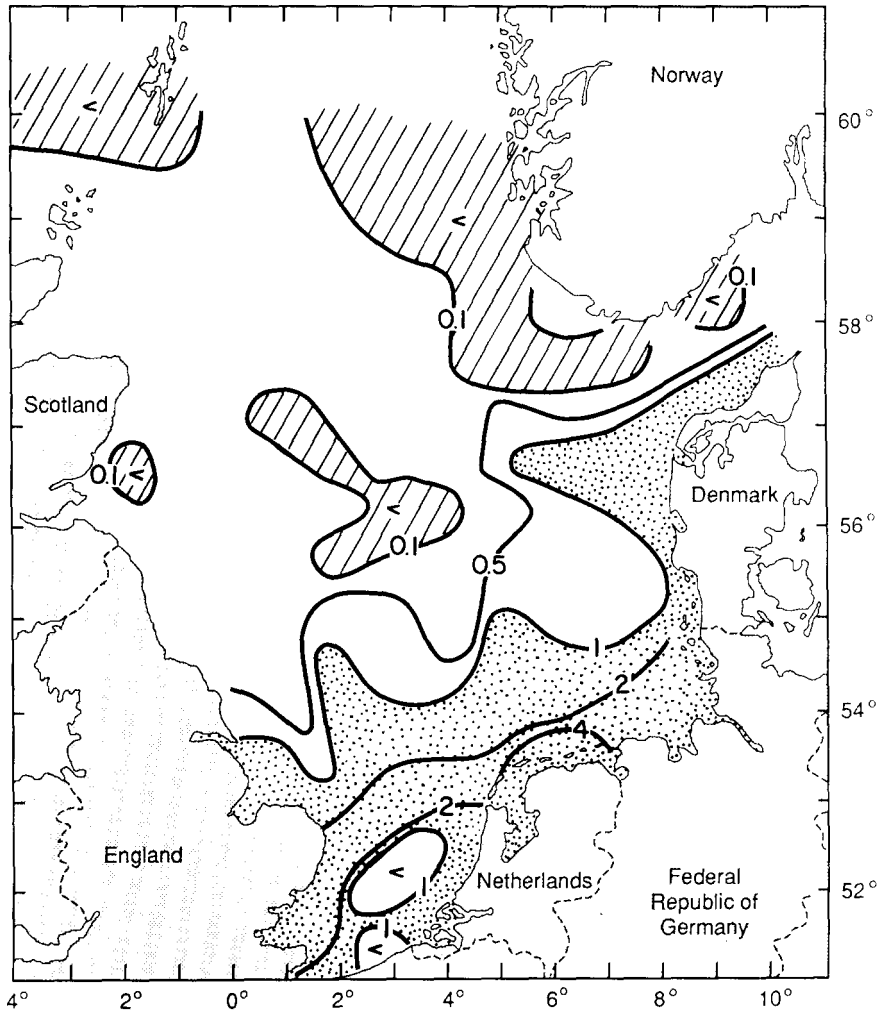
Fig. 11. Winter (1987) near-surface (5 m) distribution of nephelometer turbidity units (ZISCH
Projekt Rapport, Universität Hamburg, June 1987).

Fig. 12. Summer (1986) near-surface (5 m) distribution of nephelometer turbidity units
(ZISCH Projekt Rapport, Universität Hamburg, June 1987).

Fig. 13. The horizontal distribution of Gelbstoff at 10 m depth (HØJERSLEV, 1988); standard-
ized fluorescence units after DUURSMA (1974).

therefore the accuracy of the chlorophyll algorithms based on absorption properties, correspond closely to the low salinity waters (<34) along the eastern margin of the North Sea.
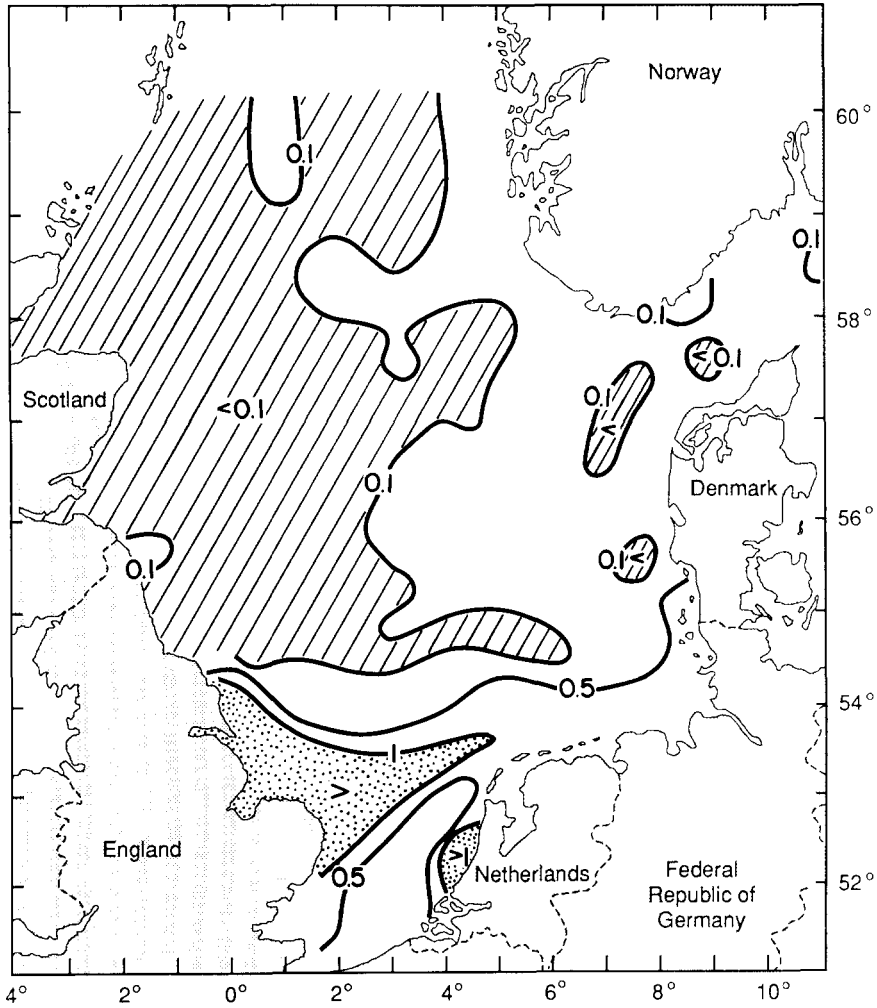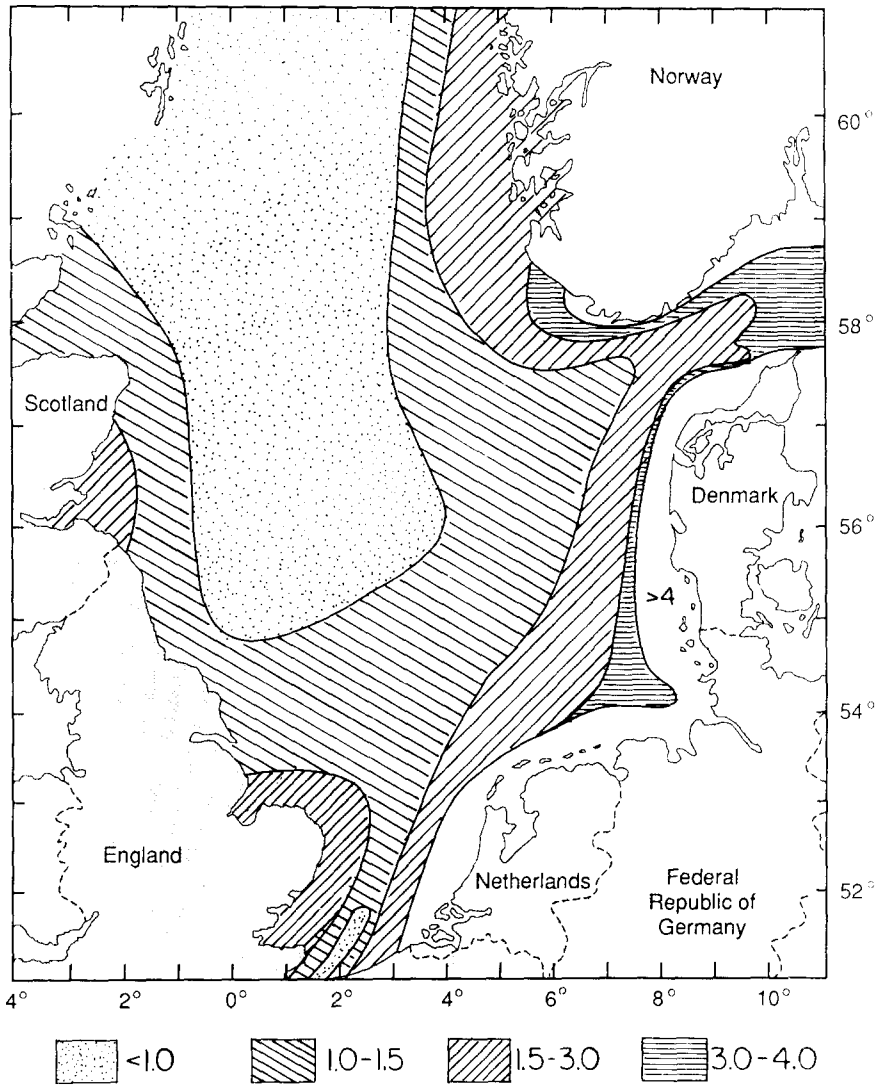
3. METHODS

3.1. Satellite sensors and applications

The data used in this study were obtained from two sensors, the AVHRR and CZCS, both of which were carried on satellites in sun-synchronous polar orbits with equator crossing times at approximately the same local time throughout the year. Table 1 lists the characteristics of the AVHRR, CZCS and their host spacecraft. The sensors construct an image by scanning the narrow aperture which admits light to the detecting system across a swath, perpendicular to the direction of flight. The continuous outputs from the detectors are digitized at such a rate that successive samples, or picture elements, represent contiguous areas on the ground. The angular size of the aperture is such that the forward motion of the spacecraft allows successive adjacent scan lines of Earth data to be added. The CZCS visible bands were optimized for ocean colour observation with narrow band-widths placed in high, medium and low regions of the chlorophyll absorption spectrum, with high signal-to-noise ratios and high sensitivity (or gain), enabling the differentiation of slight changes in water-leaving radiance. Also, the CZCS incorporated a novel mechanism whereby the scan plane could be tilted up to 20° either forward or aft of nadir in the direction of travel to avoid the detection of sunglint (specular reflection of sunlight from the sea surface) which would mask a large area of the satellite field of view.

A basic description of the processing and applications of CZCS data is given by GORDON and MOREL (1983). The major objective of the CZCS mission was to investigate the distribution in the oceans of phytoplankton, unicellular plants living in the sunlit surface layers, which contain a variety of light-absorbing photosynthetic pigments (KIRK, 1983). The most abundant pigment is generally chlorophyll a which absorbs most strongly in the blue part of the spectrum, with a secondary absorption peak at red wavelengths, while accessory pigments have absorption maxima at intermediate wavelengths. Waters with increasing abundance of phytoplankton are characterized by decreasing reflectance of blue light. Variations of reflectance in the green-yellow part of the spectrum depend on a combination of the abundance of accessory pigments and of the scattering properties of the cells (the latter is most important for diatoms and cocolithophores with external coverings of silica and calcite, respectively).

The depth to which the CZCS can "see" into the ocean is limited to approximately one attenuation length (the reciprocal of the attenuation coefficient) above which 90% of the ocean colour signal originates (SMITH, 1981). This depth is strongly wavelength dependent and for oceanic waters is typically 15 – 30 m. For relatively high pigment or turbid waters, such as in the North Sea, it is generally <15 m at the most penetrating wavelength but <1 m in certain coastal regions. Thus, the remotely sensed signal represents a depth-weighted average of surface properties, and sub-surface phytoplankton populations at or below the 10% light level are usually beyond the detection limit of the CZCS. Set against this, the satellite measurements are representative of the surface mixed layer whether it is 5 or 50 m.

Waters with optical properties dominated by phytoplankton have been named Case 1 (MOREL and PRIEUR, 1977). Algorithms for the retrieval of both pigment concentration

Table 1. Sensor characteristics (adapted from HOVIS, 1981)

	CZCS					AVHRR
Band	1	2	3	4	5	4
Spectral bandwidth (nm)	443 ± 10	520 ± 10	550 ± 10	670 ± 10	750 ± 50	10.5–12.5 µm TIROS-N, NOAA-6,8 Figs 22, 26, 38, 46 10.2–11.3 µm NOAA-7, 9 Figs 14, 18, 30, 34, 42, 50
Colour	Blue	Green	Yellow	Red	Near i.r.	Thermal i.r.
Scientific observation	Chl *a* absorption DOM	Absorption by accessory pigments		Atmospheric correction	Land/cloud/ sea discrimination	Sea surface temperature

Scattering by suspended sediments or cocolithophores

Satellite characteristics

	Nimbus-7	TIROS-N/NOAA Series
Orbit	Sun-synchronous near-polar	Sun-synchronous near-polar
North-bound crossing of equator (local times)	12.00	14.30 T-N, N-7, N-9 19.30 N-6, N-8
Nominal height	955 km	833 or 870 km
Pixel area (resolution) at nadir	0.825 × 0.825 km	1.1 × 1.1 km
Field of view	± 39.3° from nadir	± 55.4° from nadir
Swath width (area covered by field of view)	1650 km at 0° tilt 2400 km at 20° tilt	3000 km

and the diffuse attenuation coefficient utilize the ratios of the signals from bands 1 and 3, or 2 and 3 for low and high pigment waters, respectively (GORDON *et al.*, 1983a). Examples of CZCS observations of the development of phytoplankton blooms include the studies by HOLLIGAN *et al.* (1983a) and BROWN *et al.* (1985). Algorithms for estimating rates of primary production have also been developed, relying on the relationship of surface (satellite-derived) pigment estimates to total pigment integrated within the euphotic zone (EPPLEY *et al.*, 1985; PLATT, 1986; CAMPBELL and O'REILLY, 1988; PLATT and SATHYENDRANATH, 1988).

In coastal (Case 2) waters other constituents affect the ocean colour signal including suspended particulates, which may originate from bottom sediments resuspended by vertical mixing throughout the water column, from coastal erosion, or from riverine inputs. The particulates tend to increase the radiance exiting the ocean over much of the visible band by backscatter of incident light. Quantitative evaluations of backscattering have been made for suspended sediments by VIOLLIER and STURM (1984), SIMPSON and BROWN (1987), DESCHAMPS and VIOLLIER (1987) and for coccolithophores by HOLLIGAN *et al.* (1983b) and GROOM and HOLLIGAN (1987). Also present, particularly in low salinity water (<30), is dissolved organic matter (DOM) or "yellow-stuff" of both terrestrial or marine origin which absorbs light strongly at short wavelengths (BRICAUD *et al.*, 1981; HØJERSLEV, 1982; CARDER *et al.*, 1986). Estimates of pigment concentration for Case 2 waters using radiance ratios (e.g. MITCHELSON *et al.*, 1986) show larger uncertainties than for Case 1 waters.

3.2. *Methods of processing satellite data*

The data for this study were obtained from the NERC funded Satellite Receiving Station at Dundee University (CZCS and AVHRR data) and from NOAA, Washington D.C. (CZCS data). Images were processed at the Bigelow Laboratory using an Adage 3000 display processor, hosted by a MicroVAX II, and software developed at the University of Miami, and at Plymouth, using a VAX 11/750 with a model 75 I²S image processor and software written in-house.

CZCS calibration. First the raw digital data as supplied from the receiving station must be converted into radiometric quantities, usually radiance. This requires knowledge of the on-board calibration which, in the case of the CZCS, was unable to adjust for a reduction in the sensitivity of the detection system, believed to be due to a degradation in the scanning mirror (GOWER, 1987). Empirical models have been developed to allow for changes in calibration (GORDON *et al.*, 1983b; MUELLER, 1985) but the residual errors involved in the procedure may affect the accuracy of the retrieved water signal.

Atmospheric correction. Remote sensing of ocean colour is subject to considerable atmospheric contamination, which masks the water-leaving signal and may contribute up to 95% of the total detected signal (STURM, 1981). The atmosphere affects the detected radiance in two ways: the water-leaving signal is reduced, by absorption and scattering during its path to the sensor, particularly in the ozone layer, and the atmosphere scatters light into the field of view of the sensor, increasing the detected radiance. The total radiance L_T^λ at wavelength λ can be written as

$$L_T^\lambda = (L_w^\lambda t^\lambda + L_p^\lambda) \, t_{oz}^\lambda, \tag{1}$$

where L_p^λ is the path radiance, L_w^λ the water-leaving radiance, and t^λ and t_{oz}^λ are, respectively, the diffuse and ozone transmissions as described by GORDON *et al.* (1983a).

In essence the diffuse transmission comprises the Rayleigh scattering transmission, since the ozone transmission has been factored out and the aerosol transmission is assumed to be negligible. The aim of the atmospheric correction is to retrieve L_w^λ from the total radiance, ensuring the atmospheric components are estimated accurately given their high magnitude relative to L_w^λ.

The transmission terms can be calculated from the ozone concentration in a vertical column, the sun-pixel-satellite geometry and the optical depth of molecular scattering which is a function of surface atmospheric pressure.

Path radiance is caused by two processes: Rayleigh (or molecular) scattering and Mie (or aerosol) scattering. In this study we have followed GORDON *et al.* (1983a), GORDON and CASTAÑO (1987) and GORDON *et al.* (1988), who have presented correction algorithms making allowance for multiple scattering effects.

Removal of the Rayleigh scattering and ozone absorption effects leaves the transmitted water signal and the aerosol scattering radiance L_a^λ (which includes a component due to Rayleigh–aerosol scattering interaction):

$$L_c^\lambda = L_w^\lambda t^\lambda + L_a^\lambda . \tag{2}$$

The aerosol radiance, caused by haze particles suspended in the atmosphere, cannot be calculated in the same way as the Rayleigh scattering since the aerosol varies considerably in concentration, size distribution and composition, and hence in optical characteristics, both spatially and temporally. An alternative approach has been presented (GORDON, 1978) which uses the different CZCS waveband images to effect a correction. For a given aerosol type, the ratio of radiances at two wavelengths can be considered constant:

$$L_a^{\lambda 1}/L_a^{\lambda 2} \approx \tau_a^{\lambda 1} E_0^{\lambda 1}/\tau_a^{\lambda 2} E_0^{\lambda 2} = \varepsilon(\lambda_1, \lambda_2) E_0^{\lambda 1}/E_0^{\lambda 2} , \tag{3}$$

where E_0^λ is the solar irradiance incident at the top of the atmosphere and τ_a^λ is the (unknown) aerosol optical depth. Furthermore, if the aerosol size distribution is assumed to follow a Junge power law then

$$\varepsilon(\lambda_1, \lambda_2) = (\lambda_1/\lambda_2)^{-n} , \tag{4}$$

where n is the Ångström exponent. If the aerosol radiance is measured at two wavelengths where the water-leaving radiance is zero, then the Ångström exponent can be retrieved, and the aerosol radiance in other wavebands (where $L_w \neq 0$) can be estimated. Since the CZCS does not possess two such bands, an alternative method has been used for estimating n over areas in which the water-leaving radiance is known. Away from the coastline, in Case 1 waters where the concentration of phytoplankton pigments is < 0.25 mg m^{-3}, the water-leaving radiance is approximately constant at 520 and 550 nm (CZCS bands 2 and 3; GORDON and CLARK, 1981). At this level absorbing phytoplankton pigments only modify the water radiance weakly. Hence, if such "clear water" areas can be found in a scene, the Ångström exponent can be estimated and applied to the remaining image (assuming a homogeneous aerosol type) by extrapolating the aerosol radiance from the 670 nm band in which water-leaving radiance is assumed to be zero.

Application of this technique in the North Sea presents a problem since, except during late spring/summer in central and northern stratified waters, pigment concentrations may be higher than the critical value and, for much of the year, suspended sediments may dominate the ocean colour signal.

In this work an alternative approach, proposed by ARNONE and LAVIOLETTE (1984),

was used which recognizes the correlation between aerosol radiances at different wavelengths, and the lack of correlation between the water and aerosol spatial structures. This "interactive" technique can be performed by subtracting an increasing fraction of CZCS band 4 (670 nm) from bands 1, 2 and 3, until distinct aerosol spatial structure, if present, is seen to disappear. Obviously this method is subjective and may result in inaccurate values of n. However, in the absence of clear water areas it represents a better approach than using a constant (e.g. maritime aerosol) Ångström exponent for all scenes. The Ångström exponent can then be used to generate $\varepsilon(\lambda_i, \lambda_4)$ values via equation (4). These values are multiplied by 0.95, 1.0 and 1.0 for 443, 520 and 550 nm, respectively, to take account of the residual aerosol–Rayleigh interaction and the aerosol multiple scattering effects (GORDON and CASTAÑO, 1987).

To solve equation (2) for the water-leaving radiances it was assumed initially that L_w^{670} is zero. This assumption may be true in low pigment waters, but is not valid in areas of high pigment or in coccolithophore blooms. A simple linear relation, proposed for use in coccolithophore-rich waters by VIOLLIER and STURM (1984):

$$L_w^{670} = 0.15 \, L_w^{550} \, E_o^{670}/E_o^{550} \tag{5}$$

was used to account for non-zero L_w^{670}. It should however be noted that this relation will not allow accurate water-leaving radiance retrieval for sediment-laden waters where more complex, site-specific, algorithms are required (TASSAN and STURM, 1986).

The corrected images have been converted to reflectance which is independent of solar elevation (VIOLLIER et al., 1980). In order to present ocean colour features of different inherent reflectance, such as dark areas of absorption or very bright coccolithophore blooms, each image has been scaled such that the maximum (or saturation) reflectance is appropriate for the feature of interest. As far as possible a uniformity has been maintained within the colour composite and channel 3 images.

CZCS chlorophyll retrieval algorithms. One of the main aims of the CZCS mission was to obtain semi-quantitative estimates of phytoplankton biomass. This is possible since *in situ* measurements of the concentration of phytoplankton pigment "C" (chlorophyll *a* and its degradation product phaeophytin) obtained simultaneously with in-water radiance, have resulted in the development of regressions of the form:

$$C = A \, (L_w^{\lambda 1}/L_w^{\lambda 2})^B.$$

GORDON et al. (1983a) proposed for satellite retrieval of pigment the use of two such algorithms, validated by *in situ* data:

$$C1 = 1.13 \, (L_w^{443}/L_w^{550})^{-1.71}$$
$$C2 = 3.326 \, (L_w^{520}/L_w^{550})^{-2.439}$$
$$\phantom{C(mg \, m^{-3}) = }C1 \text{ for } C1 < 1.5 \text{ or } C2 < 1.5$$
$$C(mg \, m^{-3}) = C1 \text{ for } C1 < 1.5 \text{ and } C2 > 1.5$$
$$\phantom{C(mg \, m^{-3}) = }C2 \text{ for } C1 > 1.5 \text{ and } C2 > 1.5.$$

This scheme has been used to generate maps of pigment concentration presented herein.

Diffuse attenuation coefficient algorithms. The diffuse attenuation coefficient $K(\lambda)$ can be derived from satellite imagery using a two wavelength algorithm of a form similar to the chlorophyll algorithms (AUSTIN and PETZOLD, 1981; GORDON and MOREL, 1983).

Diffuse attenuation images have been processed using the relationship:

$$K490(m^{-1}) = 0.088 \, (L_w^{443}/L_w^{550})^{-1.491} + 0.022 \, .$$

AVHRR (channel 4) data. The data presented are contrast-enhanced versions of the raw digital data: no atmospheric correction has been attempted. Hence, the images represent relative sea surface temperatures and may suffer from slight apparent gradients in temperature (approximately east–west) where the satellite has viewed the sea surface through increasing atmospheric pathlengths. The sea surface temperature signal (emitted thermal infra-red) originates from a thin surface "skin-layer" of approximately 0.1 mm (ROBINSON, 1985).

Geometric remapping. All CZCS and AVHRR images presented in this Atlas have been remapped to a Mercator projection (SNYDER, 1982), using a model of the satellite orbital and viewing geometries, in order to allow precise intercomparison between the different satellite scenes.

3.3. Selection and interpretation of images

There is complete or partial CZCS coverage of the North Sea for between 1000 and 1500 days, for the period late 1978 to mid-1986. Although only a small proportion of scenes show <50% cloud cover for the whole region, many include some cloud-free areas for which useful information about surface water properties can be derived. The numbers of clear images for particular sub-areas are not known precisely, although they will reflect the trend of increased cloud cover from southeast to northwest.

Several criteria were used to select the images for the Atlas. For the section dealing with seasonal changes, which comprises the bulk of the Atlas, a series of the most cloud-free images for the period February–October was chosen. This represents the best of the archive for the North Sea as a whole. The remaining sections provide examples of other forms of information that can be derived from the archive.

The four types of processed image used in the Atlas to illustrate the seasonal changes are entirely complementary for interpretative purposes:

(a) *AVHRR infra-red images of sea surface temperature (SST).* The AVHRR channel 4 gives superior radiometric resolution (~0.1°C) compared to the CZCS channel 6. Images for the same day as the CZCS data are used, which may be received a few hours earlier or later, though in every case afternoon images have been chosen. Relatively warm temperatures appear as darker shades. Spatial variations in temperature are indicative of advective patterns for both oceanic (e.g. REID et al., 1983) and riverine water, and of differences in the degree of thermal stratification during summer (PINGREE et al., 1978; PINGREE and GRIFFITHS, 1978). The latter give rise to relatively sharp horizontal gradients in surface temperature (fronts) between warm stratified water and cool tidally mixed water. Under conditions of low wind stress, anomalously warm patches may be apparent during the day due to superficial heating of the surface layer (SAUNDERS et al., 1982).

(b) *Reflectance at 550 nm (CZCS channel 3), for sediment and coccolithophore distributions.* These images show regions of high reflectance (light shades) caused by suspended sediment in inshore and well-mixed waters (e.g. VIOLLIER and STURM, 1984; SIMPSON and BROWN, 1987) and by coccolithophores in offshore, stratified waters (HOLLIGAN et al., 1983b). On certain scenes, areas of strong absorption, probably mainly due to phytoplankton accessory pigments, are also apparent.

(c) *CZCS colour composites, for particulate distributions, and absorption by chlorophyll and DOM.* The colour composite images are produced by assigning the atmospherically corrected reflectances for channels 1 (blue), 2 (green), and 3 (yellow), respectively,

to blue, green and red colours in the image processing system, thereby giving a semi-natural colour image. Sediments are distinguished as relatively strong reflectance in channels 2 and 3 (yellow to brown colours), whereas coccolithophores show as white or bluish shades due to backscattering in all three visible bands. Clear, high salinity waters appear blue as a result of the lower absorption of blue light by seawater, in comparison to the dark areas which are indicative of additional absorbing materials (chlorophyll and yellow substances at blue wavelengths, accessory pigments at green and yellow wavelengths). The combined effects of backscattering and absorption due to these different properties (ROBINSON, 1983) give rise to intermediate colour patterns, thereby retaining all the information available from CZCS channels 1, 2 and 3, unlike the algorithms for specific properties (pigments, primary productivity) based on only two channels. It is important to note that the colour balance will be affected by any errors in calibration and atmospheric correction procedures as, of course, will be the retrieved chlorophyll concentrations and values of the diffuse attenuation coefficient.

(d) *Chlorophyll images*. The standard algorithms are affected by constituents in the water other than chlorophyll in a largely unknown manner (at least for the North Sea) so that chlorophyll distributions need to be qualified using information from the channel 3 and colour composite images. In general, spatial patterns in chlorophyll levels are likely to be preserved even though the absolute quantities might be unreliable due to co-variance between chlorophyll, dissolved organic matter and numbers of living (mainly phytoplankton) and non-living scattering particles. MITCHELSON *et al.* (1986) have shown that the radiance ratio is still positively correlated with chlorophyll in Case 2 waters, albeit with a lower sensitivity and higher variance. More problematical is the effect of yellow stuff or dissolved organic matter (DOM); TASSAN (1988), using a sensitivity analysis, demonstrated that radiance ratio algorithms overestimate the retrieved values of chlorophyll concentration by varying degrees in the presence of DOM. It appears, therefore, that useful information on the spatial distributions of phytoplankton pigment absorption can be retrieved for coastal waters, even though site-specific differences in combined water properties make it inappropriate to develop any general algorithm (HØJERSLEV, 1982).

A consistent colour scale is used for the chlorophyll images (see colour bar on reverse of Fig. 14), with chlorophyll concentrations <1.0, 1.0–2.0, 2.0–4.0 and >4.0 mg m^{-3} represented, respectively, by blue, green, yellow to orange and red shades. The greatest errors in CZCS chlorophyll retrievals will occur in the Southern Bight (see Fig. 1) due to a combination of low salinity (i.e. high DOM) and high turbidity (due to tidal mixing), in the Norwegian Channel due to low salinity, and in the winter in coastal waters of the eastern North Sea due to high turbidity.

## 4. SATELLITE IMAGES

4.1. *Seasonal images of the North Sea*

Date	AVHRR (GMT)	CZCS (GMT)	R_s (%)	Figures
21 February 1982	14.21	10.48	3.75	14–17
26 March 1982	12.54	10.35	3.75	18–21
16 April 1981	18.22	11.26	3.75	22–25
12 May 1980	14.33	11.14	3.75	26–29
15 June 1986	13.15	11.00	8.00	30–33
6 July 1983	13.10	10.18	6.00	34–37
24 July 1980	14.13	11.34	3.75	38–41
20 August 1984	14.37	11.10	3.75	42–45
6 September 1979	14.43	11.46	3.75	46–49
24 October 1985	13.01	10.42	3.75	50–53

For the seasonal section four images are presented for a standard area of the North Sea, 51.0° to 58.5°N, 3°W to 10°E (Mercator projection) in the order: AVHRR channel 4 (thermal infra-red); CZCS channel 3 (540–560 nm); CZCS colour composite; CZCS chlorophyll. In the AVHRR images, clouds appear white and land appears grey or black. In the CZCS images land and clouds are masked black. For each date, the time of the satellite pass (overhead Dundee, GMT) and the saturation reflectance R_s for the CZCS colour composite images are listed.

For each date, the state of the tide is given as the number of days before (–) or after (+) neaps and springs.
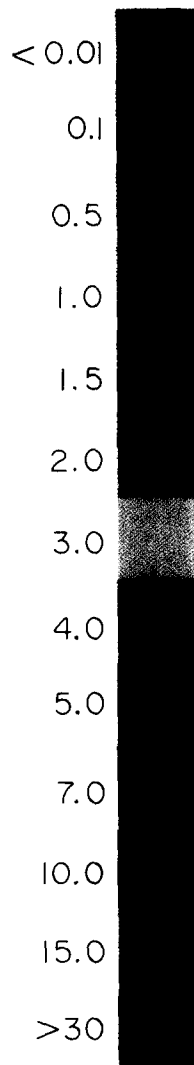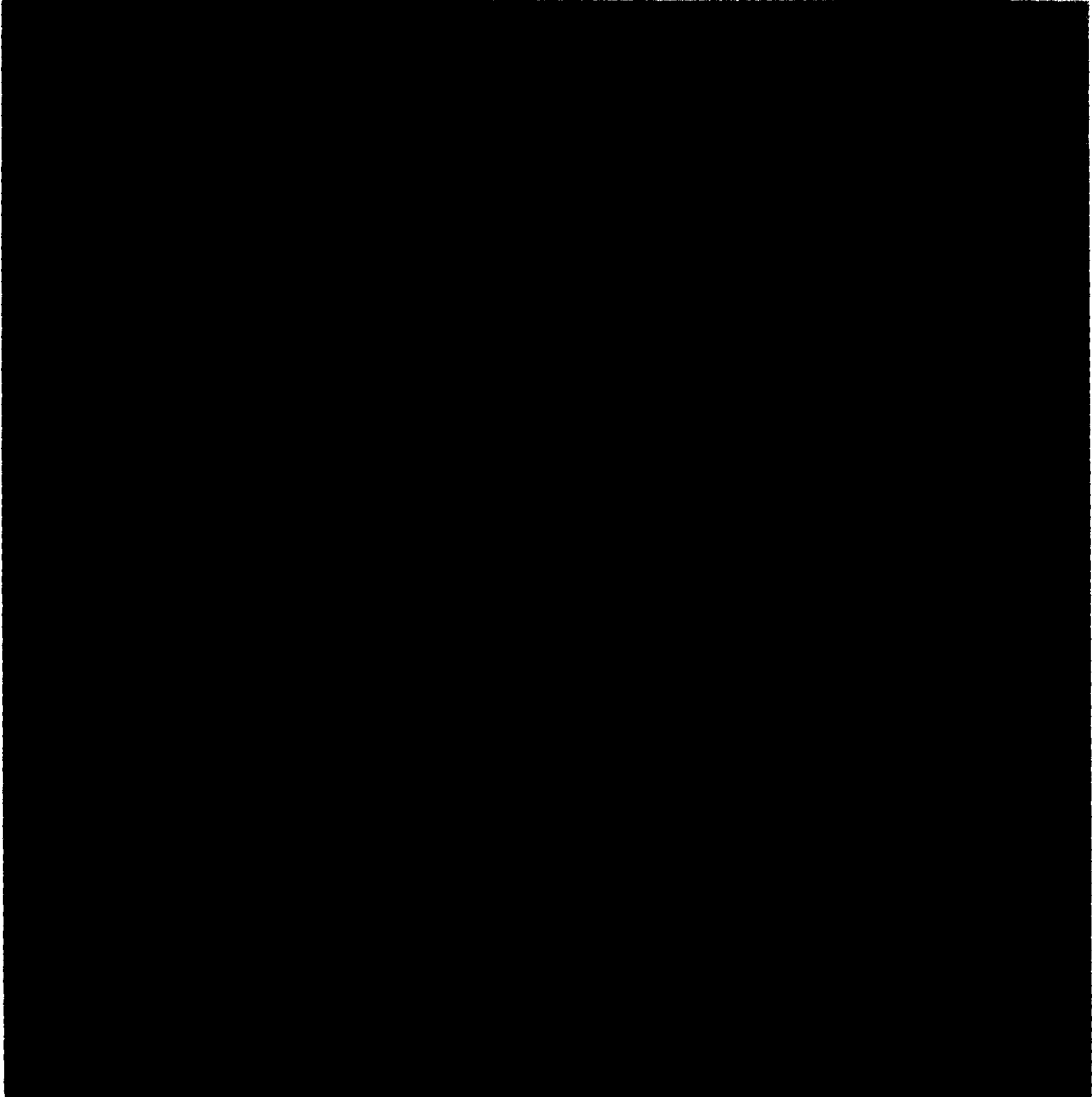
Phytoplankton pigment concentration (mg m^{-3}) used in Figs 17, 21, 25, 29, 33, 37, 41, 45, 49, 53, 56, 57, 59, 64–69, 78–83.
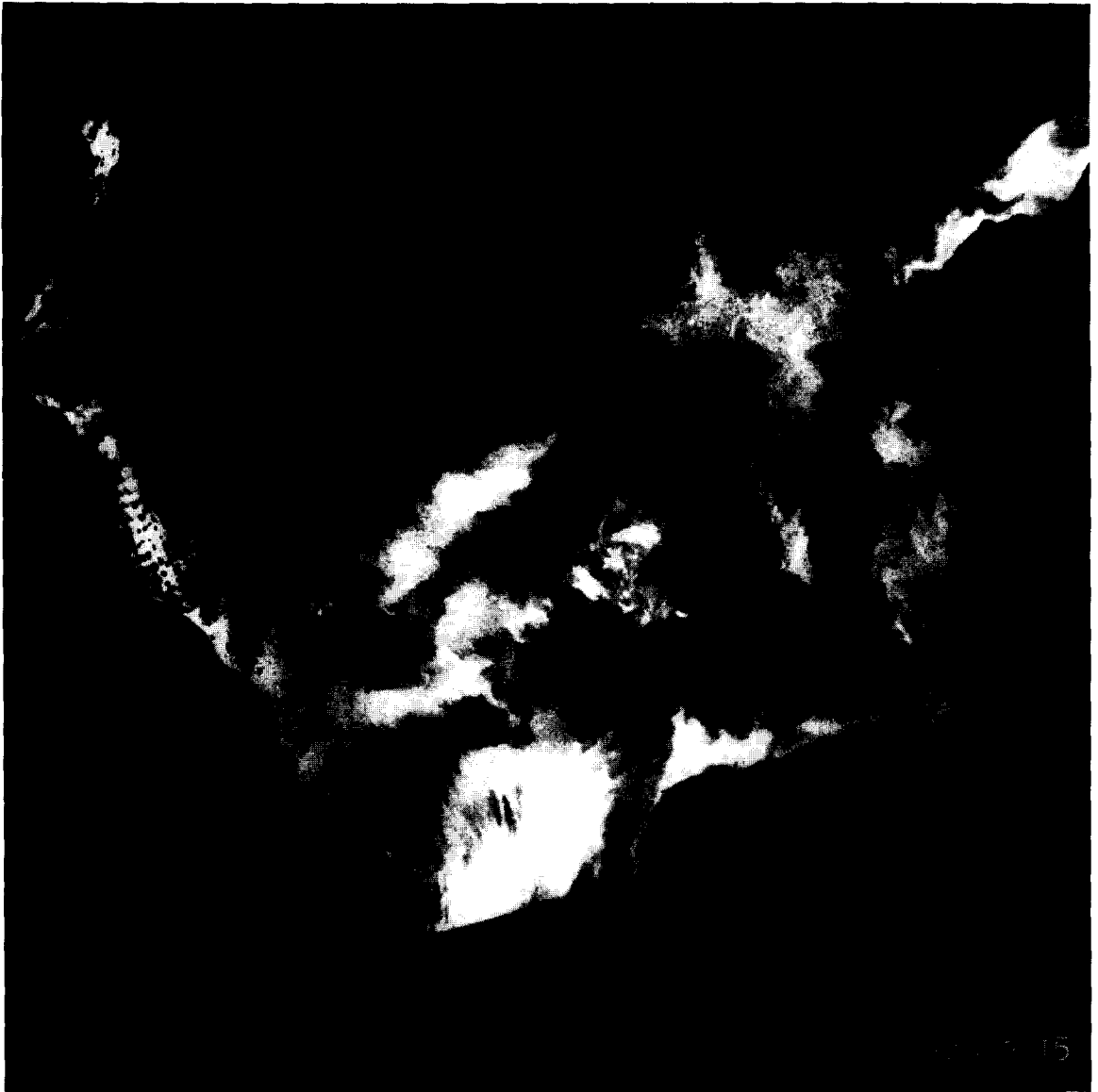
The CZCS channel 3 image (Fig. 15) shows turbid water throughout much of the southern and eastern North Sea where the water is shallow and the tides are strong (see Fig. 11; LEE and FOLKARD, 1969; VISSER, 1970; EISMA and KALF, 1979; EISMA, 1981; EISMA and IRION, 1988). The fine structure in the reflectance patterns is related in part to topographic features (see Fig. 1) and to surface temperature distributions. By contrast, the northern North Sea, although partly cloud covered, and Norwegian Channel appear relatively dark.

21 *February* 1982 (*neaps* + 3) *AVHRR* 14.21 *GMT CZCS* 10.48 *GMT* (*Figs* 14–17). The coldest surface water temperatures (Fig. 14) are seen from the coast of Norway southwards to the German Bight and Wadden Sea. Broad tongues of relatively warm water, extending from the English Channel into the Southern Bight and from the northwest along the western margin of the Norwegian Channel, indicate inflows of Atlantic water (see Figs 5 and 6). In the Southern Bight, anomalously high salinity values in late winter have been associated with warm water and early diatom blooms (REID *et al.*, 1983).

indication of absorption) to the north of Dogger Bank and north of the Norfolk Banks (cf. Fig. 1) is not known. The estimated chlorophyll concentrations (Fig. 17) range from <1.0 mg m^{-3} in the northern North Sea to >1.0 mg m^{-3} in offshore areas of the southern and eastern North Sea: these are not inconsistent with measured values for late winter (BROCKMANN and WEGNER, 1985; RICHARDSON and OLSEN, 1987). However, concentrations >4 mg m^{-3} for turbid coastal waters and the Norwegian Channel, as shown by the orange and red shades, are probably overestimates for this early time of year when solar radiation is still low.

The white (offshore) to yellow (inshore) shades in the colour composite image (Fig. 16) indicate the presence of high levels of suspended particulate material with increasing yellow colouration attributable to the absorption of blue light by DOM. The transition to the darker (low sediment reflectance, high absorption) waters of the northern North Sea is rather abrupt. The dark brown appearance of the Norwegian coastal waters is considered to result from a combination of low backscattering and of high absorption by DOM and by higher surface chlorophyll values associated with a shallow halocline (DAHL and DANIELSSEN, 1981). The cause of distinct dark patterns (an

important differences can be seen. Levels of chlorophyll (Fig. 21) were generally low, but a distinct patch is apparent over the Dogger Bank as reported by BROCKMANN and WEGNER (1985) and RICHARDSON and OLSEN (1987) for March. The warm Atlantic water in the northern North Sea shows relatively strong reflectance in the blue band of the colour composite image, whereas the water in the western central region remains dark, due to absorption.
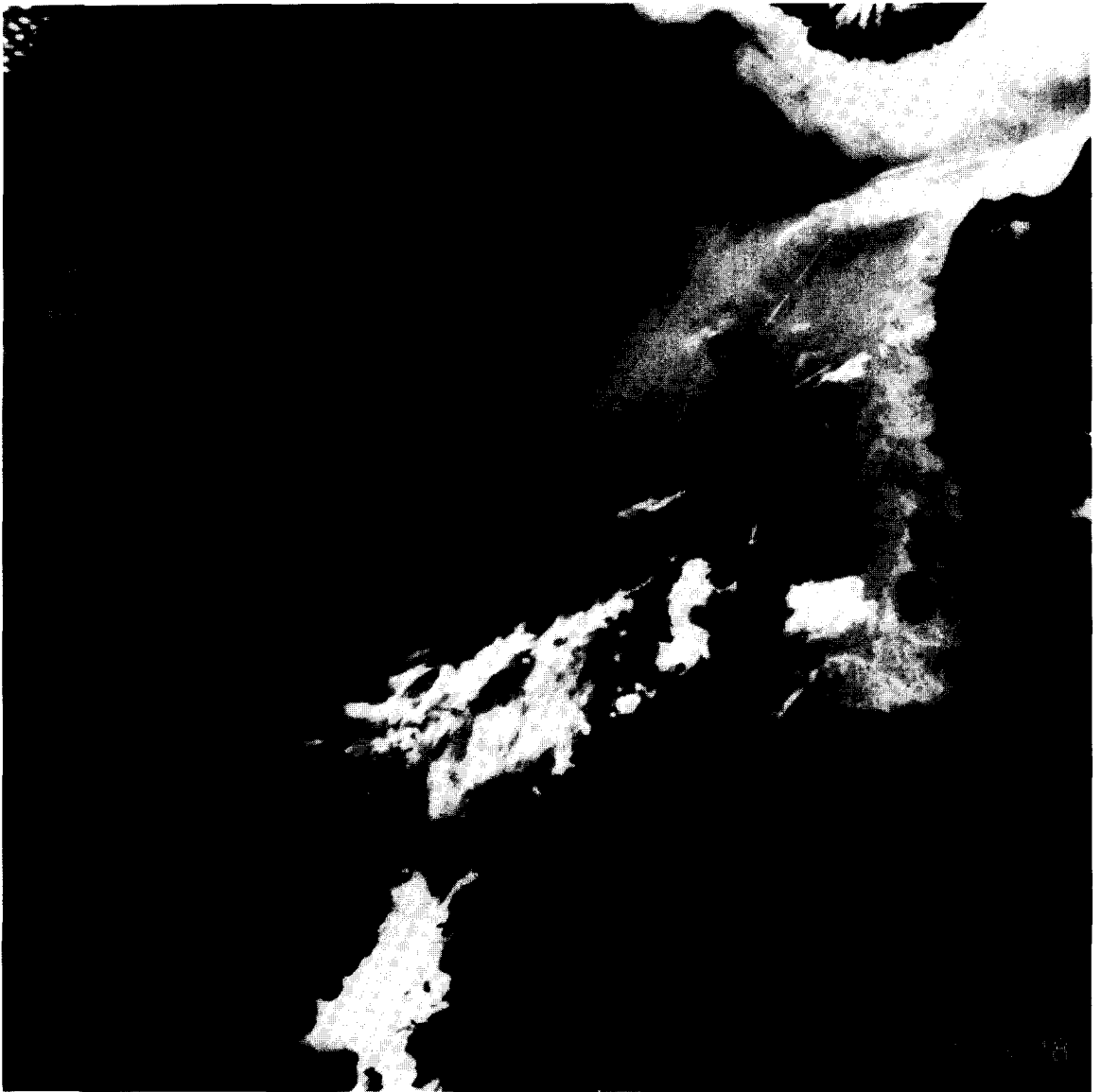
26 *March* 1982 (*springs*–1) *AVHRR* 12.54 *GMT, CZCS* 10.35 *GMT* (*Figs* 18–21). The winter distributional patterns for temperature (Fig. 18), sediment (Fig. 19) and chlorophyll (Fig. 21) shown by the February images persist through to March. While boundaries in both temperature and colour between the Norwegian coastal water, the southeastern North Sea, and the central and northwestern North Sea are still well defined, some
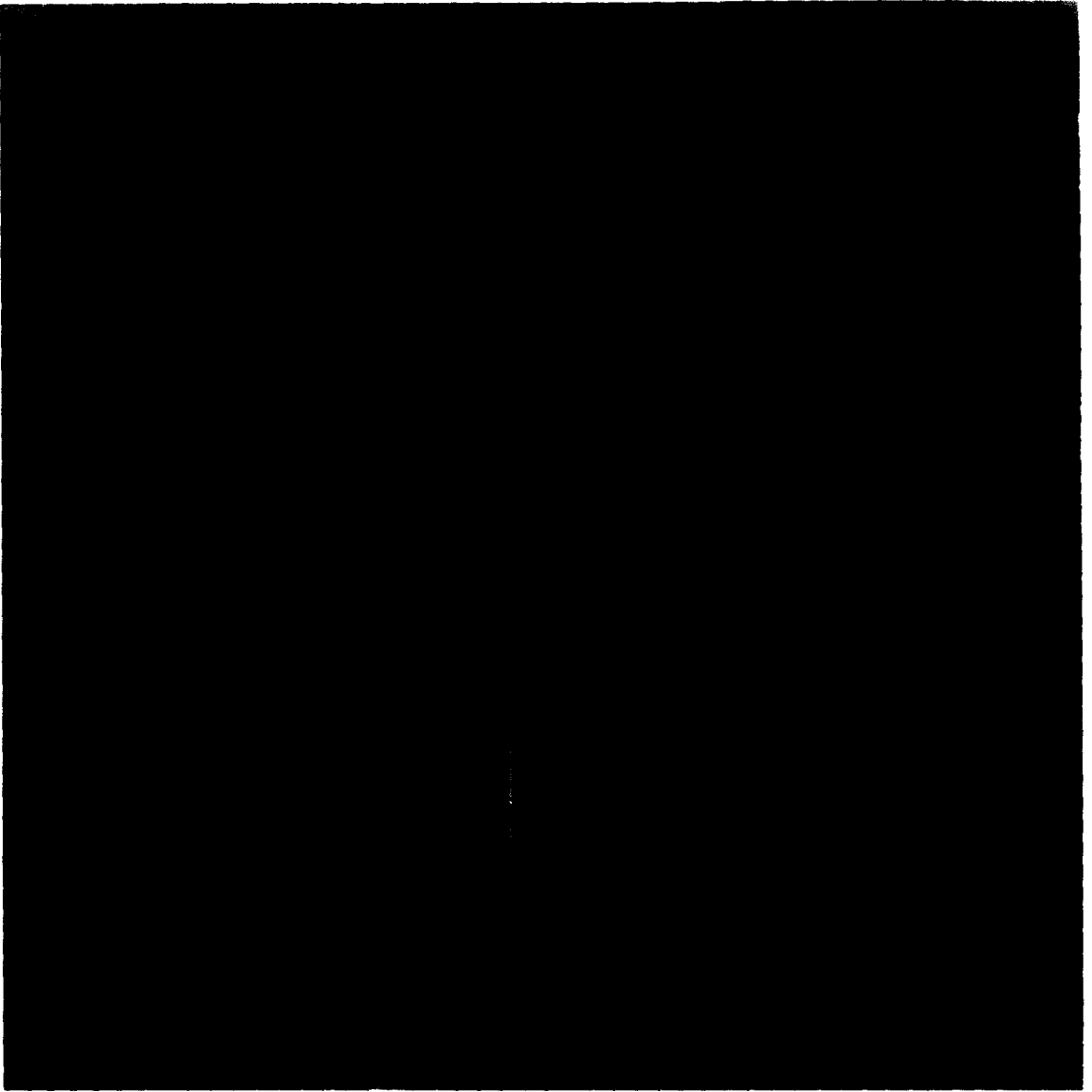
absorption in channel 3. The Norwegian Channel is also well defined in both temperature and colour, with eddies both along the boundary between the cold, fresh coastal water and the North Sea and entrained within the Norwegian current.

The plume of sediment-rich water extending northeast from the Norfolk Banks is shown clearly by many of the other CZCS images (e.g. 6 September 1979, Fig. 47) and also by ship observations (EISMA and KALF, 1979; Fig. 6).
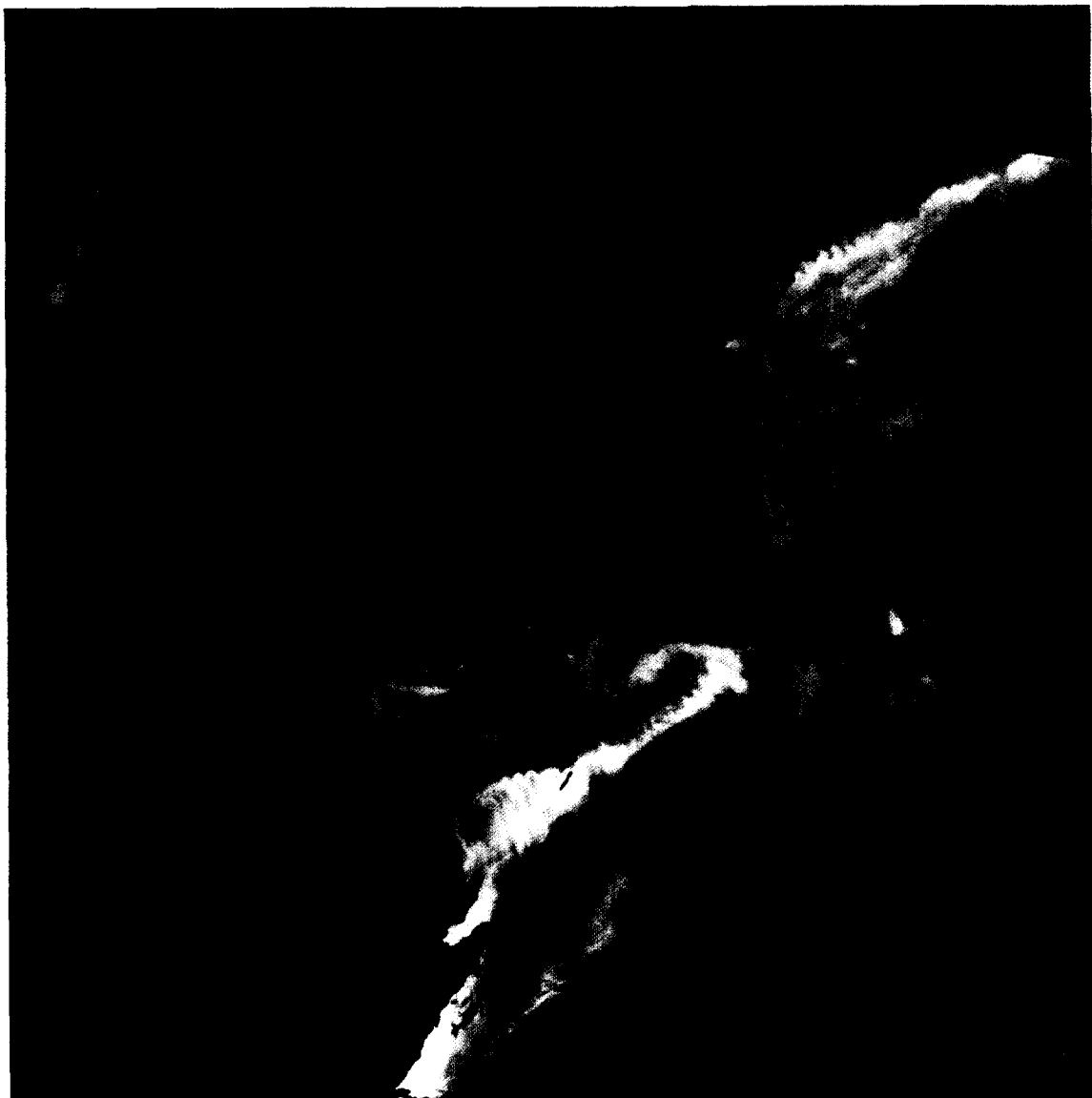
Another notable feature is the steep gradient in optical properties to the west of Denmark. The coastal band of very turbid water (Fig. 19) is somewhat narrower than in the February image (Fig. 15) and shows complex eddy-like structures along the outer boundary. Furthermore, in the colour composite image (Fig. 20), the inshore and offshore waters appear quite distinct, being separated by a narrow zone showing

The CZCS channel 3 image (Fig. 23) indicates weaker reflectance due to suspended material in the eastern North Sea than in March, probably as a result of reduced convective mixing and the initiation of the seasonal thermocline/pycnocline. A distinct plume off Horns Reef related to the local maximum in tidal mixing (Fig. 4) is still visible, but extensive dark areas, indicative of strong absorption of visible light, are the main feature of the image.

16 *April* 1981 (*neaps* + 3) *AVHRR* 18.22 *GMT, CZCS* 11.26 *GMT* (*Figs* 22–25). Compared to the images for March 1982, major differences result from the spring increases of solar warming and illumination causing greater phytoplankton production. Although surface Atlantic water from the northwest and from the English Channel remains relatively warm, the coastal waters of the eastern North Sea and off Norway are now also warm compared to the central North Sea. The higher surface temperature (Fig. 22) in the Norwegian Channel is associated with the development of a shallow pycnocline (SVANSSON, 1975) at the time of the spring snow melt.
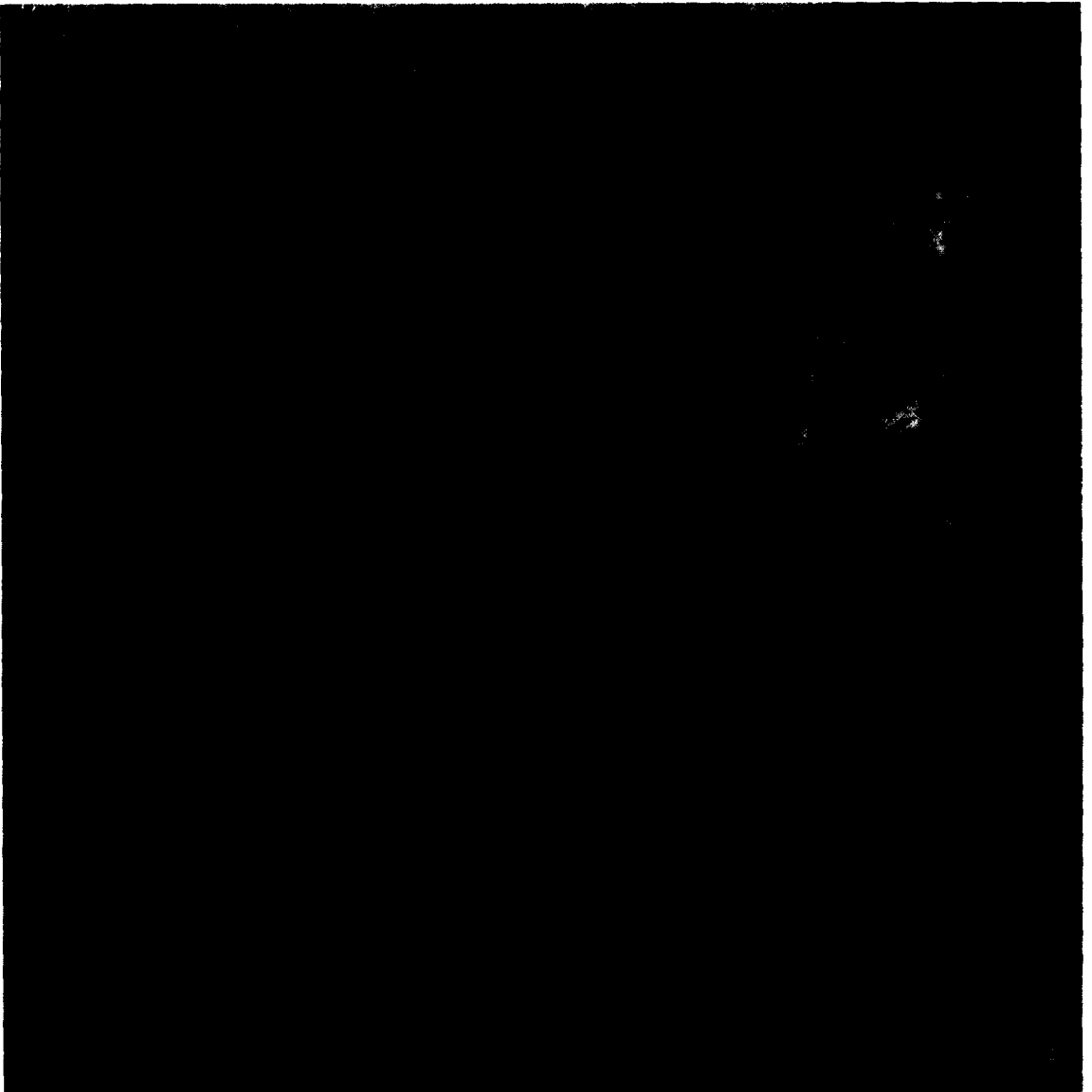
The chlorophyll algorithm (Fig. 25) gives saturated values (>45 mg m^{-3}) over an extensive area to the west of Denmark, extending into the lower salinity waters of the eastern Norwegian channel (Figs 7 and 8). Published values (e.g. RICHARDSON, 1985) indicate that concentrations >10 mg m^{-3} are unlikely at this time of year except in localized patches.

Sharp gradients in the surface chlorophyll levels are also apparent in the northern North Sea, some of which are coincident with temperature boundaries. Such features were well documented in the FLEX experiment in the northern North Sea during 1976 (e.g. STEELE and HENDERSON, 1979; GIESKES and KRAAY, 1980), although the spring bloom in that year occurred about 10 days later (WEICHART, 1980) than shown in these satellite images.

Much variability in the optical properties of surface waters is seen in the colour composite image (Fig. 24), with high sediment content (yellow) close to the coasts of Holland, Germany and Denmark, high chlorophyll and/or DOM (dark shades) in much of the offshore eastern North Sea, Norwegian Channel and northwestern area, and relatively clear water (blue) in the central northern North Sea. The white shades to the east of the cloud edge in the lower half of the image area are caused by a temporary sensitivity drop (backlash) following sensor saturation over clouds (MUELLER, 1988).
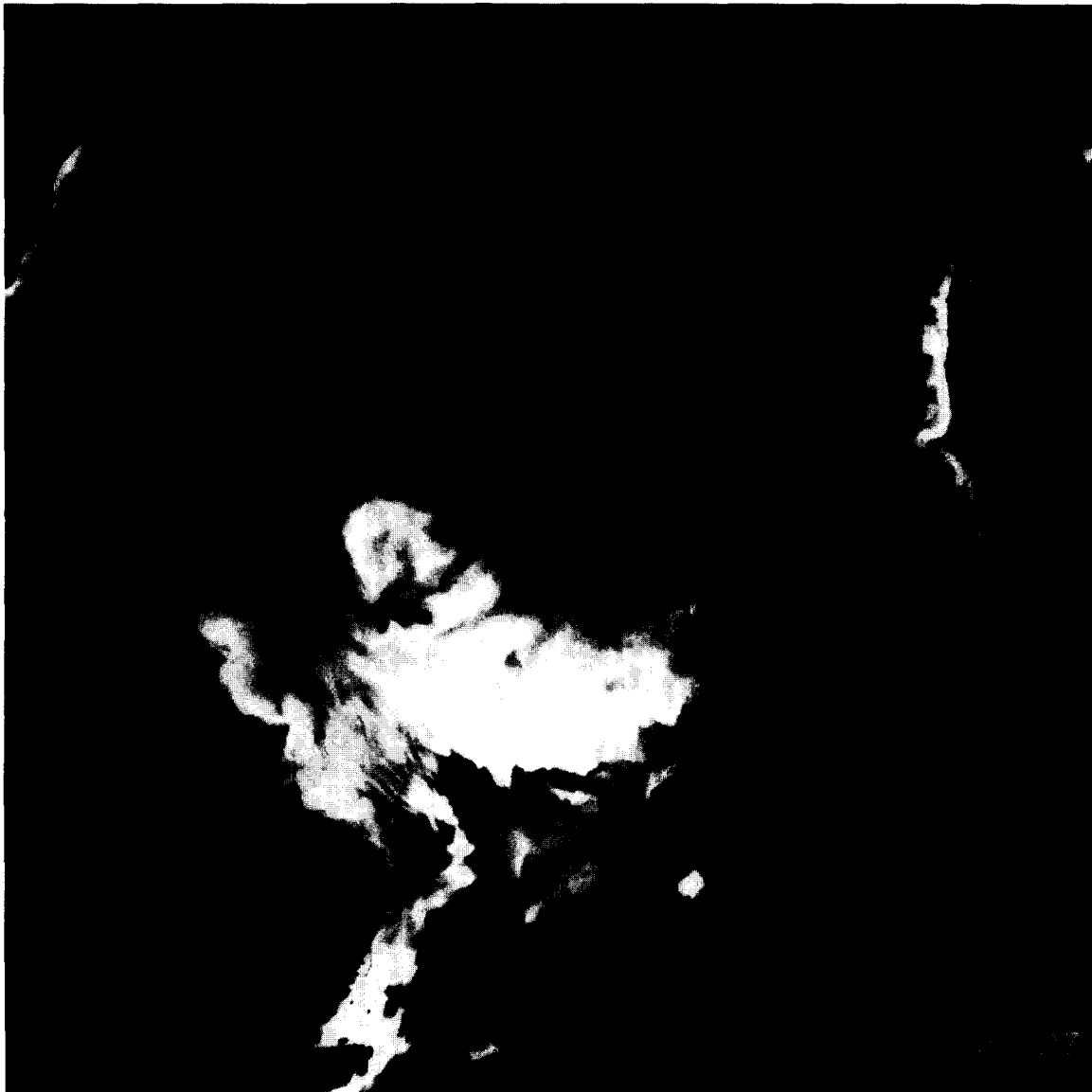
Reflectance due to suspended sediments (Fig. 27) remains strong in the western part of the Southern Bight, over Dogger Bank and along the coastal fringes of Scotland and Denmark. In contrast, parts of the central and eastern Southern Bight appear dark, and both the colour composite (Fig. 28) and chlorophyll (Fig. 29) images indicate that this is due to absorption by relatively high concentrations of phytoplankton chlorophyll and accessory pigments. Much of the variability in optical properties also appears to be related to chlorophyll distributions in the central and northern North Sea. The Norwegian coastal current is an exception, with low reflectance in all three colour bands and only intermediate chlorophyll values. This combination of properties is attributable to lower salinity water containing significant quantities of DOM.

12 *May* 1980 (*springs*–3) *AVHRR* 14.33 *GMT*, *CZCS* 11.14 *GMT* (*Figs* 26–29). By mid-May, the seasonal thermocline has become established over most of the northern and central North Sea. Variations in surface temperature (Fig. 26) are small, with the eastern North Sea somewhat warmer than the central region. The warmest water is seen in the Southern Bight associated with the English Channel inflow and in the plume of the River Rhine, which is characterized by fine-scale structure.
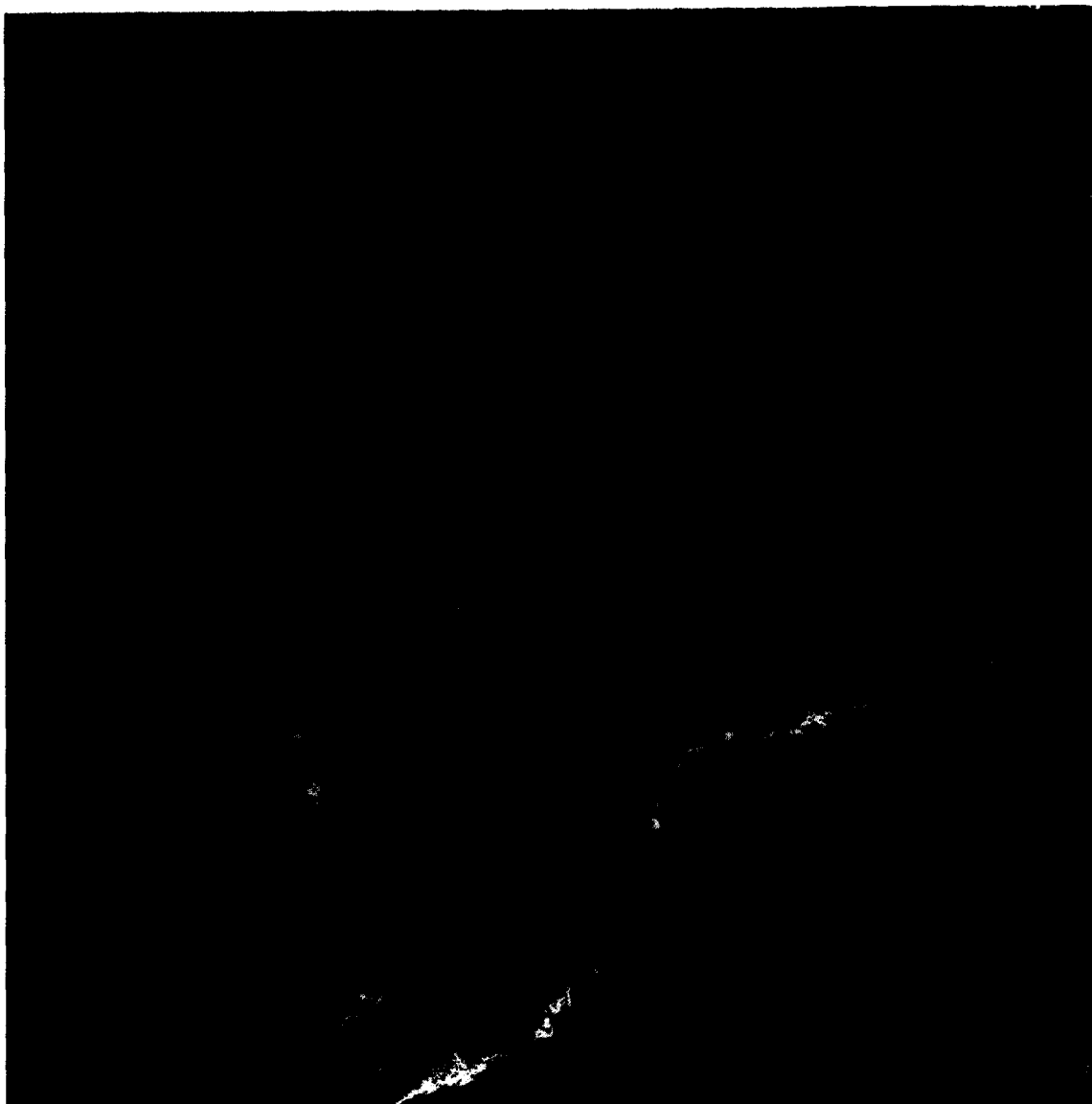
In the Southern Bight and eastern coastal waters, high chlorophyll concentrations persist throughout May (e.g. GIESKES and KRAAY, 1977; VELDHUIS et al., 1986), particularly in association with the annual bloom of Phaeocystis (LANCELOT et al., 1987) which extends along the Dutch and German coasts at this time of year. The very low channel 3 reflectances in these regions may be the result of absorption by the accessory pigments of Phaeocystis.
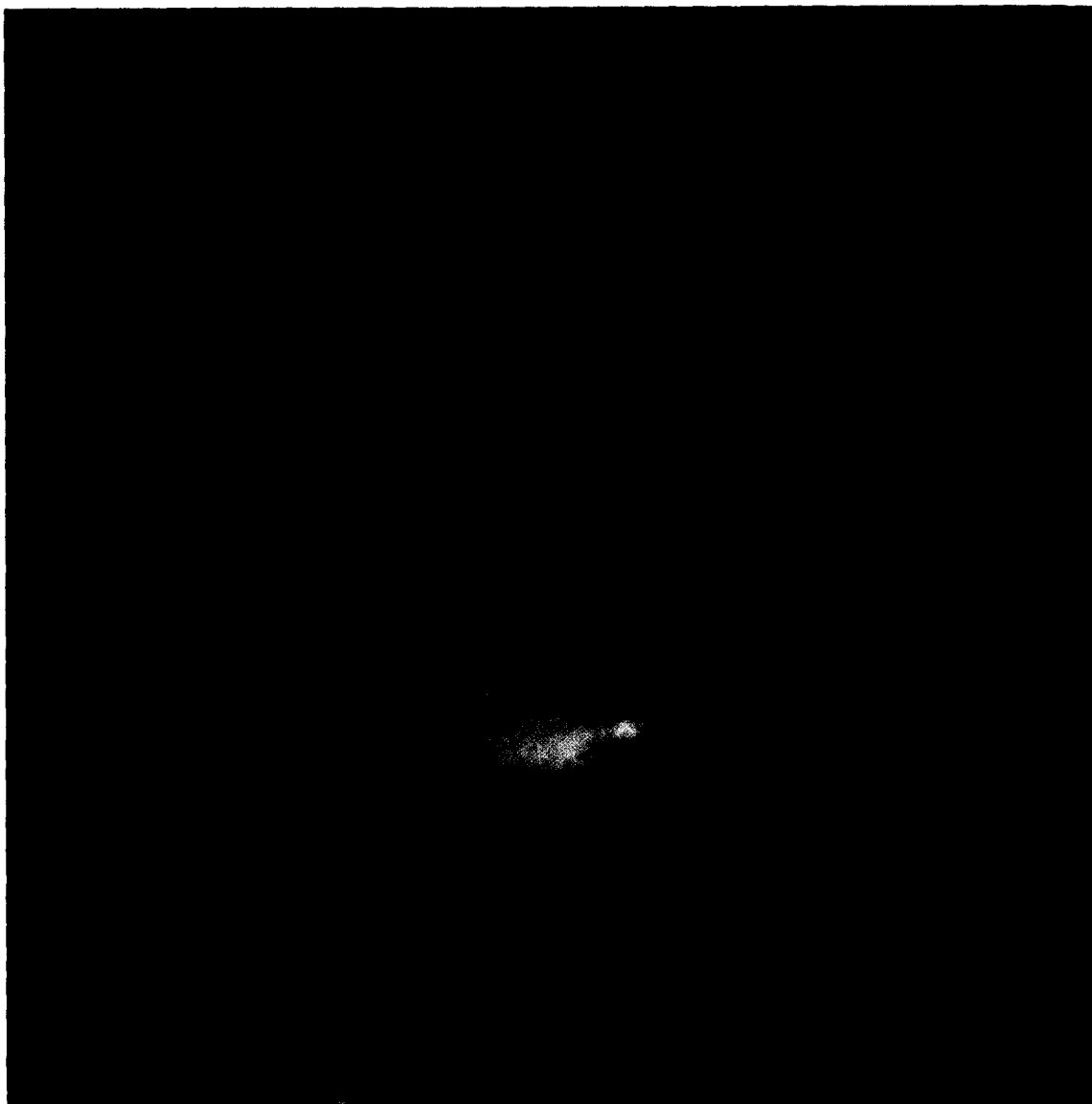
As shown in the image for 16 April 1981 (Fig. 25), the distribution of chlorophyll is very patchy in the central and northern North Sea, although the smaller size of patches and generally lower chlorophyll values suggest that the spring bloom is declining by mid-May. Ship measurements of chlorophyll (e.g. WEICHART, 1980; GIESKES and KRAAY, 1983) confirm that maximum chlorophyll levels are generally reached in late April or early May.

With neap tides, the reflectance due to suspended material in the tidally mixed waters of the Southern Bight is generally low (Fig. 31). In contrast, in the central North Sea and off northeast Scotland extremely bright features are apparent with maximum reflectance values calculated to be 20%. Evaluation of similar features in the Celtic Sea (HOLLIGAN et al., 1983b; GROOM and HOLLIGAN, 1987) and of anomalous conditions of optical backscattering in the northern North Sea (DOERFFER et al., 1984) show the cause to be populations of the coccolithophore, *Emiliania huxleyi*, in which the main backscattering component is probably the detached plates or coccoliths of calcium carbonate (BRICAUD and MOREL, 1986). Such blooms, other examples of which have been illustrated by SINGH et al. (1983) and HOLLIGAN (1987), occur each year in the North Sea (see also Figs 60–63).

Figure 30

15 *June* 1986 (*neaps*–1) *AVHRR* 13.15 *GMT, CZCS* 11.00 *GMT* (*Figs* 30–33). The main features in sea surface temperature (Fig. 30) are a zone of warm water along the coasts of Holland, Germany and southwest Norway, and a diffuse region of relatively high temperatures across the central North Sea between two areas of cloud. The latter is attributed to superficial daytime heating under conditions of low wind stress (SAUNDERS *et al.*, 1982). The temperature gradients associated with tidal fronts across the southern North Sea (see Fig. 4) are relatively weak, except in an area to the northwest of the Dutch coast where a narrow band of cool water probably marks the southern extent of thermal stratification.
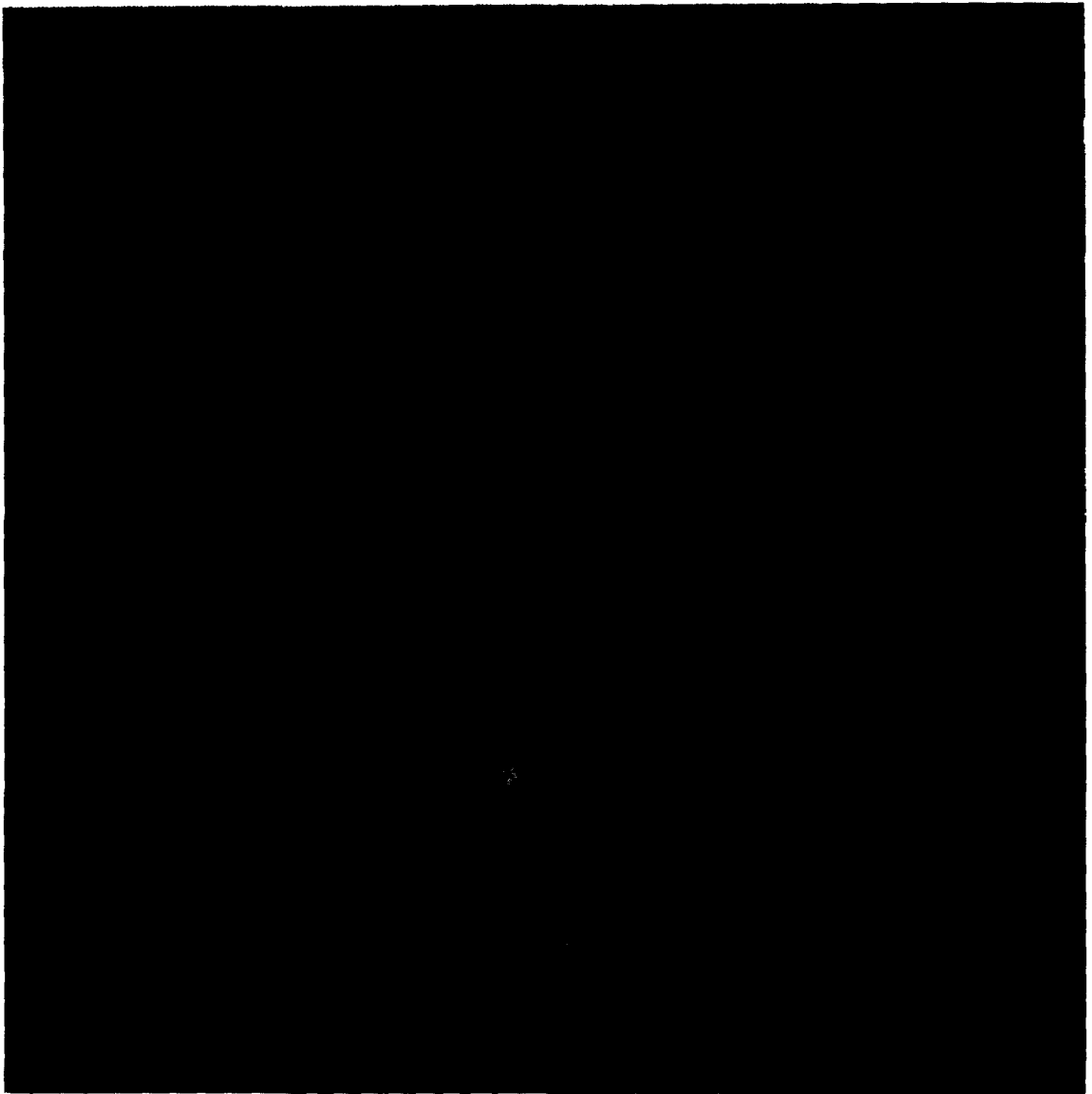
The estimated chlorophyll levels (Fig. 33) are generally low except in the Southern Bight and eastern coastal waters. The dark areas on the colour composite image and the corresponding higher chlorophyll values are evidence for persistent phytoplankton growth in these tidally mixed and turbid coastal waters during mid-summer when conditions of solar irradiance are optimal: this in turn suggests that the availability of nutrients is generally not a limiting factor for primary production in these regions.

In the colour composite image (Fig. 32) the coccolithophores appear white due to saturation, surrounded by blue indicative of low surface chlorophyll levels over much of the central and northern North Sea. The darker shades in the Southern Bight in both the channel 3 and colour composite images are interpreted as due to light absorption by higher pigment concentrations in mid-summer; these tend to mask the reflectance by suspended particulate matter characteristic of the winter months. The Norwegian coastal waters which show minimum surface salinities in summer also appear dark.

Both the channel 3 (Fig. 35) and colour composite (Fig. 36) images show an extensive coccolithophore bloom in the northern North Sea extending as a plume into the southern Skagerrak between the Norwegian Channel and Danish coastal waters. The remainder of the cloud-free area appears relatively dark on the channel 3 image since a high saturation level for reflectance was used in the processing procedure to show the structure within the coccolithophore bloom. A second colour composite (see inset), processed with a lower saturation value for reflectance, shows optical variability for the waters of the central and southern North Sea in greater detail, although the detail within the bloom is lost. Some increase in reflectance, possibly due to suspended matter, is apparent south of Dogger Bank and there are spectral shifts from blue shades in the central North Sea to yellow/brown shades along the coasts of Denmark and Norway.

6 *July* 1983 (*neaps* + 2) *AVHRR* 13.10 *GMT*, *CZCS* 10.18 *GMT* (*Figs* 34–37). The southern North Sea is masked by cloud in these images. The highest surface temperatures (Fig. 34) are seen in the shallow waters west of Denmark and in the Skagerrak, with a broad area of relatively warm water extending west from the Norwegian Channel towards the central North Sea. The tidal front east of Aberdeen is barely discernible.
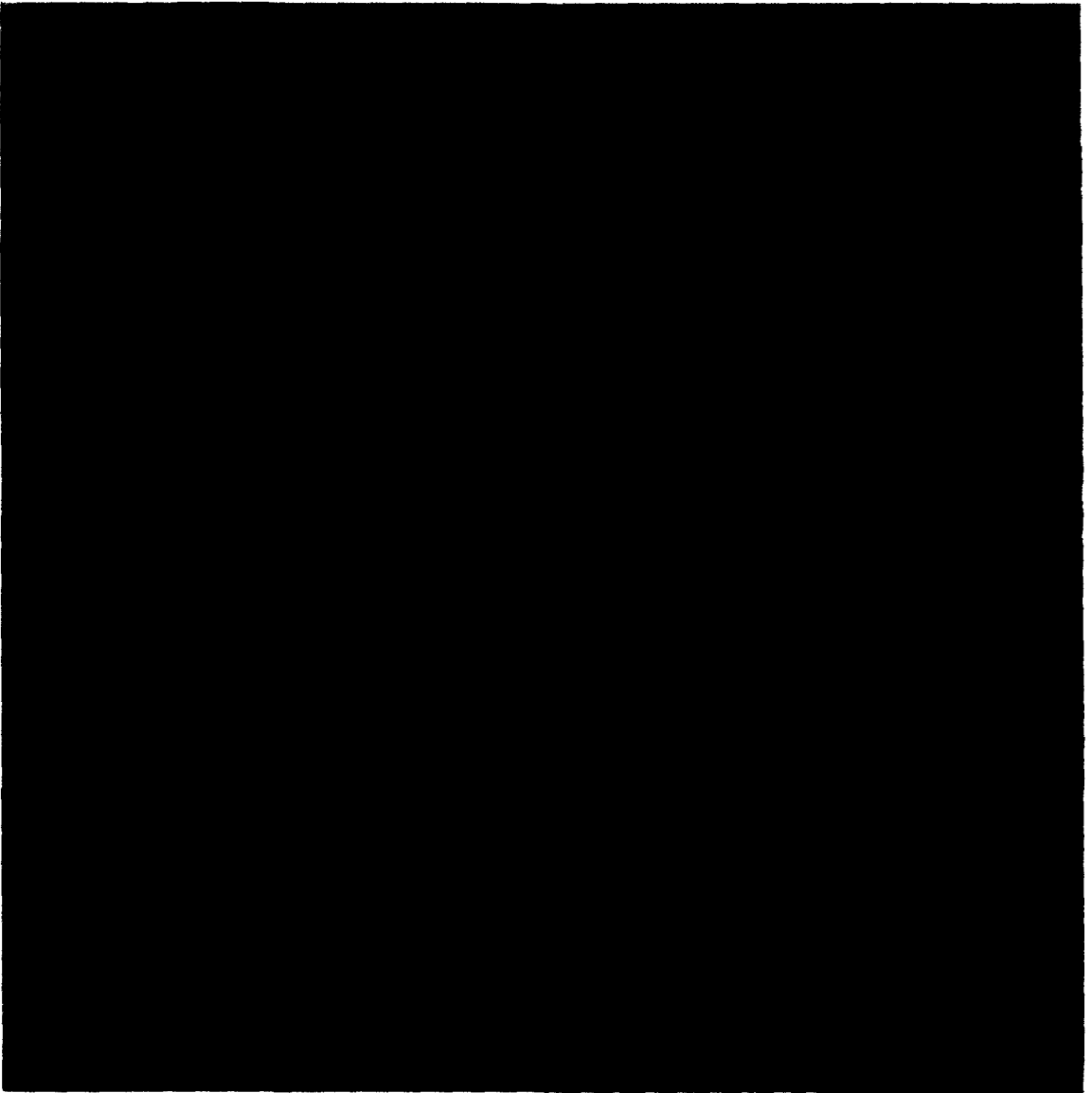
east of the Orkney Islands (Fig. 4). Only part of the coccolithophore bloom along the western edge of the Norwegian Channel appears as a region of elevated chlorophyll concentration. The very sharp gradient in coccolith abundance between the North Sea and Norwegian Channel suggests that mixing of surface waters across this boundary is restricted, perhaps due to density gradients associated with changes in salinity (see Fig. 8).

There is a correspondence between higher surface temperatures and the presence of coccolithophores in the northeastern North Sea, but this relationship with temperature does not hold for the area of coccolithophores further to the west.
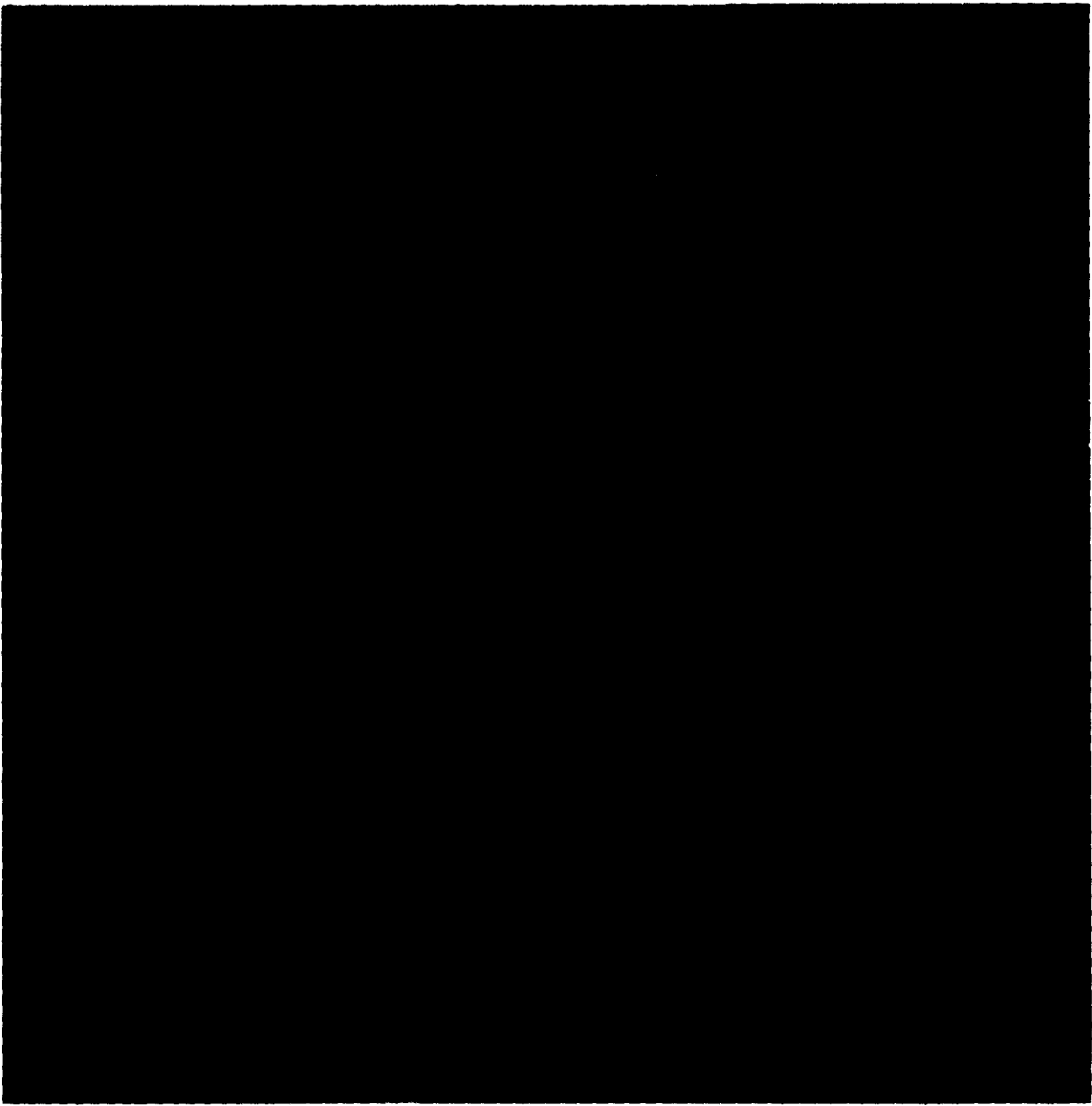
Levels of surface chlorophyll (Fig. 37) are generally low, especially in the central North Sea where estimated values are <0.5 mg m^{-3} over a wide area. Higher values are seen in coastal waters and in the northwest of the image in association with the tidal front
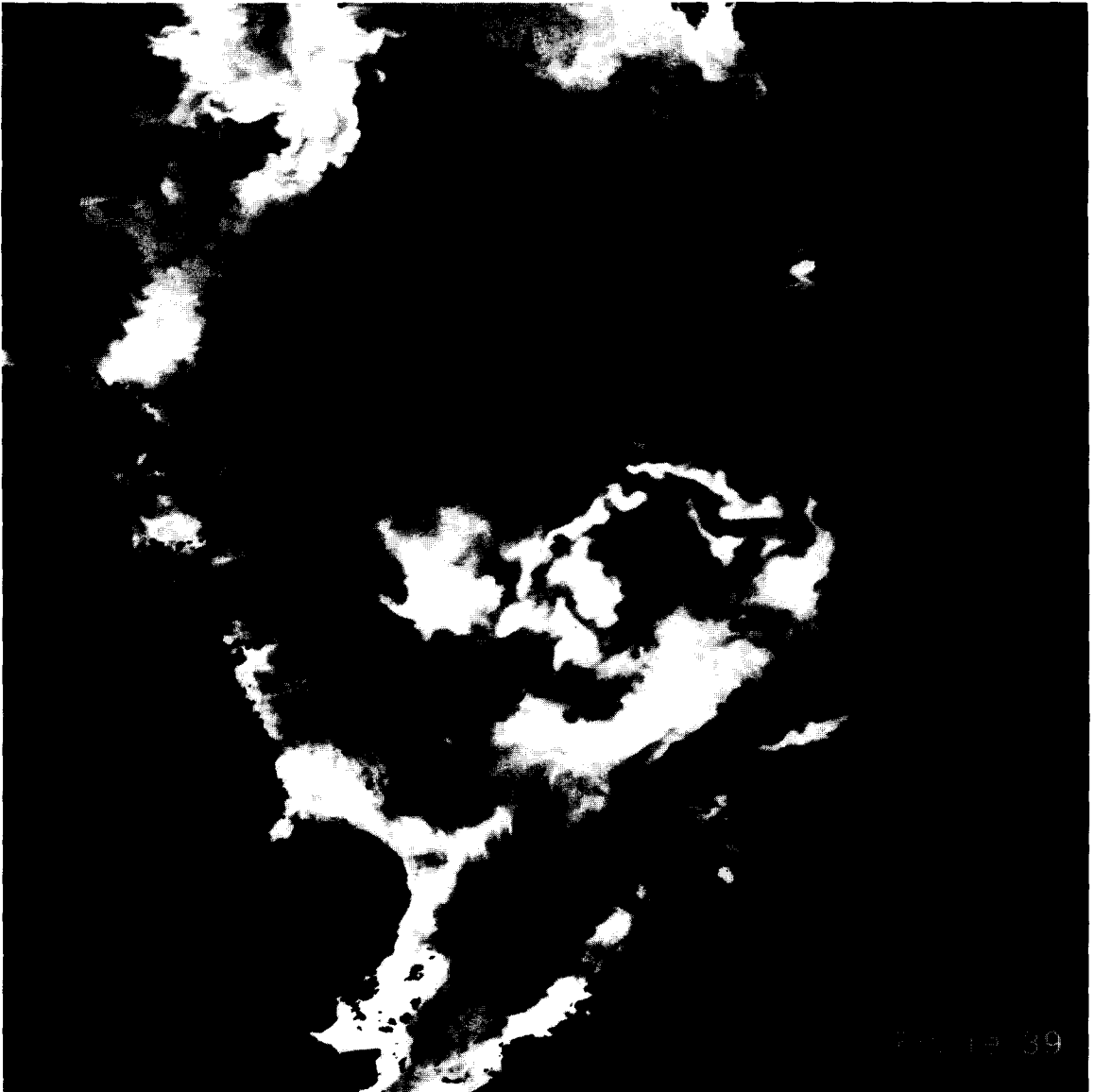
Areas of high reflectance in the channel 3 image (Fig. 39) are interpreted, on the basis of spectral shifts in the colour composite image (Fig. 40), as a combination of coccolitho-phores (white to blue shades) in the northern and central North Sea and of suspended matter (white to yellow shades) in the Southern Bight. The cause of the somewhat diffuse patches of reflectance over Dogger Bank and to the northwest of the Dutch coast is uncertain. The yellowish, as opposed to bluish, colours are suggestive of suspended sediments although resuspension due to vertical mixing is likely to have been relatively weak at neap tides.

24 *July* 1980 (*neaps* + 2) *AVHRR* 14.13 *GMT*, *CZCS* 11.34 *GMT* (*Figs* 38–41). The warmest surface water (Fig. 38) is seen again in the eastern and northern North Sea (see Fig. 6), with relatively sharp thermal fronts extending along the western margin of the Norwegian Channel and from the southern Skagerrak into the central North Sea.

the colour composite. The estimated chlorophyll values for coccolithophore waters range from >3 mg m^{-3} east of Scotland to <0.5 mg m^{-3} in the central North Sea. In mid-summer a well-defined sub-surface chlorophyll maximum is characteristic of the thermally stratified waters of the central and northern North Sea (e.g. GIESKES and KRAAY, 1984) typically at a depth of 25 m which is at or below the vertical detection limit of the CZCS sensors (one attenuation length) even for clear, chlorophyll-poor waters.

The levels of surface chlorophyll (Fig. 41) are higher generally than on the image for 6 July 1983. Areas of elevated chlorophyll concentration, corresponding to dark regions on the colour composite image, extend well offshore along the Dutch coast in association with the outflow of the River Rhine, and along the east coasts of Scotland and England; note the presence of cirrus clouds in the Southern Bight which appear as dark patches in
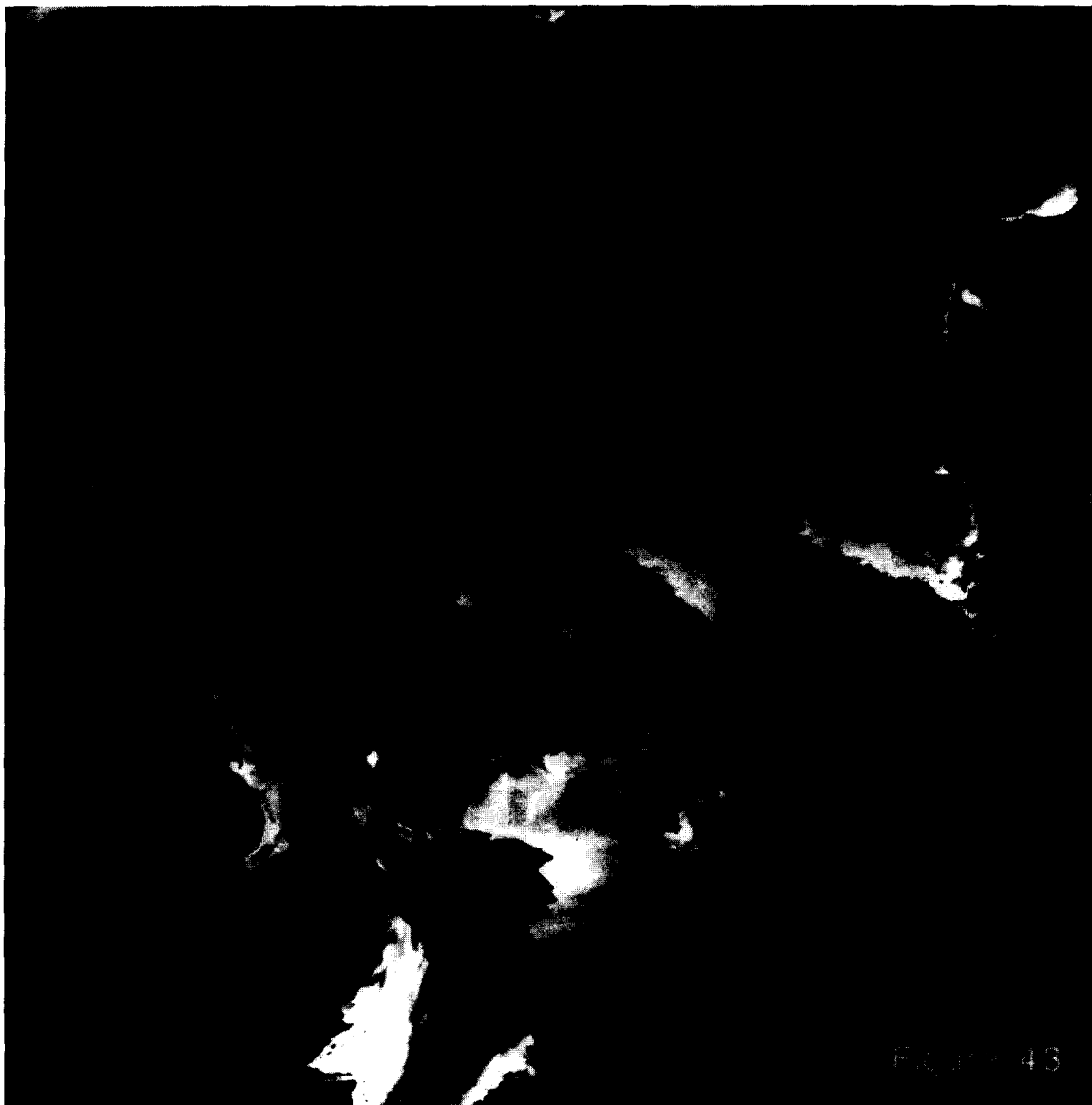
The reflectance in channel 3 (Fig. 43) is weak except for the River Thames estuary where high levels of suspended material are apparent. In the colour composite image (Fig. 44) the main part of the North Sea appears uniformly blue, with spectral variations in reflectance only in the Southern Bight and immediate coastal waters especially off Holland and Denmark. There is no evidence for the presence of coccolithophores. The Norwegian coastal waters are uniformly dark, presumably indicative of the absorption of blue light by DOM.

20 *August* 1984 (*neaps*−2) *AVHRR* 14.37 *GMT, CZCS* 11.10 *GMT* (*Figs* 42–45). The main features of the thermal image (Fig. 42), apart from a broad area of daytime superficial heating in the central North Sea, are the tidal fronts between warm stratified water and cold mixed water off Aberdeen and east of Flamborough Head. A plume of cold water extends offshore from Horns Reef, and relatively warm water is seen within the westward-flowing Norwegian coastal current. The northeastern North Sea appears generally cooler than waters to the west and south, in marked contrast to the surface temperature distributions on the July images.
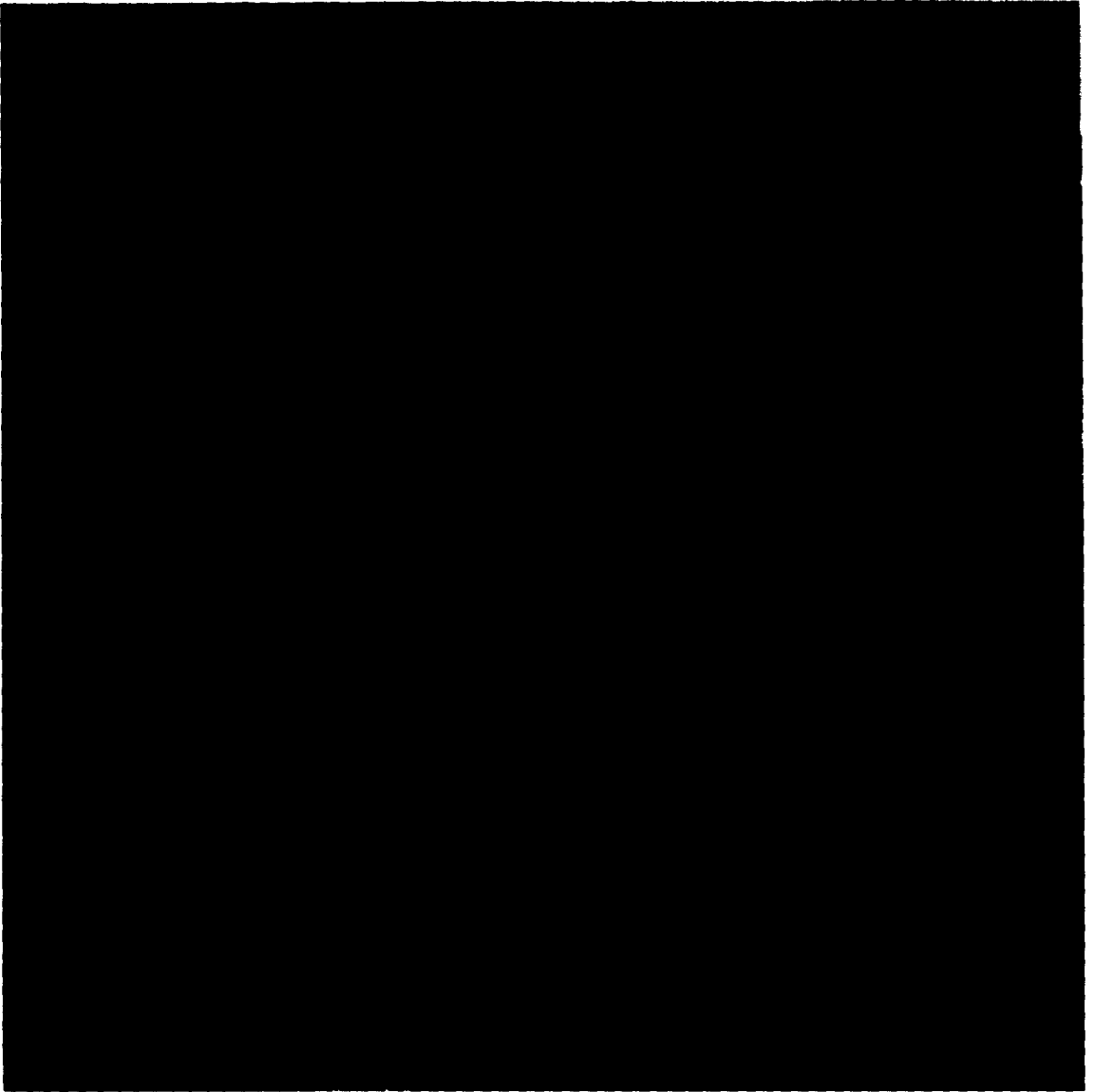
channel 3 and colour composite images). The image for 24 August 1984 (Fig. 83), shows no obvious feature in the surface chlorophyll distribution off the Danish coast. Low chlorophyll levels over much of the central and northern North Sea are typical of CZCS scenes for the period between early July and early September.

The highest levels of chlorophyll (Fig. 45) are shown for the southeastern North Sea. High chlorophyll patches to the east of clouds are erroneous and caused by detector backlash after saturation over cloud (note the light areas to the right of the clouds in the
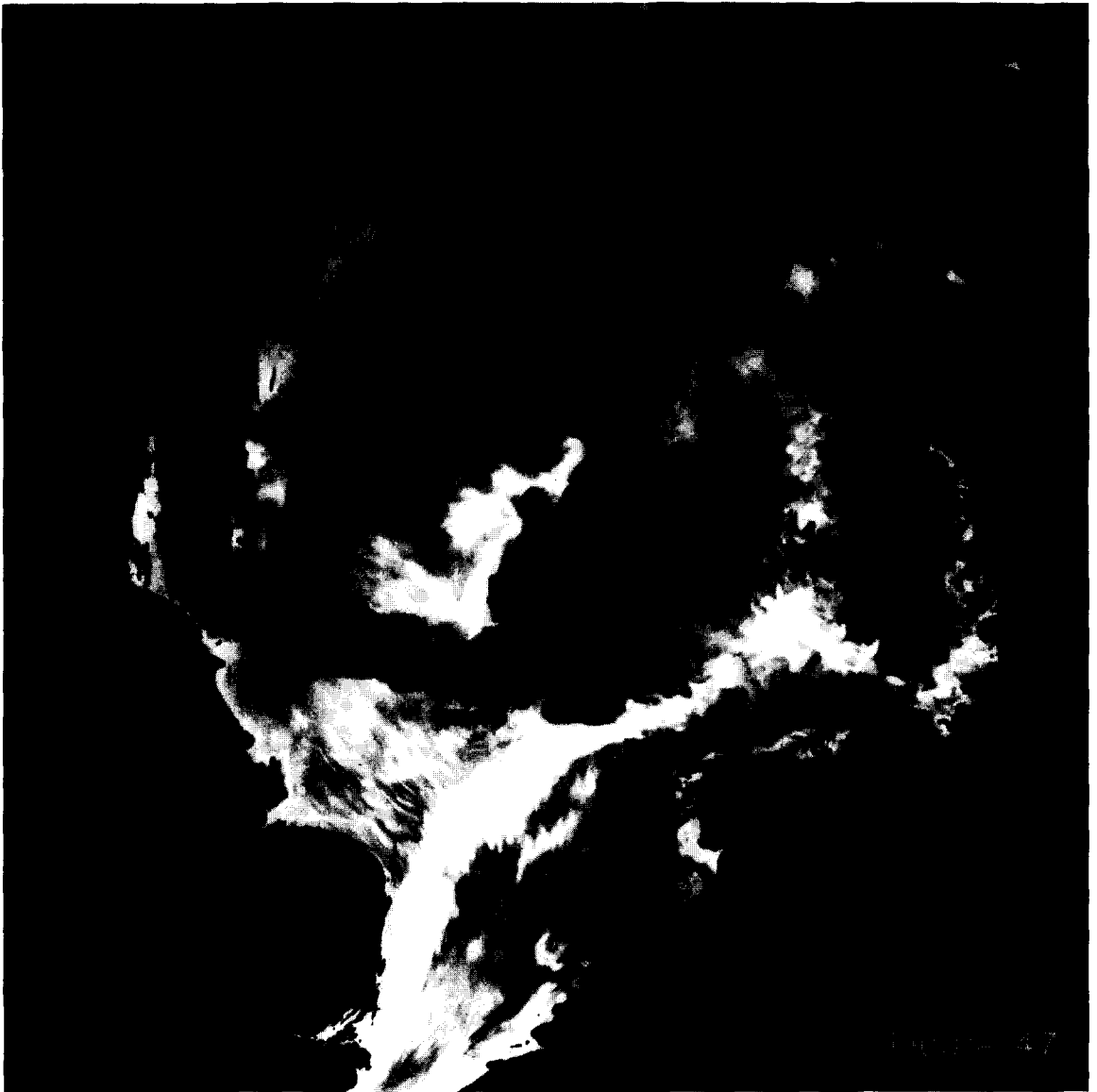
The channel 3 image (Fig. 47) shows relatively high reflectance across most of the Southern Bight at a period of spring tides and as thermal stratification begins to break down. Particularly bright features are seen over Dogger Bank and in a band extending northeast from the coast of eastern England and then north to the west of Denmark.

6 *September* 1979 (*springs*–1) *AVHRR* 14.43 *GMT*, *CZCS* 11.46 *GMT* (*Figs* 46–49).
The thermal image (Fig. 46) shows warm surface water extending through the English
Channel into the Southern Bight and eastern North Sea, and the edge of relatively warm
water in the Norwegian Channel. By contrast, the coolest temperatures appear along the
east coast of England south of the Flamborough Head tidal front.
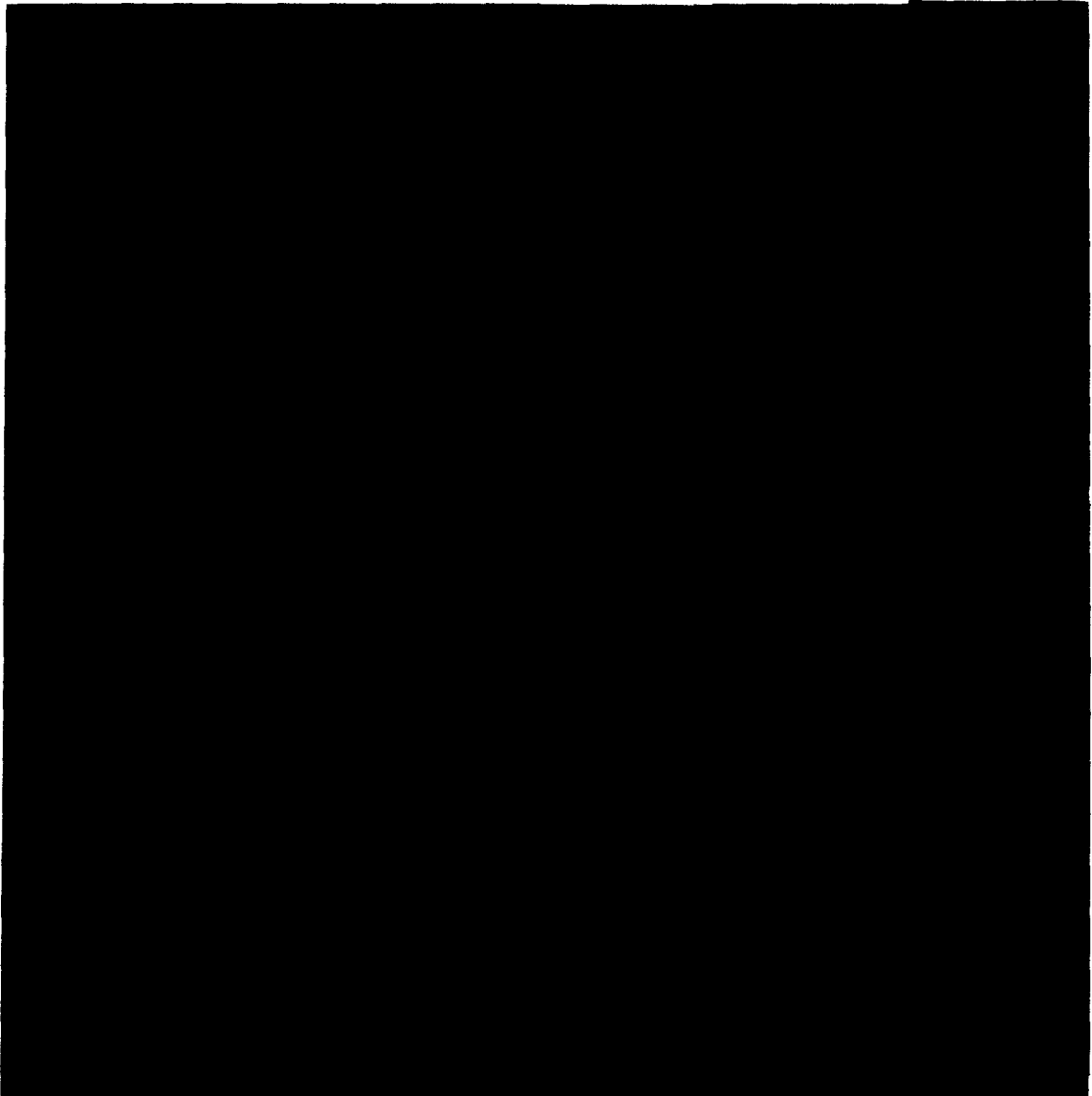
The chlorophyll image (Fig. 49) indicates low chlorophyll concentrations over most of the scene, with higher values confined to coastal waters and to areas of high reflectance. The analysis by FISCHER and DOERFFER (1987), using an inverse technique to distinguish pigments from sediments and dissolved material, gives chlorophyll levels up to 10 mg m^{-3}, and for the northwestern North Sea, RICHARDSON et al. (1986) observed levels up to 4 mg m^{-3} in 1984.

In the colour composite (Fig. 48) the higher reflectances over the Dogger Bank appear bluish-white and superficially resemble the coccolithophore signatures of the summer period.

The channel 3 image (Fig. 51) is similar to that for 6 September 1979 (except that the Dogger Bank does not show as an area of high reflectance) and also to those for the winter months (e.g. Figs 15 and 19).

24 *October* 1985 (*neaps* + 2) *AVHRR* 13.01 *GMT*, *CZCS* 10.42 *GMT* (*Figs* 50–53). Relatively warm water in the southeastern North Sea is the dominant feature of the thermal image (Fig. 50). Relatively cool water extends from the north along the western boundary of the Norwegian Channel giving rise to complex patterns of surface temperature in the western Skagerrak.
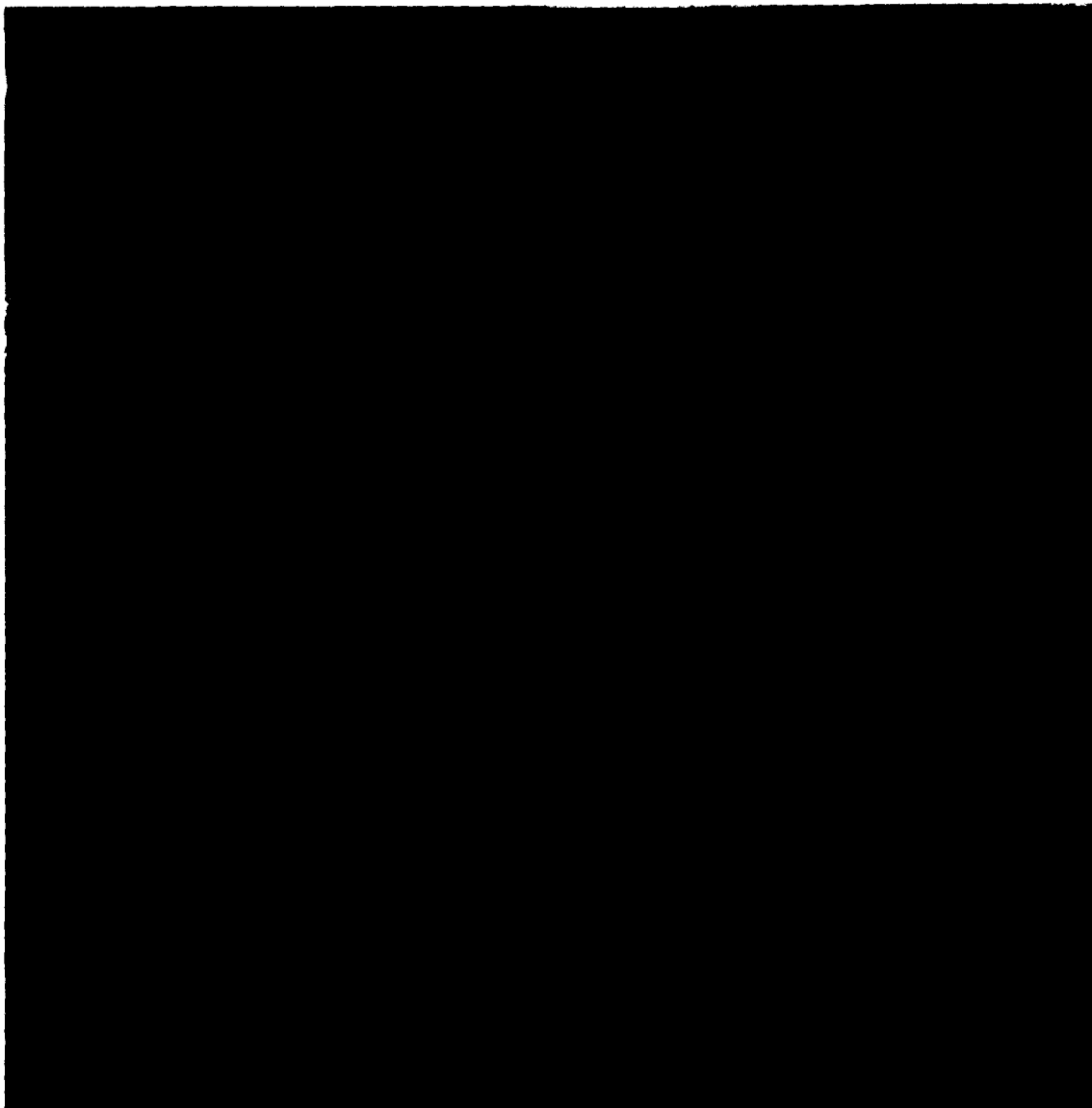
The main part of the central North Sea has a very grainy appearance in both the colour composite and chlorophyll (Fig. 53) images with no obvious structure related to topographic or hydrographic conditions. The reasons for this are unknown. By late October the sun is low in the sky so that low solar illumination at the sea surface may present problems for the standard algorithms.

At intermediate distances (10–30 km) from the coasts of Holland and Germany the water appears dark in both the channel 3 and colour composite (Fig. 52) images, indicative of higher chlorophyll levels than in surrounding waters.

4.2. *Comparisons between CZCS imagery and ship observations*

In this and subsequent sections the satellite pass time (overhead at Dundee), geographical range and, where appropriate, reflectance saturation (%) are given for each date.

Southern Bight, May 1986:
 Colour composite images, 50.5° to 54.5°N, 0.0° to 6.5°E, for:
  4 May (10.20 GMT, 3.75%) Fig. 54,
  13 May (11.20 GMT, 3.75%) Fig. 55.
 Chlorophyll image overlaid with chlorophyll measurements and ship track for 7–13
  May, 50.5° to 54.5°N, 0.5° to 7.0°E, for:
  13 May (11.20 GMT) Fig. 56.

East Central North Sea, 1984 and 1985, 53.5° to 56.9°N, 4.5° to 10.5°E:
 Chlorophyll image overlaid with chlorophyll measurements for:
 24 August 1984 (10.39 GMT) Fig. 57.
 Diffuse attenuation coefficient image overlaid with Secchi disc measurements for:
  24 August 1984 (10.39 GMT) Fig. 58.
 Chlorophyll image overlaid with chlorophyll measurements for:
 24 October 1985 (10.42 GMT) Fig. 59.

The evaluation of CZCS imagery of the North Sea is limited severely by the lack of contemporary optical data over appropriate time and space scales. Few detailed optical studies have been undertaken (e.g. HØJERSLEV, 1982), and to the best of our knowledge, there is no extensive set of chlorophyll measurements that matches up to a clear CZCS image of the North Sea. In this section, three examples of CZCS scenes are presented, for which some information from ships on the distributions of chlorophyll and Secchi disc values are available. A fourth example, based upon data for the Skagerrak, has been discussed by AARUP *et al.* (1987, 1989): the satellite-derived chlorophyll values were generally higher than the *in situ* measurements, but the combination of low surface salinities (high DOM) in the Baltic outflow and of suspended sediments along the Danish coast will affect the accuracy of the chlorophyll algorithm.
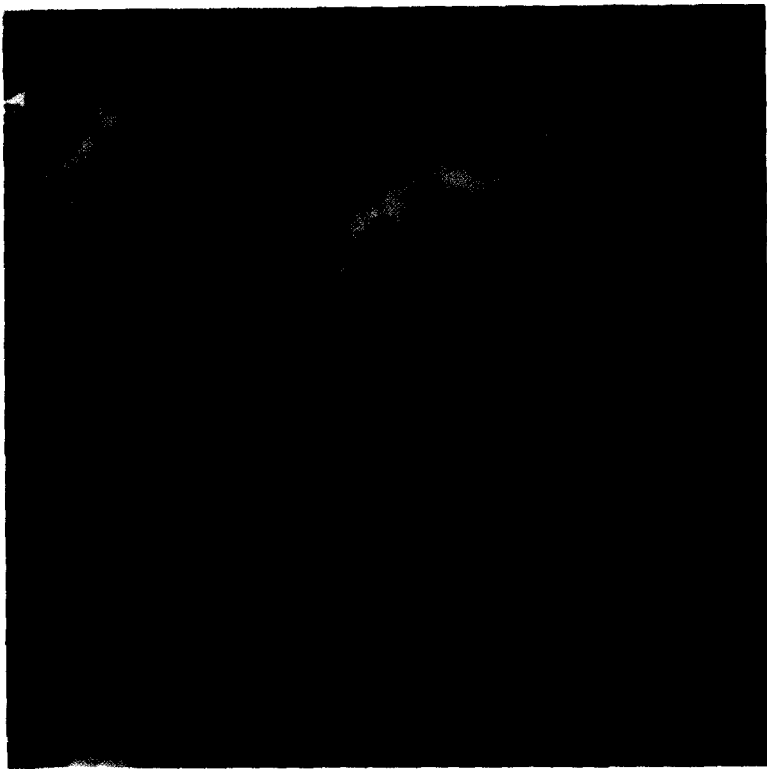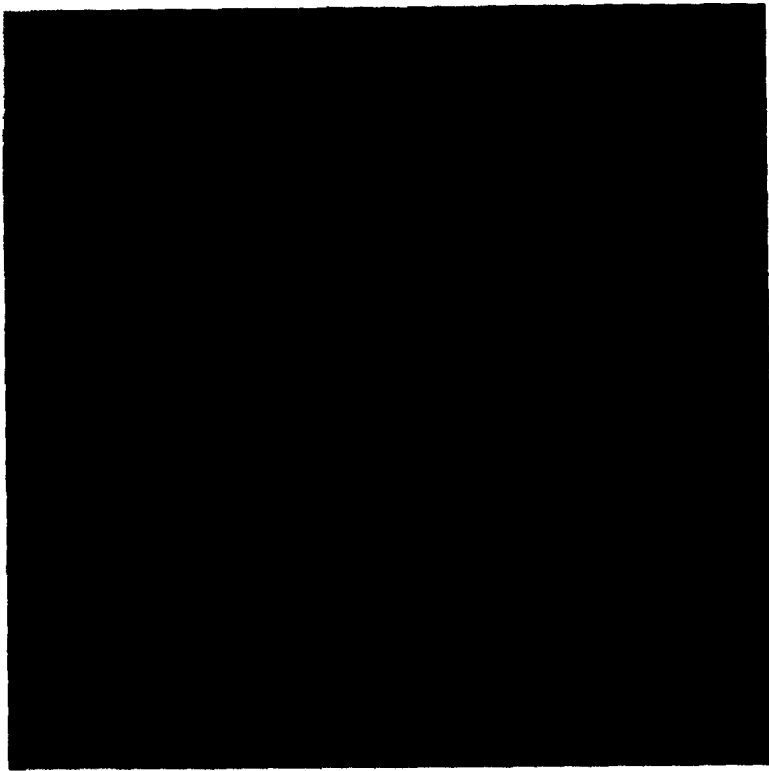
Southern Bight, May 1986 (*Figs* 54–56). In a study of the annual bloom of the colonial flagellate, *Phaeocystis pouchetii*, along the coast of Holland (P. M. HOLLIGAN, unpublished data) in May 1986, strong offshore gradients in surface chlorophyll were observed north of the River Rhine estuary as in previous years (GIESKES and KRAAY, 1977; VELDHUIS *et al.*, 1986). Colour composite images for 4 May (10.20 GMT) (Fig. 54) and 13 May 1986 (11.20 GMT) (Fig. 55) show the bloom as dark areas (strong absorbance of light by chlorophyll and accessory pigments) which are in strong contrast to adjacent light areas where backscattering by suspended material dominates the optical signal. Over the 9 day period which includes spring tides on 9 May, the effects of advection towards the northeast (~4 km d^{-1}) are clearly seen. At the same time, the main part of the *Phaeocystis* population in the Rhine plume becomes more tightly constrained against the coast of Holland, with the outer (western) boundary appearing as a pattern of fringes or finger-like projections.

The chlorophyll image for 13 May (Fig. 56) shows saturation of the algorithm (>45 mg m^{-3} chlorophyll a) in the most dense part of the bloom, where measured concentrations were as high as 50 mg m^{-3}. The secondary patch of chlorophyll to the west was also composed of *Phaeocystis*. The correlation between ship and satellite for the general distributional pattern of chlorophyll was surprisingly good for these Case 2 waters, perhaps due to the dominance of the optical properties by the high levels of chlorophyll. This suggests that instruments such as the CZCS have the potential to provide useful data on trends in phytoplankton abundance (e.g. CADEE and HEGEMAN, 1986) that are the
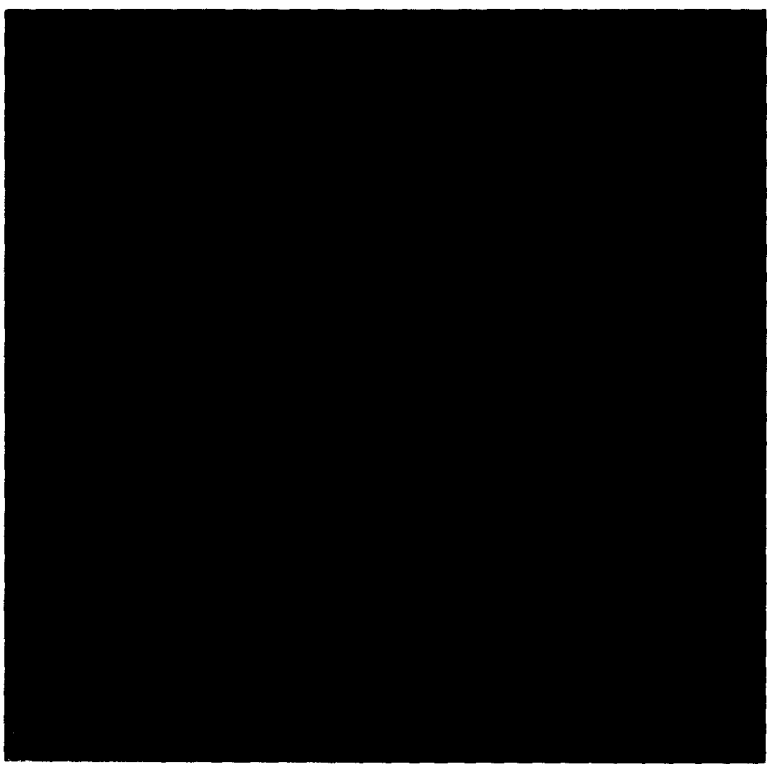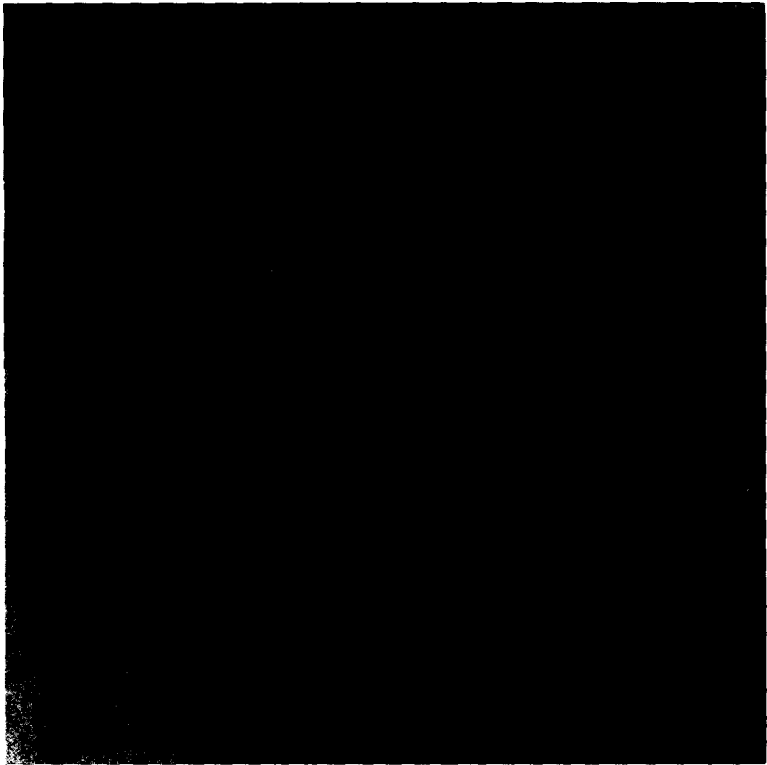
result of increasing eutrophication in the Southern and German Bights (POSTMA, 1985; RADACH and BERG, 1986).

East Central North Sea 1984 *and* 1985 (*Figs* 57–59). Measurements of surface chlorophyll and Secchi disc values made on two cruises (20–30 August 1984 and 22–31 October 1985) are compared qualitatively to satellite images of chlorophyll and diffuse attenuation for 24 August 1984 (10.39 GMT) (Figs 57 and 58) and of chlorophyll for 24 October 1985 (10.42 GMT) (Fig. 59), respectively. In the first case, the offshore extent of the chlorophyll patch in the frontal region to the southeast of Horns Reef corresponds closely to the gradient of chlorophyll seen on the CZCS image, but the maximum levels within the patch are not well described by the satellite. The autumn data show the highest levels of chlorophyll inshore with relatively good agreement between the ship and satellite values, particularly off Horns Reef. Offshore the surface abundance of phytoplankton is greater than in the summer; both methods give chlorophyll values of ~2 mg m^{-3}.
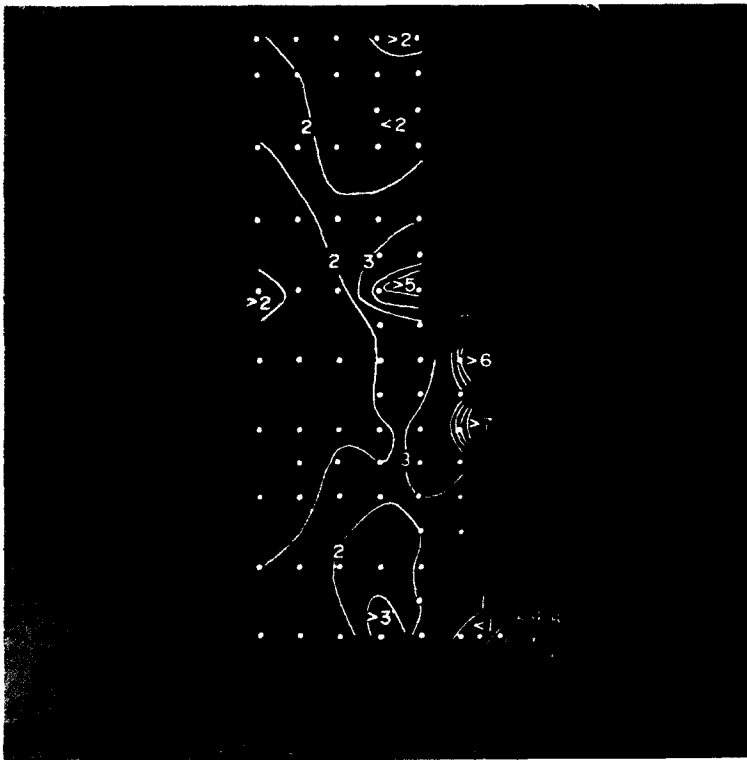
4.3. *Annual coccolithophore blooms* (*Figs* 60–63)

CZCS colour composite images for:
  12 July 1979 (54.0° to 61.0°N, 4.0°W to 9.0°E, 10.38 GMT, 9%) Fig. 60;
  2 July 1981 (54.0° to 61.0°N, 3.0°W to 10.0°E, 11.06 GMT, 6%) Fig. 61;
  12 July 1982 (54.0° to 61.0°N, 4.0°W to 9.0°E, 10.57 GMT, 9%) Fig. 62;
  3 August 1982 (54.0° to 61.0°N, 3.0°W to 10.0°E, 10.48 GMT, 6%) Fig. 63.

Satellite visible band images have shown that coccolithophore blooms are a regular feature of the North Sea each summer (late May to August) (see Figs 32, 36 and 40 for the years 1980, 1983 and 1986). Extensive populations were also seen in 1979, 1981 and 1982, but not in 1985 when very few CZCS images of the North Sea were received. The coccolithophore blooms are characterized by their large extent, their persistence for 3–6 weeks when they tend to act as a passive tracer of water movement, and their variable distribution from year to year. From plankton records it is almost certain that only one species, *Emiliania huxleyi*, is abundant in the North Sea, but remarkably little is known about the hydrographic factors that determine the distribution of this organism or the rate at which it sheds coccoliths.

The presence of *E. huxleyi* has been related to the inflow of Atlantic water into the North Sea (DOERFFER *et al.*, 1984) and some of the most extensive populations appear to the northeast of the Scottish mainland. The species also occurs regularly in Norwegian coastal waters with salinities <30 as well as in the central North Sea away from direct oceanic influence. Although Atlantic waters may be an important source for *E. huxleyi* each spring, factors other than salinity are likely to be important in controlling the growth of summer populations.

Within coccolithophore blooms, maximum underwater reflectance values are typically 20–25% for CZCS channel 3 (GROOM and HOLLIGAN, 1987), corresponding to a surface coccolith density of the order of 10^5 ml^{-1} (HOLLIGAN *et al.*, 1983b). Considerable variations are seen in the spectral composition of the reflectance signature, especially around the margins of the patches; these are attributable to variable ratios of coccolith backscattering, chlorophyll absorption, and absorption by water and dissolved constituents (BRICAUD and MOREL, 1986). The characteristic trend in time from greenish to bluish shades is considered to be related to the decrease in the ratio of cells to coccoliths as the populations age (GROOM and HOLLIGAN, 1987).
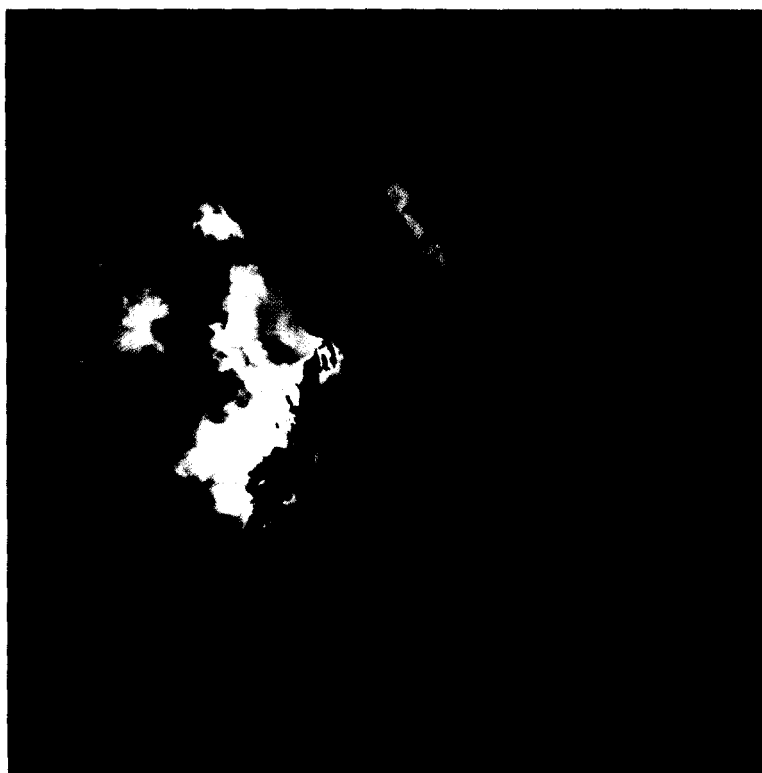
4.4. *Development of the spring phytoplankton bloom in* 1980

The best time series of clear CZCS scenes for the North Sea was received between late April and mid-May 1980. Two sets of images are presented here, for the east central North Sea (west of Denmark) and for the northwestern North Sea; these illustrate certain dynamic features during the period of the spring phytoplankton outburst. The appearance of the whole North Sea on 12 May 1980 has been described in an earlier section (Figs 26–29).

Danish coastal waters:
   CZCS chlorophyll images, 53.5° to 58.3°N, 3.7° to 12.3°E, for:
        23 April (10.28 GMT) Fig. 64;
        2 May (09.49 GMT) Fig. 65;
        5 May (10.45 GMT) Fig. 66;
        12 May (11.14 GMT) Fig. 67;
        13 May (09.50 GMT) Fig. 68;
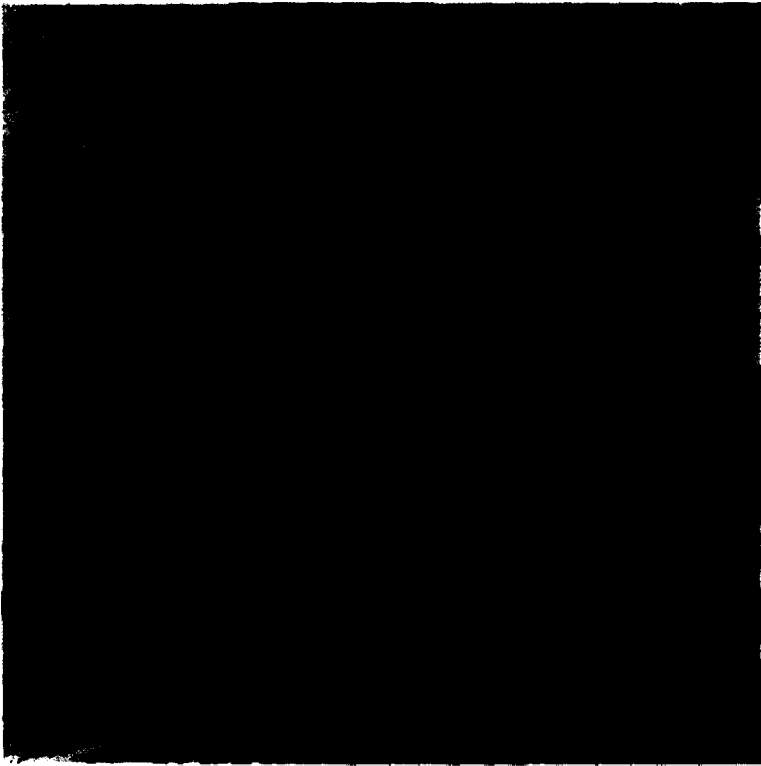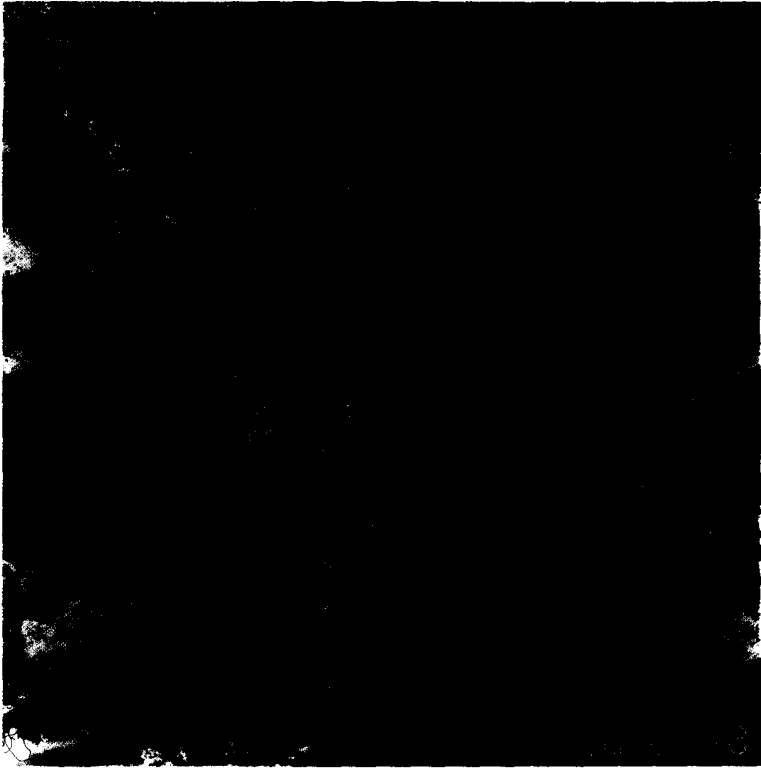   17 May (11.04 GMT): Fig. 69.

From 23 April to 17 May high levels of chlorophyll persisted to the west of Denmark, as well as along the coast of east Holland, in the German Bight, and in the Kattegat.

Although there are many chlorophyll measurements for this time of year (e.g. RICHARDSON *et al.*, 1985) to substantiate the development of diatom and *Phaeocystis* blooms, the spatial and temporal extent of such blooms has not been described in any detail from ship observations. These CZCS images show persistent phytoplankton populations to the west and north of Horns Reef, although the hydrographic conditions determining their distribution are not well documented.

Comparison of the scenes for 12, 13 and 17 May (Figs 67, 68 and 69) illustrate the rapidity with which changes in the surface structure can occur, presumably as a result of a combination of physical and biological forcing factors. Features with linear dimensions of 20 km or more appear and disappear, whereas others, such as the plume extending off Horns Reef, are remarkably persistent. The interpretation of such images, in terms of biological production rates, is a considerable challenge for the future.
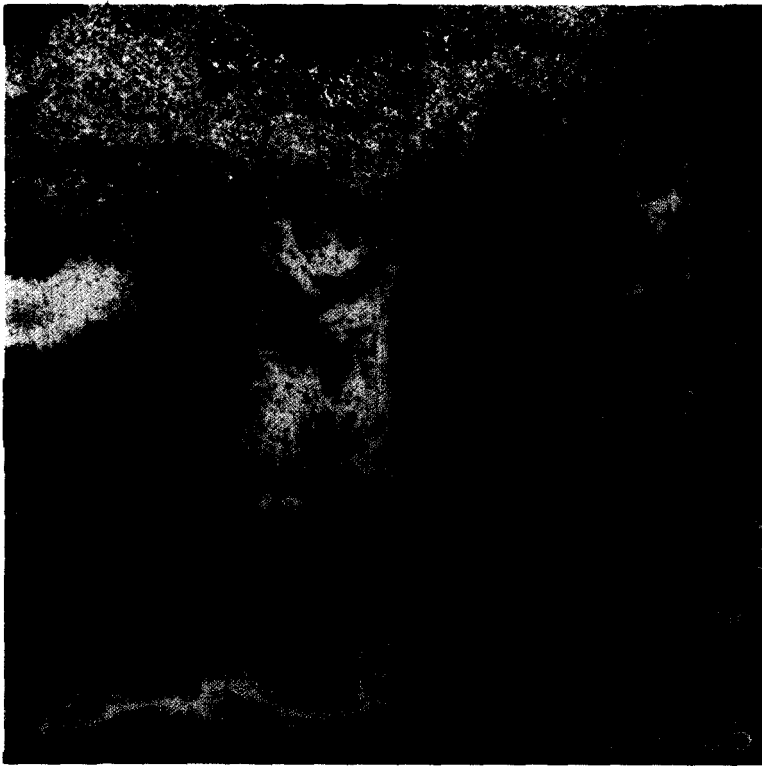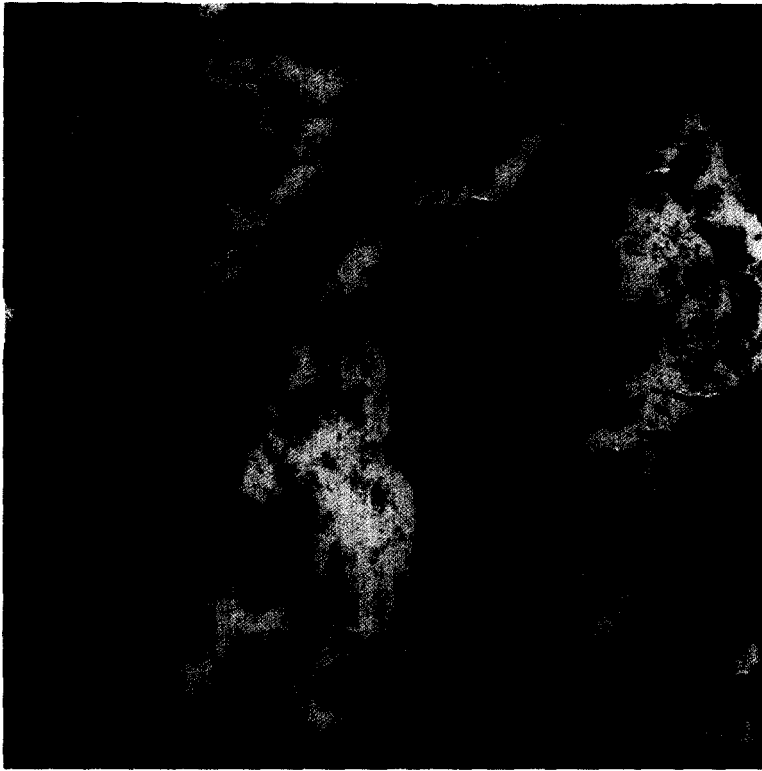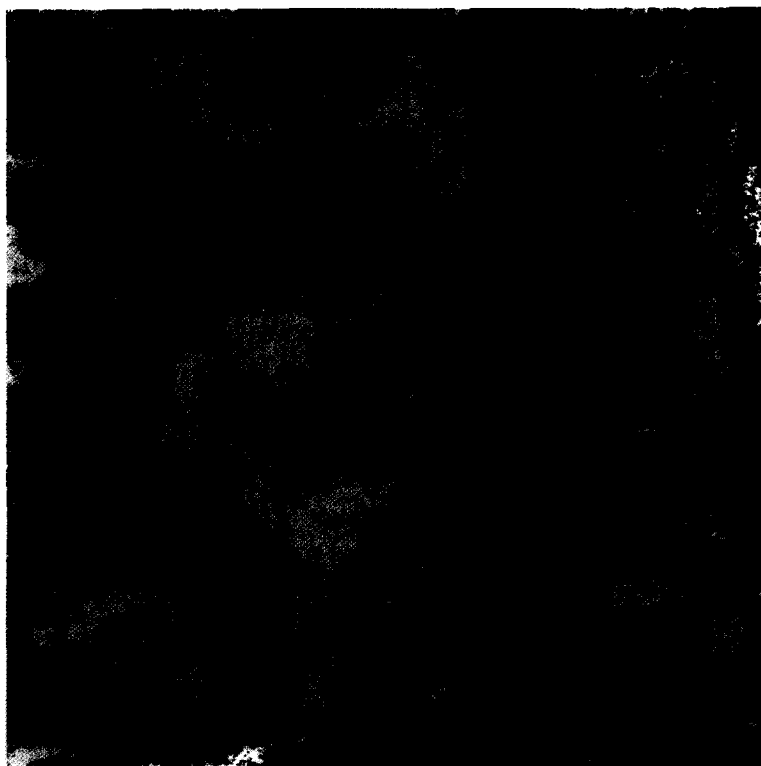
Northwestern North Sea:

CZCS colour composite images, 54.9° to 58.5°N, 3.0°W to 3.5°E, for:
12 May (11.14 GMT, 3.75%) Fig. 70;
15 May (10.27 GMT, 3.75%) Fig. 71;
18 May (11.23 GMT, 3.75%) Fig. 72;
17 May (11.04 GMT, 3.75%) Fig. 73.

This sequence of colour composite images shows considerable heterogeneity in the optical properties of the open North Sea at the start of the annual production cycle. The patchiness in water properties at this time of year has been documented through the application of continuous recording instruments. For example, STEELE and HENDERSON (1979) demonstrated for the FLEX box (Fladen Ground, just to the north of the area shown here) strong local gradients in temperature and chlorophyll which were correlated in some instances and not in others. Furthermore, over periods of a few days, these gradients shifted within the advective field and, for chlorophyll, grew weaker or stronger according (presumably) to the developmental stage of the phytoplankton population.

The main features of the images are two darker regions to the east of Scotland and east of England. In the former, there was a general reduction in reflectance between 12 and 15 May, followed by the reverse trend and the sudden appearance of bright patches (coccolithophores) offshore between 15 and 18 May. To the south, a marked decline in chlorophyll over the whole period was apparent, leading by 18 May to "blue" water conditions typical of the summer. A persistent bright feature is seen in the southeastern quadrant of each image, probably due to suspended material in water over the northern part of Dogger Bank. In both regions, numerous changes in the structure of small-scale eddies are apparent. Rapid changes both in chlorophyll concentrations (WEICHART, 1980) and in species composition (GIESKES and KRAAY, 1983) have been reported from the North Sea during the spring. The 10 days leading to 18 May had been almost cloud-free, so that conditions for phytoplankton growth had been near ideal. From satellite images alone, it can not be determined whether sinking of the plant cells under conditions of nutrient depletion, or mortality due to zooplankton grazing was the cause of the general decline in surface chlorophyll. Also it is uncertain, from this image, whether the increase in reflectance was caused by coccolith production or a reduction in chlorophyll absorption. It should be noted that although Figs 70–73 were produced with the same saturation reflectance as Fig. 28, the latter is noticeably darker – this is due to differences in the processing of each set of prints and gives some indication of the problems encountered with the reproduction of near real-colour composites.
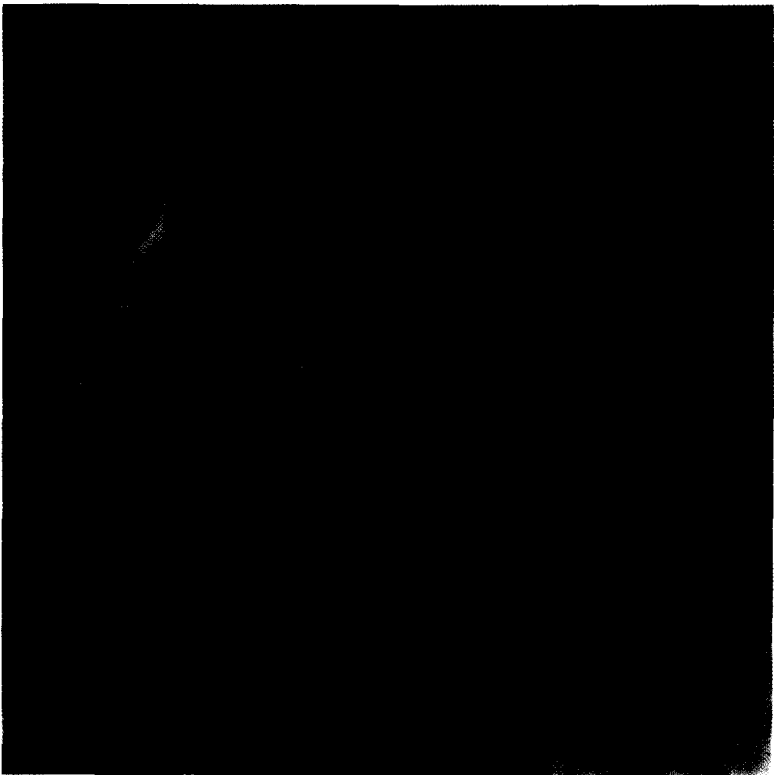
4.5. *Advection and mixing processes in the Skagerrak* (*Figs* 74–77)

CZCS channel 3 images for June 1982, 56.0° to 59.2°N, 6.0° to 12.0°E:
   19 June (10.18 GMT) Fig. 74;
   21 June (10.54 GMT) Fig. 75;
   22 June (11.12 GMT) Fig. 76;
   23 June (09.48 GMT) Fig. 77.

Hydrographic investigations in the Skagerrak have demonstrated how the distributions of surface water properties are determined by a combination of surface flows westward out of the Baltic, along the Norwegian coast and towards the northeast along the north Danish coast (SVANSSON, 1975; LARSSON and RHODE, 1979; DAHL and DANIELSSEN, 1981), and of downwelling/upwelling along the coast depending on the strength of the prevailing winds. Geostrophic effects can also induce upwelling-type conditions in the central part of the Skagerrak, through upward doming of the seasonal pycnocline (PINGREE *et al.*, 1982).

These channel 3 CZCS images show how rapidly surface properties in the Skagerrak can change over a period of 5 days. The patterns represent a combination of dark areas (absorption by chlorophyll and dissolved material), bright areas offshore (probably coccolithophores), and bright areas inshore (suspended sediments) along the immediate Danish coast and around islands in the Kattegat. The effect of cyclonic circulation in the Skagerrak can be discerned, with certain features being stretched due to shear, as well as small eddies being formed and dissipated with the general flow field.

Figure 78

Figure 76

Figure 77

.
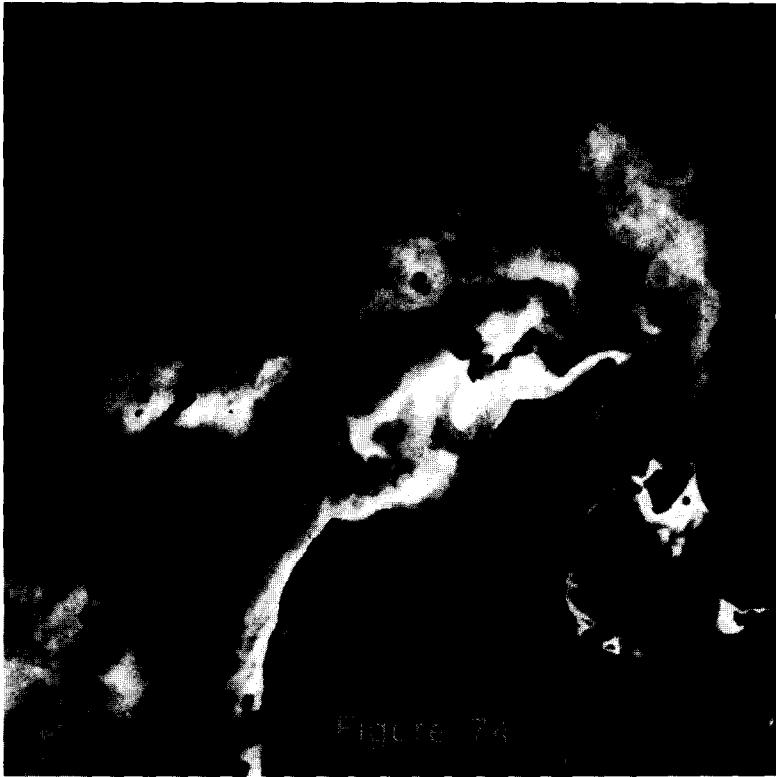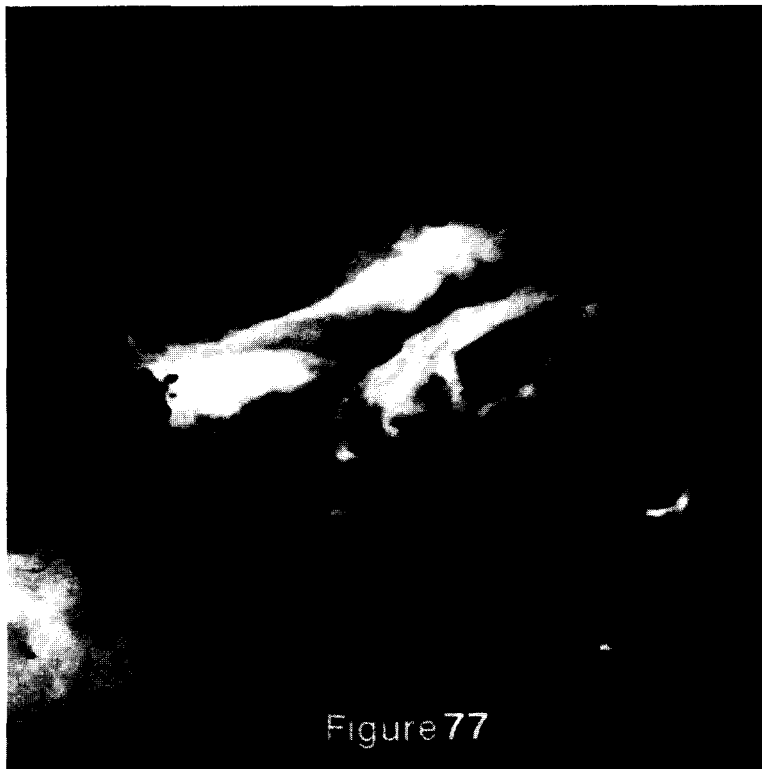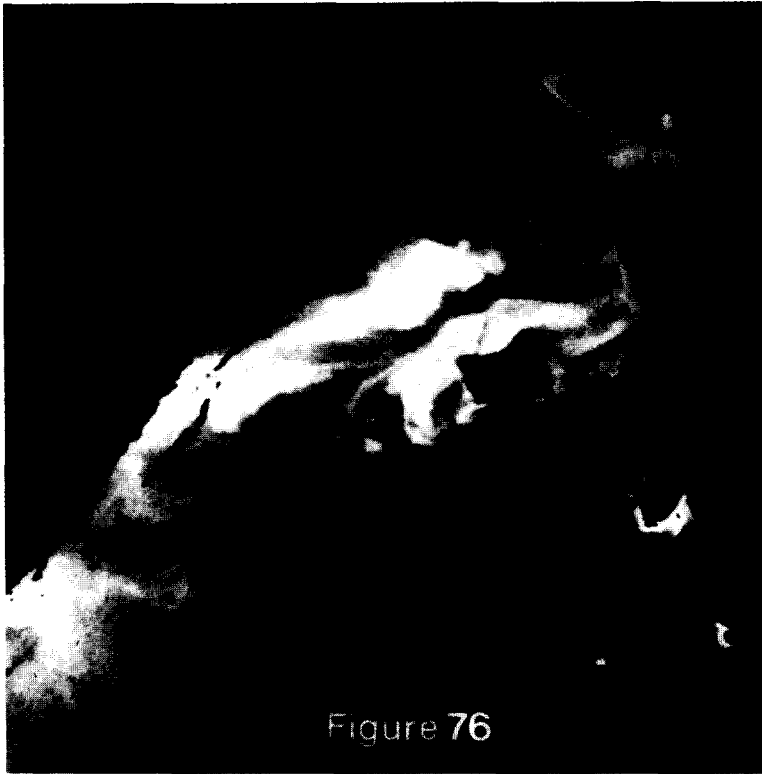
4.6. *Summer chlorophyll in the German Bight* (*Figs* 78–83)

CZCS chlorophyll images, 53.0° to 56.9°N, 3.6° to 10.4°E, for:
 30 August 1979 (11.18 GMT) Fig. 78;
 26 July 1980 (10.29 GMT) Fig. 79;
 5 September 1981 (12.13 GMT) Fig. 80;
 1 August 1982 (10.10 GMT) Fig. 81;
 23 July 1983 (10.18 GMT) Fig. 82;
 24 August 1984 (10.39 GMT) Fig. 83.

CZCS images for the German Bight indicate that relatively high surface chlorophyll levels are characteristic of the region between July and early September. The highest chlorophyll values are seen generally close to the coast and in the Elbe estuary, both locations where sediments will influence the optics of the water. However, intermediate chlorophyll levels (yellow to green shades) usually extend well offshore in marked contrast to the blue, chlorophyll-poor waters of the more stratified central North Sea.

There have been several reports of dinoflagellate blooms in the German Bight at this time of year (GILLBRICHT, 1983; DOERFFER *et al.*, 1984) which can affect surface pH values (WEICHART, 1985) and, through subsequent oxidation processes, cause depletion of oxygen below the pycnocline (DYER *et al.*, 1983). Also, there is strong evidence for a consistent increase in the general abundance of phytoplankton, probably in response to higher inputs of nutrients from the rivers (RADACH and BERG, 1986).

Reference to the island of Helgoland provides an indication of annual variability at local scales which is typical of ephemeral dinoflagellate blooms and of differences, from one summer to the next, in hydrographic conditions. In these images the water around Helgoland ranges from blue to red and is not necessarily representative of the main area of the German Bight. The problems of extrapolating from observations at one locality, whether from satellites or ships, are well illustrated.
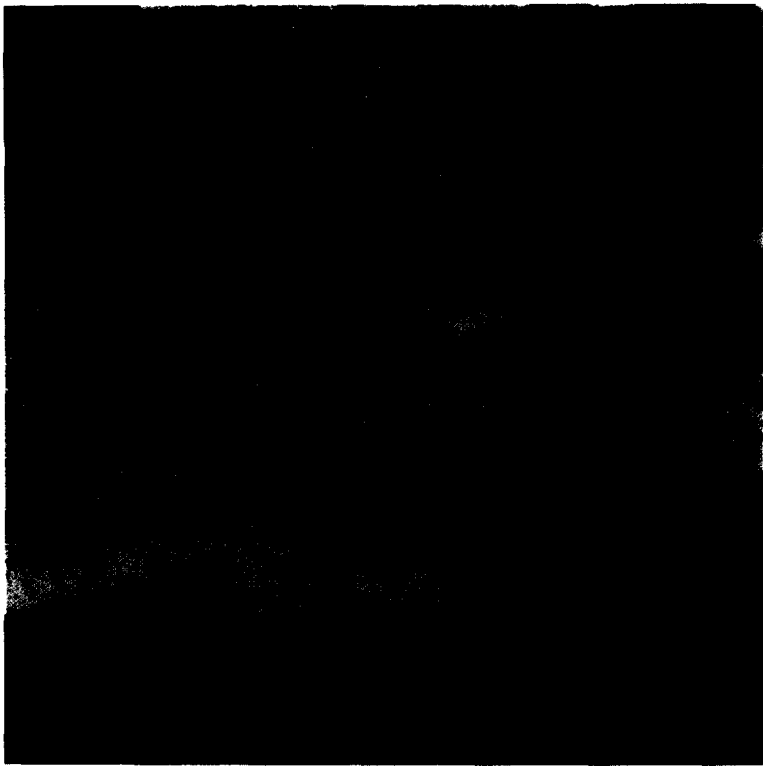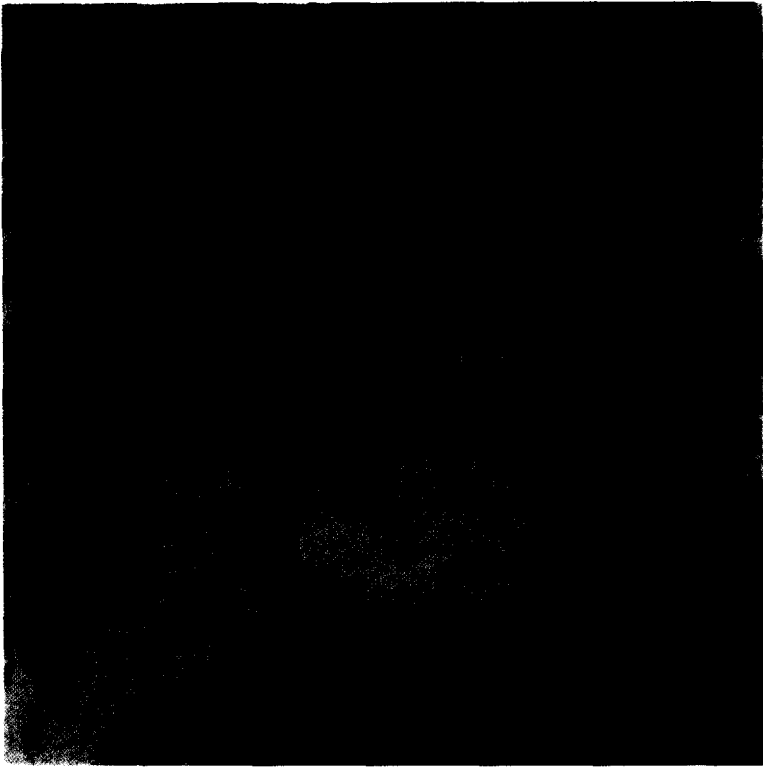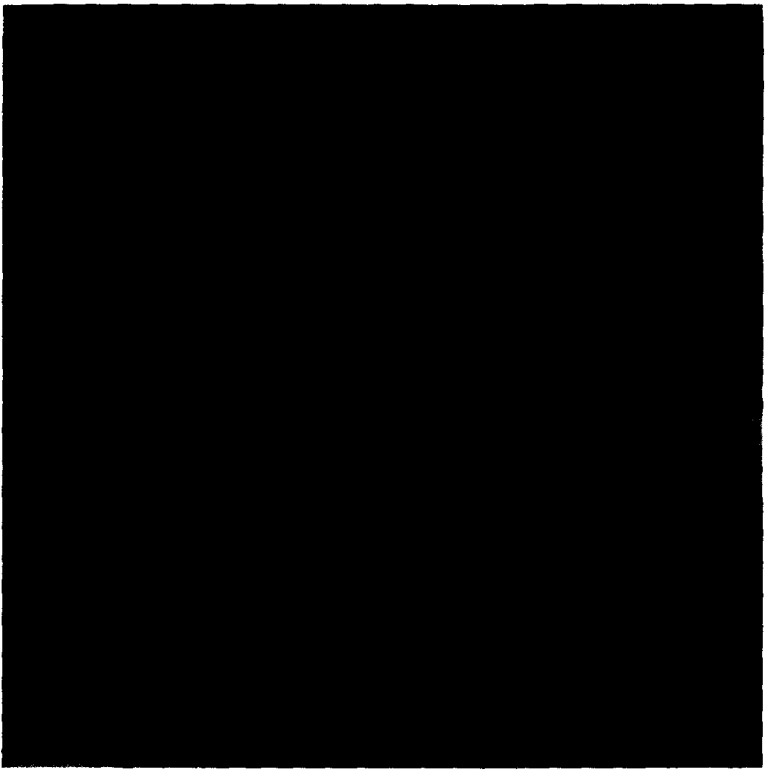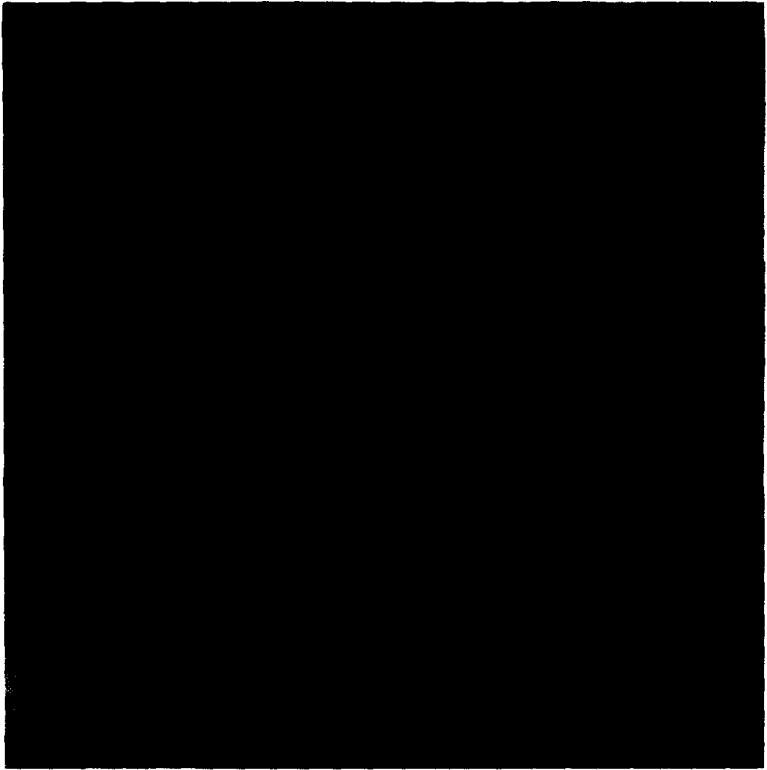
5. CONCLUSIONS

The seasonal series of CZCS and AVHRR (thermal) satellite images show the complexity of surface phytoplankton, suspended sediment and temperature distributions in the North Sea. Many of the main features have been recognized previously, through standard sampling procedures from ships, but the superior spatial (~1 km) and temporal (1 day in the absence of clouds) resolution of satellite sensors allows a much better appreciation of the variability within the ecosystem as a whole. Each CZCS scene represents a synoptic picture of patterns in optical properties that can be related to hydrographic (e.g. tidal fronts, river plumes, advection) and topographic features. The structural detail and rapidity of change is, in many cases, remarkable and not well understood in a mechanistic sense. Applications for this new information have yet to be developed but will certainly include improved validation and interpretation of ship observations and of hydrodynamic models (e.g. BACKHAUS, 1985).

Seasonal changes in the North Sea, including the effects of thermal stratification and tidal mixing on surface suspended matter and on the development of phytoplankton blooms, are well documented by the imagery. The significance of physical processes in determining the distributions of biological properties, which has received much attention through recent interdisciplinary studies on tidal fronts, is reinforced by the correlations that exist between thermal and optical structures.

Although remote sensing alone will not resolve all the outstanding problems of estimating primary productivity in the North Sea (HOLLIGAN, 1989), it will provide for the first time an objective framework for extrapolating from *in situ* experimental measurements of photosynthetic activity. Important questions are also raised about the significance of optical properties (absorption by plant pigments and DOM, backscattering by coccoliths and suspended sediment) in relation to warming of the surface mixed layer in spring and summer.

The images of blooms of diatoms and *Phaeocystis* in the spring and coccolithophores in the summer, of chlorophyll distributions in the German Bight, and of reflectance patterns in the Skagerrak demonstrate the potential importance of remote sensing for investigations of a wide range of ecological and water quality problems in coastal seas. Recent events in the North Sea (MILNE, 1987), which include the effects of various types of pollution and of toxic algal blooms, demonstrate the need for continuous monitoring of offshore waters as can only be achieved through the use of satellites. In this context, it is necessary to recognize that there are many apparently local effects along the coast which result from events offshore; these affect the water properties over relatively large temporal and spatial scales.

There are many features in the images that show boundary conditions typical of mixing processes in the water and can be related to known hydrographic and topographic features, but are difficult to interpret in terms of specific optical properties. This problem is caused both by a lack of appropriate ground truth measurements and by considerable uncertainties in algorithms for quantitative determinations of constituents such as chlorophyll and suspended sediment. In order to improve the present crude methods of interpretation for the visible band images, a data base of simultaneous hydrographic and remote sensing (satellite or aircraft) measurements covering the full range of water types in the North Sea is required. Towed instrument packages including optical sensors, such as the Undulating Oceanographic Recorder (AIKEN and BELLAN, 1986), must be deployed to obtain the necessary temporal and spatial resolution of *in situ* information.

Algorithm development will depend upon improved satellite sensors to deal with the special problems of Case 2 coastal waters. In particular the accurate estimation of chlorophyll requires a second blue channel at around 410 nm in order to take account of absorption by dissolved organic matter (BRICAUD et al., 1981; SATHYENDRANATH et al., 1987) independently of absorption by chlorophyll. The signal-to-noise performance of any blue channel is also important, in relation both to the relatively high levels of blue-absorbing materials in coastal waters and to sensitivity in the winter months when surface irradiance is low. New algorithms to supplement purely empirical methods of distinguishing chlorophyll, dissolved organic material, coccoliths and suspended sediments (e.g. VIOLLIER and STURM, 1984; FISCHER and DOERFFER, 1987) are required for future sensors that will have more visible channels than the CZCS [e.g. the Moderate-Resolution Imaging Spectrometer (MODIS) planned for the Space Station in the mid-1990s]. Some progress in this direction will be possible with the proposed Sea-viewing Wide-Field-of-View Sensor (SeaWIFS).

In the meantime there is the question of what further work can be done with the extensive CZCS archive for the North Sea. Explaining the causes and understanding the effects (both biological and chemical) of the variability in optical properties of surface waters of the North Sea shown by the CZCS images should be an integral part of new observational and modelling studies of the North Sea which are aimed at better control and prediction of water quality. Although the various problems of interpreting colour data for Case 2 waters (HØJERSLEV, 1982) cannot be ignored, site-specific studies in the North Sea (e.g. the FLEX area, HØJERSLEV, 1982), as well as in the English Channel (VIOLLIER and STURM, 1984) and Irish Sea (MITCHELSON et al., 1986; SIMPSON and BROWN, 1987), indicate that appropriate processing and statistical techniques can provide reliable information on water properties including plant pigment concentrations. The apparent consistency in seasonal and sub-regional (coastal vs offshore, mixed vs stratified waters) change in the CZCS images needs to be quantitatively evaluated. Furthermore, sequences of images (e.g. Figs 64–69; 70–73 and 74–77; also see BOXALL and ROBINSON, 1987) provide an important independent method of assessing experimental and theoretical results on advective processes.

In the longer term, the CZCS archive of the North Sea will become an important set of data for assessing long-term trends in an ecosystem that continues to be heavily affected by man's activities. Distinguishing the influences on plankton distributions and productivity of natural variations in climate (COLEBROOK, 1979, 1986; RADACH, 1984) and of changing inputs of inorganic nutrients (POSTMA, 1985) and other pollutants is already the subject of much debate (REID, 1978; CADEE and HEGEMAN, 1986; RADACH and BERG, 1986). The use of satellites to monitor trends in optical properties represents a powerful new technique in attempts to determine the direct impact of human interference in the North Sea.

REFERENCES

AARUP T., S. B. GROOM and P. M. HOLLIGAN (1987) The processing and interpretation of North Sea CZCS imagery. ICES C.M. 1987/C; 31, 14 pp.

AARUP T., S. B. GROOM and P. M. HOLLIGAN (1989) CZCS imagery of the North Sea. Netherlands Journal of Sea Research, in press.

AIKEN J. and I. BELLAN (1986) Synoptic optical oceanography with the Undulating Oceanographic Recorder. Proceedings of SPIE, 637, 221–229.

ARNONE R. A. and P. E. LAVIOLETTE (1984) A method of selecting optimal Ångström coefficients to obtain quantitative ocean color data from Nimbus-7 CZCS. Proceedings of SPIE, 489, 187–193.

AUSTIN R. W. and T. J. PETZOLD (1981) The determination of the diffuse attenuation coefficient of sea water using the coastal zone color scanner. In: Oceanography from space, J. R. F. GOWER, editor, Plenum Press, New York, pp. 239–256.

BACKHAUS J. O. (1985) A three-dimensional model for the simulation of shelf-sea dynamics. Deutsche Hydrographische Zeischrift, 38, 165–187.

BACKHAUS J. O. and E. MAIER-REIMER (1983) On seasonal circulation patterns in the North Sea. In: North Sea dynamics, J. SUNDERMANN and W. LENZ, editors, Springer-Verlag, New York, pp. 63–84.

BOXALL S. R. and I. S. ROBINSON (1987) Shallow sea dynamics from CZCS imagery. Advances in Space Research, 7, 37–46.

BRICAUD A. and A. MOREL (1986) Light attenuation and scattering by phytoplanktonic cells: a theoretical modeling. Applied Optics, 25, 571–580.

BRICAUD A., A. MOREL and L. PRIEUR (1981) Absorption by dissolved organic matter of the sea (yellow substance) in the UV and visible domains. Limnology and Oceanography, 26, 43–53.

BROCKMANN U. H. and G. WEGNER (1985) Hydrography, nutrient and chlorophyll distribution in the North Sea in February 1984. Archiv für Fischereiwissenschaft, 36, 37–45.

BROWN O. B., R. H. EVANS, J. W. BROWN, H. R. GORDON, R. C. SMITH and K. S. BAKER (1985) Phytoplankton blooming off the U.S. east coast: A satellite description. Science, 229, 163–167.

CADEE G. C. and J. HEGEMAN (1986) Seasonal and annual variation in Phaeocystis pouchetii (Haptophyceae) in the westernmost inlet of the Wadden Sea during the 1973 to 1985 period. Netherlands Journal of Sea Research, 20, 29–36.

CAMPBELL J. W. and J. E. O'REILLY (1988) Role of satellites in estimating primary productivity on the northwest Atlantic continental shelf. Continental Shelf Research, 8, 179–204.

CARDER K. L., R. G. STEWARD, J. H. PAUL and G. A. VARGO (1986) Relationships between chlorophyll and ocean color constituents as they affect remote-sensing reflectance models. Limnology and Oceanography, 31, 403–413.

COLEBROOK J. M. (1979) Continuous plankton records: seasonal cycles of phytoplankton and copepods in the North Atlantic Ocean and the North Sea. Marine Biology, 51, 23–32.

COLEBROOK J. M. (1986) Environmental influences on long-term variability in marine plankton. Hydrobiologia, 142, 309–325.

DAHL E. and D. S. DANIELSSEN (1981) Hydrography, nutrients and phytoplankton in the Skagerrak along the section Torungen–Hirtshals, January–June 1980. In: The Norwegian coastal current, R. SAETRE and M. MORK, editors, University of Bergen, pp. 294–310.

DESCHAMPS P. Y. and M. VIOLLIER (1987) Algorithms for ocean colour from space and application to CZCS data. Advances in Space Research, 7, 11–19.

DOERFFER R., V. AMANN and H. VAN DER PIEPEN (1984) Remote sensing of exceptional plankton blooms. Presented at the special meeting on the causes, dynamics and effects of exceptional marine blooms and related events, ICES, Copenhagen, 4–5 October 1984. A3 poster.

DUURSMA E. K. (1974) The fluorescence of dissolved organic matter in the sea. In: Optical aspects of oceanography, N. JERLOV and A. S. NIELSON, editors, Academic Press, New York, pp. 237–256.

DYER M. F., J. G. POPE, P. D. FRY, R. J. LAW and J. E. PORTMANN (1983) Changes in fish and benthos catches off the Danish coast in September 1981. Journal of the Marine Biological Association of the United Kingdom, 63, 767–775.

EISMA D. (1981) Supply and deposition of suspended matter in the North Sea. *Special Publications of the International Association of Sediment*, **5**, 415–429.

EISMA D. and J. KALF (1979) Distribution and particle size of suspended matter in the Southern Bight of the North Sea and the Eastern Channel. *Netherlands Journal of Sea Research*, **13**, 298–324.

EISMA G. and J. KALF (1987) Distribution, organic content and particle size of suspended matter in the North Sea. *Netherlands Journal of Sea Research*, **21**, 65–85.

EISMA D and G. IRION (1988) Suspended matter and sediment transport. In: *Pollution of the North Sea: an assessment*, W. SALOMONS, B. L. BAYNE, E. K. DUURSMA and U. FORSTNER, editors, Springer-Verlag, New York, pp. 20–35.

EPPLEY R. W., E. STEWART, M. R. ABBOTT and U. HEYMANN (1985) Estimating ocean primary production from satellite chlorophyll. Introduction to regional differences and statistics for the Southern California Bight. *Journal of Plankton Research*, **7**, 57–70.

FISCHER J. and R. DOERFFER (1987) An inverse technique for remote detection of suspended matter, phytoplankton and yellow substance from CZCS measurements. *Advances in Space Research*, **7**, 21–26.

FRASER J. H. (1965) Zooplankton indicator species in the North Sea. Series of Atlases on the Marine Environment, Folio 8, W. WEBSTER, editor, American Geographical Society, New York.

GIENAPP H. (1982) Optical properties of seawater in the German Bight and the mouth of the Elbe; the 1978 CZCS pre-launch experiment of the Deutsches Hydrographisches Institut (DHI). Part 2. *Deutsche Hydrographische Zeitschrift*, **35**, 135–167.

GIENAPP H. and B. STURM (1983) Ein CZCS-postlaunch-experiment uber der Deutschen Bucht und seine Auswertung im Hinblick auf die dortigen Gelbstoffund Schwebstoffgehalte sowie die Frontendynamik. *Deutsche Hydrographische Zeitschrift*, **36**, 97–128.

GIESKES W. W. C. and G. W. KRAAY (1977) Primary production and consumption of organic matter in the southern North Sea during the spring bloom of 1975. *Netherlands Journal of Sea Research*, **11**, 146–167.

GIESKES W. W. C. and G. W. KRAAY (1980) Primary productivity and phytoplankton pigment measurements in the northern North Sea during FLEX '76. *Meteor Forschungergebnisse*, **A22**, 105–112.

GIESKES W. W. C and G. W. KRAAY (1983) Dominance of Cryptophyceae during the phytoplankton spring bloom in the central North Sea detected by HPLC analysis of pigments. *Marine Biology*, **75**, 179–185.

GIESKES W. W. C. and G. W. KRAAY (1984) Phytoplankton, its pigments and primary production at a central North Sea station in May, July and September 1981. *Netherlands Journal of Sea Research*, **18**, 51–70.

GILLBRICHT M. (1983) Eine "red tide" in der sudlichen Nordsee und ihre Beziehungen zur Umwelt. *Helgoland Meeresunters*, **36**, 393–426.

GORDON H. R. (1978) Removal of atmospheric effects from satellite imagery of the oceans. *Applied Optics*, **17**, 1631–1636.

GORDON H. R. and D. CLARK (1981) Clear water radiances for atmospheric correction of Coastal Zone Color Scanner imagery. *Applied Optics*, **20**, 4175–4180.

GORDON H. R. and A. MOREL (1983) Remote assessment of ocean color for the interpretation of satellite visible imagery. In: *Lecture notes on coastal and estuarine studies*, Springer Verlag, New York, 114 pp.

GORDON H. R. and D. J. CASTAÑO (1987) Coastal Zone Color Scanner atmospheric correction algorithm: multiple scattering effects. *Applied Optics*, **26**, 2111–2122.

GORDON H. R., D. CLARK, J. BROWN, O. BROWN, R. EVANS and W. BROENKOW (1983a) Phytoplankton pigment concentrations in the Middle Atlantic Bight: comparison of ship determinations and CZCS estimates. *Applied Optics*, **22**, 20–36.

GORDON H. R., J. BROWN, O. BROWN, R. EVANS and D. CLARK (1983b) Nimbus-7 CZCS: reduction of its radiometric sensitivity with time. *Applied Optics*, **22**, 3929–3931.

GORDON H. R., J. W. BROWN and R. H. EVANS (1988) Exact Rayleigh scattering calculations for use with the Nimbus-7 Coastal Zone Color Scanner. *Applied Optics*, **27**, 862–871.

GOWER J. F. R. (1987) Introduction to oceanography from space. *Advances in Space Research*, **7**, 1–2.

GROOM S. B. and P. M. HOLLIGAN (1986) Remote sensing of coccolithophore blooms. *Advances in Space Research*, **7**, 73–78.

HOLLIGAN P. M. (1987) The physical environment of exceptional phytoplankton blooms in the Northeast Atlantic. *Rapports et Proces-Verbaux des Reunions, Conseil International pour l'Exploration de la Mer*, **187**, 9–18.

HOLLIGAN P. M. (1989) Primary productivity in the shelf seas of northwest Europe. *Advances in Botanical Research*, **16**, (in press).

HOLLIGAN P. M., M. VIOLLIER, C. DUPOUY and J. AIKEN (1983a) Satellite studies on the distribution of chlorophyll and dinoflagellate blooms in the western English Channel. *Continental Shelf Research*, **2**, 81–96.

HOLLIGAN P. M., M. VIOLLIER, D. S. HARBOUR, P. CAMUS and M. CHAMPAGNE-PHILIPPE (1983b) Satellite and ship studies of coccolithophore production along a continental shelf edge. *Nature*, **304**, 339–342.

HOVIS W. A. (1981) The Nimbus-7 Coastal Zone Color Scanner. In: *Oceanography from space*, J. GOWER, editor, Plenum Press, New York, pp. 213–225.

HØJERSLEV N. K. (1982) Bio-optical properties of the Fladen Ground: "*Meteor*"–FLEX-75 and FLEX-76. *Journal du Conseil, Conseil International pour l'Exploration de la Mer*, **40**, 272–290.

HØJERSLEV N. K. (1988) Natural occurrences and optical effects of Gelbstoff. København Universitet Geofysisk Institut. Copenhagen Report No. 50, 30 pp.

KIRK J. (1983) *Light and photosynthesis in aquatic ecosystems*. Cambridge University Press, Cambridge, 401 pp.

LANCELOT C., G. BILLEN, A. SOURNIA, T. WEISSE, F. COLIJN, M. J. W. VELDHUIS, A. DAVIES and P. WASSMANN (1987) Phaeocystis blooms and nutrient enrichment in the continental coastal zones of the North Sea. *Ambio*, **16**, 38–46.

LARSSON A. M. and J. RHODE (1979) Hydrographical and chemical observations in the Skagerrak, 1975–1977. Report 29. Ocean Institute of Goteborg University.

LEE A. J. (1980) North Sea: physical oceanography. In: *The northwest European Shelf seas: the sea bed and the sea in motion*, F. T. BANNER, M. B. COLLINS and K. S. MASSIE, editors, Elsevier, Amsterdam, pp. 467–493.

LEE A. J. and A. R. FOLKARD (1969) Factors affecting turbidity in the southern North Sea. *Journal du Conseil, Conseil International pour l'Exploration de la Mer*, **32**, 291–302.

LEE A. J. and J. W. RAMSTER, editors (1981) *Atlas of the seas around the British Isles*. M.A.F.F., Lowestoft, U.K. Her Majesty's Stationery Office Publication.

MILNE R. (1987) Pollution and politics in the North Sea. *New Scientist* (19 Nov.), 53–58.

MITCHELSON E. G., N. J. JACOB and J. SIMPSON (1986) Ocean colour algorithms from the case 2 waters of the Irish Sea in comparison to algorithms from case 1 waters. *Continental Shelf Research*, **5**, 403–415.

MOREL A. and L. PRIEUR (1977) Analysis of variations in ocean color. *Limnology and Oceanography*, **22**, 709–722.

MORK M. (1981) Experiments with theoretical models of the Norwegian coastal current. In: *The Norwegian coastal current*, R. SAETRE and M. MORK, editors, University of Bergen, pp. 518–552.

MUELLER J. (1985) Nimbus-7 CZCS: confirmation of its radiometric sensitivity decay rate through 1982. *Applied Optics*, **24**, 1043–1047.

MUELLER J. L. (1988) Nimbus-7 CZCS: Electronic overshoot due to cloud reflectance. *Applied Optics*, **27**, 438–440.

PINGREE R. D. and D. K. GRIFFITHS (1978) Tidal fronts on the shelf seas around the British Isles. *Journal of Geophysical Research*, **83**, 4615–4622.

PINGREE R. D. and D. K. GRIFFITHS (1980) Currents driven by a steady uniform wind stress on the shelf seas around the British Isles. *Oceanologica Acta*, **3**, 227–232.

PINGREE R. D., P. M. HOLLIGAN and G. T. MARDELL (1978) The effects of vertical stability on phytoplankton distributions in the summer on the northwest European Shelf. *Deep-Sea Research*, **25**, 1011–1028.

PINGREE R. D., P. M. HOLLIGAN, G. T. MARDELL and R. P. HARRIS (1982) Vertical distribution of plankton in the Skagerrak in relation to doming of the seasonal thermocline. *Continental Shelf Research*, **1**, 209–219.

PLATT T. (1986) Primary production of the ocean water column as a function of surface light intensity: algorithms for remote sensing. *Deep-Sea Research*, **33**, 149–163.

PLATT T. and S. SATHYENDRANATH (1988) Oceanic primary production: estimation by remote sensing at local and regional scales. *Science*, **241**, 1613–1620.

POSTMA H. (1985) Eutrophication of Dutch coastal waters. *Netherlands Journal of Zoology*, **35**, 348–359.

PRAHM-RODENWALD G. (1980) The hydrographic situation in the North Sea in August 1980. *Annales Biologiques*, **37**, 84–87.

RADACH G. (1984) Variations in the plankton in relation to climate. *Rapports et Proces-Verbaux des Reunions, Conseil International pour l'Exploration de la Mer*, **185**, 234–254.

RADACH G. and J. BERG (1986) Trends in den Konzentrationen der Nahrstoffe und des phytoplanktons in der Helgolander Bucht (Helgoland Reede Daten). *Berichte der Biologischen Anstalt Helgoland*, **2**, 1–63.

REID P. C. (1978) Continuous plankton records: large-scale changes in the abundance of phytoplankton in the North Sea from 1958 to 1973. *Rapports et Proces-Verbaux des Reunions, Conseil International pour l'Exploration de la Mer*, **172**, 384–389.

REID P. C., H. G. HUNT and T. D. JONAS (1983) Exceptional blooms of diatoms associated with anomalous hydrographic conditions in the Southern Bight in early 1977. *Journal of Plankton Research*, **5**, 755–765.

REID P. C., A. H. TAYLOR and J. A. STEPHENS (1988) The hydrography and hydrographic balances of the North Sea. In: *Pollution of the North Sea: an assessment*, W. SALOMONS, B. L. BAYNE, E. K. DUURSMA and U. FORSTNER, editors, Springer-Verlag, New York, pp. 3–19.

RICHARDSON K. (1985) Plankton distribution and activity in the North Sea/Skaggerrak–Kattegat frontal area in April 1984. *Marine Ecology Progress Series*, **26**, 233–244.

RICHARDSON K. and O. VAGN OLSEN (1987) Winter nutrient concentrations and primary production in the Eastern North Sea. ICES C.M./C: 23, 5 pp.

RICHARDSON K., M. R. HEATH and S. M. PEDERSEN (1986) Studies of a larval herring (*Clupea harengus* L.) patch in the Buchan area. III. Phytoplankton distribution and primary productivity in relation to hydrographic features. *Dana*, **6**, 25–36.

Robinson I. S. (1983) Satellite observations of ocean colour. *Philosophical Transactions of the Royal Society*, **309**, 415–432.

Robinson I. S. (1985) *Satellite oceanography: an introduction for oceanographic and remote sensing scientists.* Ellis Horwood, Ltd., Chichester, 455 pp.

Sathyendranath S., L. Prieur and A. Morel (1987) An evaluation of the problems of chlorophyll retrieval from ocean colour, for case 2 waters. *Advances in Space Research*, **7**, 27–30.

Saunders R. W., N. R. Ward, C. F. England and G. E. Hunt (1982) Satellite observations of sea surface temperature around the British Isles. *Bulletin of the American Meteorological Society*, **63**, 267–272.

Simpson J. H. and J. Brown (1987) The interpretation of visible band imagery of turbid shallow seas in terms of the distribution of suspended particulates. *Continental Shelf Research*, **7**, 1307–1313.

Singh S. M., A. P. Cracknell and J. A. Charlton (1983) Comparison between CZCS data from 10 July 1979 and simultaneous *in situ* measurements for southeastern Scottish waters. *International Journal of Remote Sensing*, **4**, 755–784.

Smith R. C. (1981) Remote sensing and depth distribution of ocean chlorophyll. *Marine Ecology Progress Series*, **5**, 359–361.

Snyder J. P. (1982) Map projections used by the Geological Survey. U.S. Geological Survey Bulletin, 1532, 313 pp.

Steele J. H. and E. W. Henderson (1979) Spatial patterns in North Sea plankton. *Deep-Sea Research*, **26**, 955–963.

Sturm B. (1981) The atmospheric correction of remotely sensed data and the qualitative determination of suspended matter in marine water surface layers. In: *Remote sensing in meteorology, oceanography and hydrology*, A. P. Cracknell, editor, Ellis Harwood Ltd, pp. 163–197.

Svansson A. (1985) Physical and chemical oceanography of the Skagerrak and the Kattegat. I. Open sea conditions. Fisheries Board of Sweden, Institute of Marine Research, Report No. 1, 88 pp.

Sørensen B. M. (1979) The North Sea Ocean Color Scanner Experiment 1977. Joint Research Center, Ispra, Italy, 126 pp.

Tassan S. (1988) The effect of dissolved "yellow substance" on the quantitative retrieval of chlorophyll and total suspended sediment concentrations from remote measurements of water colour. *International Journal of Remote Sensing*, **9**, 787–797.

Tassan S. and B. Sturm (1986) An algorithm for the retrieval of sediment content in turbid coastal waters from CZCS data. *International Journal of Remote Sensing*, **7**, 643–655.

Veldhuis M. J. W., F. Coljin and L. A. H. Venekamp (1986) The spring bloom of *Phaeocystis pouchetii* (Haptophyceae): observations in Dutch coastal waters of the North Sea. *Netherlands Journal of Sea Research*, **20**, 37–48.

Viollier M. and B. Sturm (1984) CZCS data analysis in turbid coastal waters. *Journal of Geophysical Research*, **89**, 4977–4985.

Viollier M., D. Tanre and P. Y. Deschamps (1980) An algorithm for remote sensing of water color from space. *Boundary Layer Meterology*, **18**, 247–267.

Visser M. P. (1970) The turbidity of the southern North Sea. *Deutsche Hydrographische Zeitschrift*, **35**, 97–117.

Weichart G. (1980) Chemical changes and primary production in the Fladen Ground area (North Sea) during the first phase of a spring phytoplankton bloom. *"Meteor" Forschungsergebnisse*, **22**, 79–86.

Weichart G. (1985) High pH values in the German Bight as an indication of intensive primary production. *Deutsche Hydrographische Zeitschrift*, **38**, 93–117.

APPENDIX

To assist future work on the CZCS imagery, the following services and facilities are available to users.

The complete global set of CZCS imagery is archived at:

National Climate Data Center,

Satellite Data Services Division,

Washington, DC 20233,

U.S.A.

and

National Space Science Data Center (NSSDC),

NASA Goddard Space Flight Center,

Greenbelt, MD 20771,

U.S.A.

For North European areas including the North Sea, the satellite receiving station at the University of Dundee holds a complete archive for these areas from August 1979.

The Satellite Receiving Station,
Dept of Applied Physics and Electronic &
  Manufacturing Engineering,
The University,
Dundee DD1 4HN,
Scotland, U.K.

The cloud cover and the quality of the CZCS imagery can be assessed to some extent from (a) microfilms of raw imagery (available from the National Climate Data Center) and (b) the chlorophyll processed CZCS image archive. This archive will be distributed on videodisk together with a PC/VAX based browsing system to a number of NASA-funded research institutions in 1989.